Improving Trajectory Predictions for Short Baseline Line-of-Bearing Tracking Systems

Gary L. Durfee
Andrew A. Thompson

ARL-TR-961   February 1996

19960220 076

DTIC QUALITY INSPECTED 1

NOTICES

REPORT DOCUMENTATION PAGE

Form Approved
OMB No. 0704-0188

1. AGENCY USE ONLY *(Leave blank)*	2. REPORT DATE **February 1996**	3. REPORT TYPE AND DATES COVERED Final, Jun 93–Jul 95

4. TITLE AND SUBTITLE
Improving Trajectory Predictions for Short Baseline Line-of-Bearing
Tracking Systems

5. FUNDING NUMBERS

PR: 1L162618AH80

6. AUTHOR(S)

Gary L. Durfee and Andrew A. Thompson

7. PERFORMING ORGANIZATION NAME(S) AND ADDRESS(ES)

U.S. Army Research Laboratory
ATTN: AMSRL-WT-WB
Aberdeen Proving Ground, MD 21005-5066

8. PERFORMING ORGANIZATION REPORT NUMBER

ARL-TR-961

9. SPONSORING/MONITORING AGENCY NAME(S) AND ADDRESS(ES)

10. SPONSORING/MONITORING AGENCY REPORT NUMBER

11. SUPPLEMENTARY NOTES

12a. DISTRIBUTION/AVAILABILITY STATEMENT

Approved for public release; distribution is unlimited.

12b. DISTRIBUTION CODE

13. ABSTRACT *(Maximum 200 words)*

This report investigates methods for analyzing and improving the tracking performance of short baseline line-of-bearing (LOB) systems. Such a system might be placed on an armored vehicle in order to track an incoming threat projectile and make an accurate prediction of the threat's future location (at a specific time) so that an appropriate reaction can be initiated. The processes for estimating the trajectory of a projectile over the terminal portion of its flight are discussed. LOB, range, and radial speed sensor information were considered. Three statistical estimation methods for predicting a target's trajectory are discussed: recursive least squares, weighted least squares, and Kalman filter estimation. Simulation analyses were performed for six sensor/estimator configurations for five attack azimuths and two intercept ranges. It is shown that the inherent geometry of a short-baseline LOB system leads to large errors in the system's ability to determine range, whereas the determination of cross-range is less affected by the geometry. Simulation results are presented for all sensor/estimator combinations, and the relative improvements of each are discussed. One result shows that range sensors can greatly improve the performance of inherently bad LOB sensors but that care must be taken in properly formulating the LOB/range sensor estimation routines so as not to bias the results. Another result shows that it is important to allow the incoming threat projectile to approach as close as is feasible to improve the quality of the LOB observations and thus the overall estimation.

14. SUBJECT TERMS

trajectory estimation, line-of-bearing, target tracking, target detection

15. NUMBER OF PAGES
99

16. PRICE CODE

17. SECURITY CLASSIFICATION OF REPORT UNCLASSIFIED	18. SECURITY CLASSIFICATION OF THIS PAGE UNCLASSIFIED	19. SECURITY CLASSIFICATION OF ABSTRACT UNCLASSIFIED	20. LIMITATION OF ABSTRACT SAR

INTENTIONALLY LEFT BLANK

ACKNOWLEDGMENTS

INTENTIONALLY LEFT BLANK

TABLE OF CONTENTS

LIST OF FIGURES

Figure		Page

LIST OF TABLES

INTENTIONALLY LEFT BLANK

1. INTRODUCTION

Projectile tracking systems that use line-of-bearing (LOB) sensors to triangulate the projectile's locations, to predict its trajectory, tend to suffer from large position estimation errors created by the errors in the LOB sensor's ability to accurately measure the angle to the target. These position errors, especially range errors, are exacerbated in tracking systems for which the target range is significantly greater than the LOB sensor separation distance. A conceptual system of LOB sensors on an armored vehicle for tracking incoming threat projectiles (to predict a time and location to intercept and somehow defeat such threats) will experience errors when the separation of the LOB tracking sensors is small compared with the distance to the incoming threat.

When the situation dictates that the LOB sensors angle-to-target accuracy cannot be significantly improved (due to costs or technology limitations), then other techniques are necessary to improve such tracking systems. For instance, including additional sensors to measure other projectile attributes and/or statistical filtering techniques and algorithms for processing the incoming estimation data to improve the tracking system's performance.

This report discusses the processes used to assist in the development or improvement of a subsystem for estimating the trajectory of a projectile over the terminal portion of its flight. Three types of sensor information are considered. LOB measurements indicate the direction from the sensor to the projectile (in this context, the projectile is also referred to as the "target"). Range measurements estimate the distance from the sensor to the target. Radial speed measurements indicate the speed of the target in the direction to the sensor. (Throughout this report, a sensor that measures radial speed is referred to as a "velocity" sensor.) In addition to the desired sensor signals, measurements typically contain noise, and the noise distribution of a sensor is determined by both engineering and environmental factors.

Several simulations were used to develop trajectory estimation algorithms. These algorithms were then embedded in a system simulation that allowed a parametric analysis of their ability to estimate the trajectory of a projectile. Using the system simulation, a conceptual system's ability to estimate the trajectory of a projectile is evaluated based on a suite of sensors and the accuracy of the individual sensors. This approach is used to predict the accuracy of sensors necessary for the characterization of the terminal trajectory.

The report proceeds by first discussing line-of-bearing measurements and then considering the effects of adding radial speed and range information. A discussion of the geometry associated with LOB sensor systems is included, since LOB systems serve as the base case for all comparisons. A scenario of interest is described along with the system simulation model used for the investigations. Next, the types of simulated generic sensors (LOB, velocity, and range) are examined. A brief description of each of the

1

estimation techniques (recursive least squares [RLS], weighted least squares [WLS], and Kalman filter) is included so that the reader may be aware of their differences. Finally, the results and conclusions for the system simulation runs, for various scenarios of interest, are presented and discussed.

This report will show that the inherent geometry of a short-baseline LOB system leads to large errors in the system's ability to determine range, whereas the determination of cross-range is not so affected by the geometry. Simulation results are presented for six sensor/estimator combinations, and the relative strengths of each are discussed. One result will show that range sensors can greatly improve the performance of inherently bad LOB sensors but that care must be taken in properly formulating the LOB/range sensor estimation routines so as not to bias the results. Another result will show that it is important to allow the incoming threat projectile to approach as close as is feasible to improve the quality of the LOB observations and thus the overall estimation.

2. BACKGROUND

An LOB measurement determines the direction from a point to a target. An estimate of a target's location is found by combining the measurements from two physically separated LOB sensors (where the LOB sensor locations are known). This estimate is usually called a fix or a cut. The distance between the two LOB sensors is referred to as the baseline, and the distance to the target from the center of the baseline is the range. The system boresight is the portion of the perpendicular bisector of the baseline in the halfplane into which the sensors are directed. The off-boresight angle is the angle between the boresight and the direction to the target. These relationships are shown in Figure 1. To standardize across many situations, the range is measured using the length of the baseline as the unit of measurement; thus a target range of four "baselines" is actually four times the sensor separation distance.

Many systems use LOB information to locate distant objects. A central assumption for these systems is that the LOB location errors are adequately modeled by bivariate Gaussian distributions. These systems typically use weighted averages to estimate a target's location. Weighted averages for bivariate data are discussed in Alexander (1980) and Thompson (1991a).

A discussion in Thompson and Durfee (1992) illustrates that these location errors are not necessarily Gaussian. In some situations, reasonable errors lead to calculations of implausible target locations. In addition, it was demonstrated that the distribution of location errors is skewed in the direction of increasing range; thus, bias is a problem.

In Thompson and Durfee (1993), the properties of the errors associated with LOB locations are investigated, and guidelines are suggested for various assumptions about LOB location errors. The concept of the stability ratio is introduced and used:

ON-BORESIGHT

TARGET
PATH

LOB(S1)

LOB(S2)

OFF-BORESIGHT
ANGLE

TARGET
LOCATION

RANGE

S1

S2

BASELINE
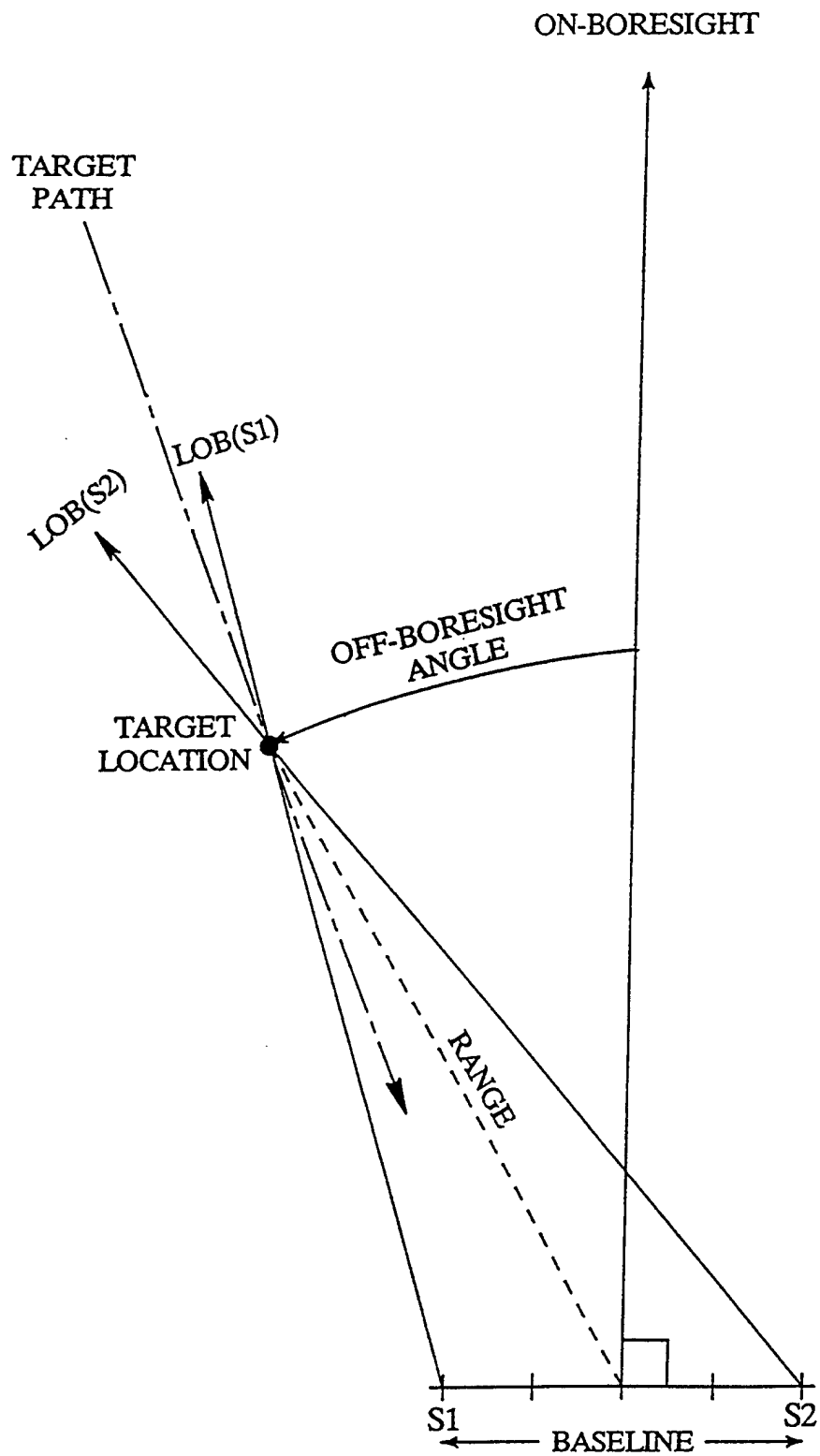
Figure 1.   **Basic Definitions of LOB System Geometry**

3

1) to determine the possibility of encountering implausible LOB locations,

2) as a means of predicting the existence and magnitude of estimator bias,

3) to determine the applicability of using a bivariate normal distribution for modeling LOB errors,

4) for determining the utility of closed form models to predict the covariance of LOB locations.

A range measurement used in conjunction with one LOB measurement gives a target location estimate. The error structure for range-LOB estimates is discussed in Thompson (1991b). Radial speed measurements are used to improve the estimates of the target's speed and trajectory. The radial speed measurement is assumed to be a projection of the actual velocity onto the direction from the sensor to the target.

3. GEOMETRIC CONSIDERATIONS FOR LOB SYSTEMS

The geometry for a two-sensor angle-only LOB system is described in this section, and the importance of the range-to-baseline ratio is discussed.

The geometric or physical relationship between the sensors and the target is a fundamental determinant of system performance. This is addressed by an assessment of system performance at a set of locations or through a measure of the situational geometry. One measure is the range-to-baseline ratio, a descriptor that is particularly useful, as its meaning is clear and easy to visualize. A more precise measure of the system performance is the stability ratio. This ratio is defined as half the angle connecting the sensors to the target divided by the standard deviation of the LOB measurement errors. Large values of the stability ratio indicate stable estimates of location, while values less than three indicate instability. The stability ratio is discussed in Thompson and Durfee (1993).

When the angle between the bearing lines from two sensors to the target is small, measurement errors can have a drastic effect on the estimate of the target location. Figure 2 shows the geometry for a simple two-dimensional LOB system. In this Figure, S1 and S2 represent two angle-only sensors separated by a distance of 2 units (i.e., 1 baseline = 2 units). These sensors are viewing a target at a distance of 4 units (or 2 baselines) resulting in a range-to-baseline ratio of 2:1. The true lines of bearing from S1 and S2 intersect at the "True Target Location." On both sides of the bearing lines from S1 and S2 are drawn rays (dashed lines) that bracket hypothetical angular excursions between ±3.0°. The area formed by the intersection of the four angular excursion rays

4
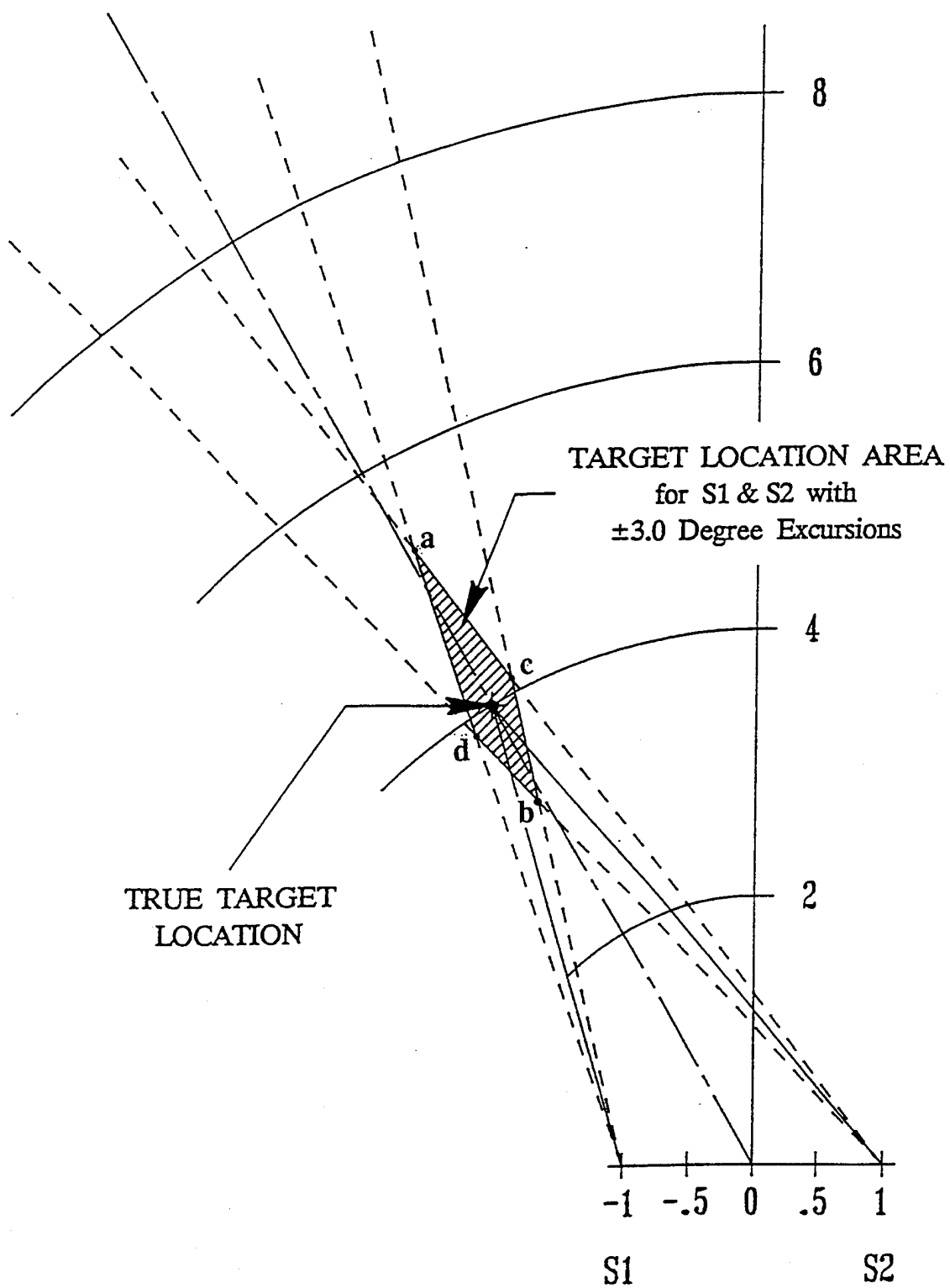
Figure 2. Two Dimensional LOB System Geometry with 2:1 Range-to-Baseline Ratio

5

from S1 and S2 provides an example of the extreme area in which the target might be observed (the hatched area in Figure 2 enclosed by a, b, c, and d). Note that the range axis (b to a) of the hatched area is significantly greater than the cross-range axis (d to c) and that the range axis is greater than 2 units long. A target actually located at 4 units might appear to be anywhere from 3 to more than 5 units away. If the hypothetical ±3.0° angular excursions are actually the one-standard deviation (or 1σ) LOB sensor accuracy (normal distribution with zero mean assumed), then ~47% of the time the target will be observed within the hatched area (in Figure 2) and ~53% of the time the target will be outside the hatched area. Consider also that if the ±3.0° angular excursions are thought of as actual 3σ values (for a ±1.0° LOB sensor accuracy), then ~99% of the time the target will be observed within the hatched area.

Figure 3 shows the result of relocating the sensors from S1 to S3 and from S2 to S4, giving a sensor separation of 1 unit. This results in a range-to-baseline ratio of 4:1 (or a range of 4 baselines). In this Figure, the "Target Location Area" from S1 and S2 (2 unit baseline separation) in Figure 2 is displayed as the darker cross-hatched area, while the "Target Location Area" for S3 and S4 (1 unit baseline separation) is displayed as the hatched area (which includes the cross-hatched area). In Figure 3, note that halving the sensor separation has very little effect on the the cross-range axis. However, the reduced sensor separation has caused a large increase in the length of the range axis. In this case, the extreme spread of the range excursions is now more than 5 units long and the target, at a true range of 4, will have extreme range excursions of 2.5 and 7.7 units away. This indicates that the actual distribution is not symmetric about the mean and is skewed in range. Therefore, targets will more likely appear at ranges further than, rather than closer to, their true range.

Further examples of the effects of LOB system geometry on range and cross-range estimates for various angular excursions are plotted in the next two figures where graphs have been used, rather than drawings, so that larger range-to-baseline ratios can be presented. In Figures 4 and 5, negative extreme range excursion values indicate an observed target location nearer than the true location and positive extreme range excursion values indicate an observed target location further than the true location. Additionally, negative extreme cross-range excursions indicate a target location left of the true location and positive values indicate a target location right of the true location. The effects of changing the range-to-baseline ratio on extreme range and cross-range excursions are plotted in Figure 4 for small angular excursions of 0.05°, 0.10°, and 0.50°. To use Figure 4, a range to target (in baselines) is selected on the x-axis (which corresponds to the "0" value on the abscissa) and the range (Figure 4a) or cross-range (Figure 4b) variation about the selected range is read from the Y-axis. Note that in these figures, "Far Range" corresponds to the farthest point (a) in the hatched area of Figure 2, "Near Range" the nearest point (b) in the hatched area of Figure 2, "Right Cross-Range"

6
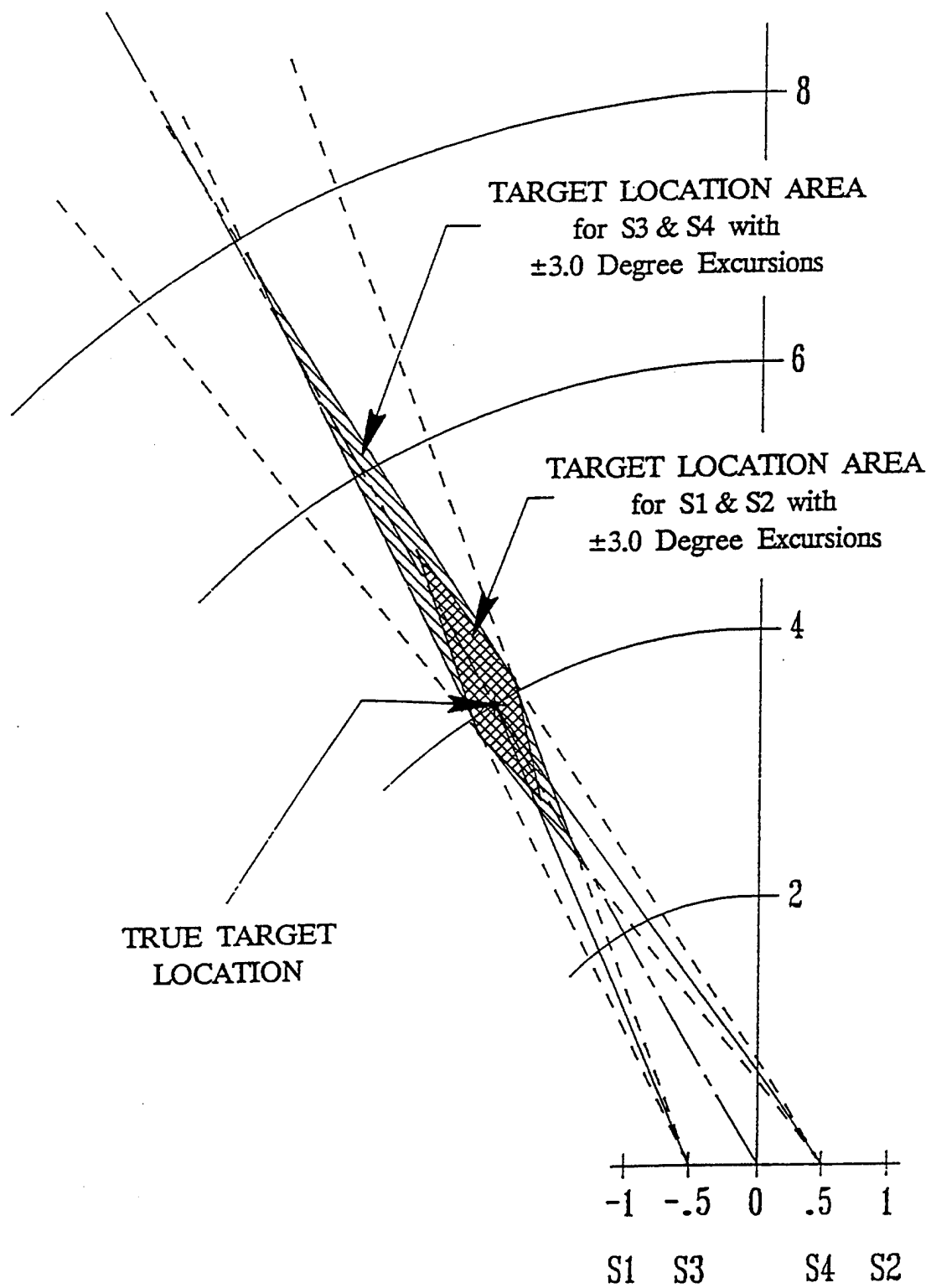
Figure 3. Two Dimensional LOB System Geometry with 4:1 Range-to-Baseline Ratio

(a)
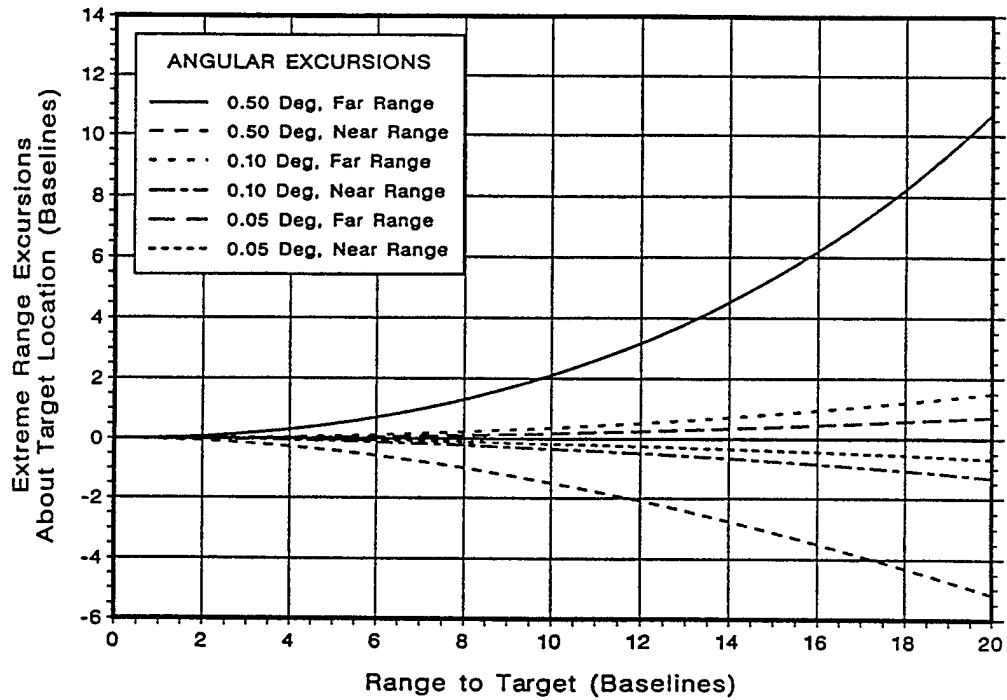
(b)
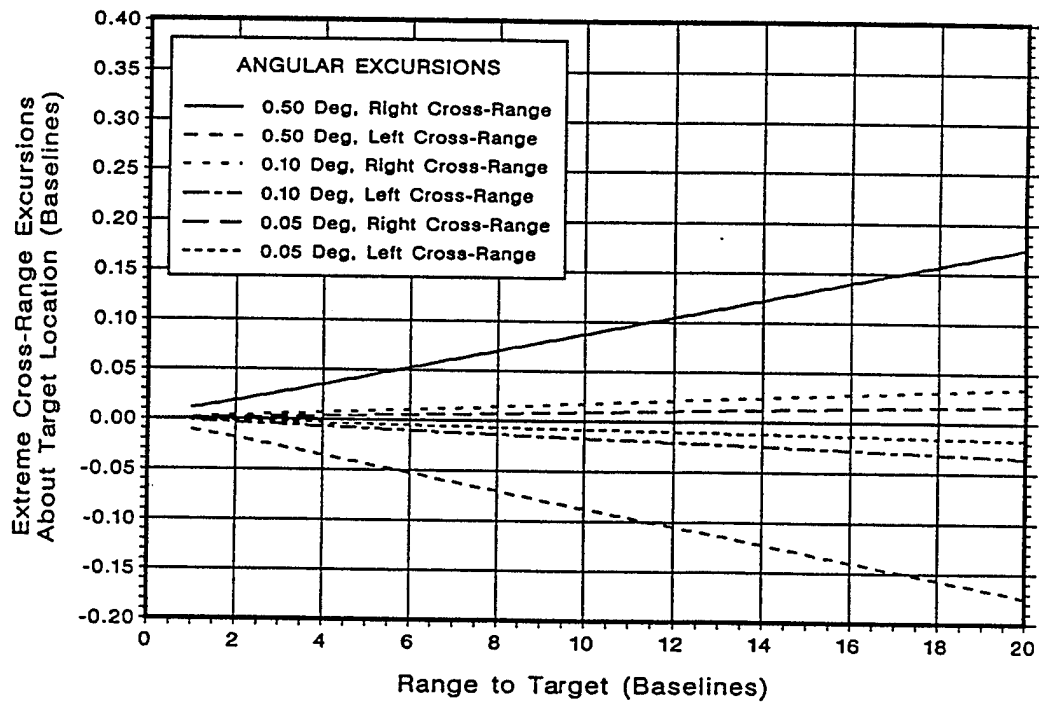
Figure 4. Extreme Geometric Excursions for 0.05 to 0.50 Degree LOB Systems, Target On-Boresight: (a) Range and (b) Cross-Range

(a)
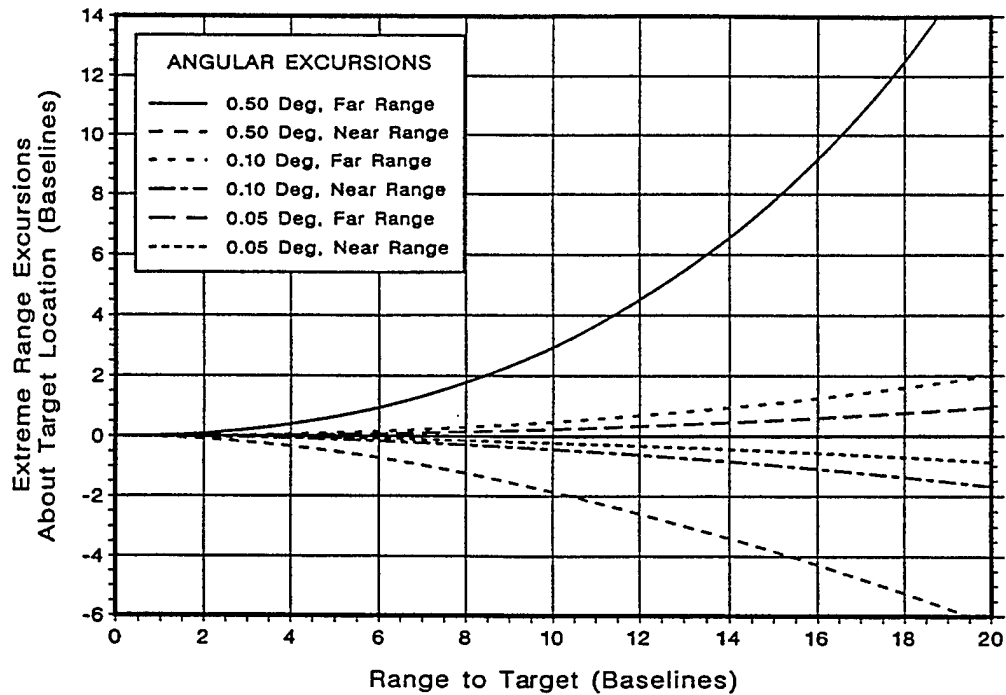
(b)
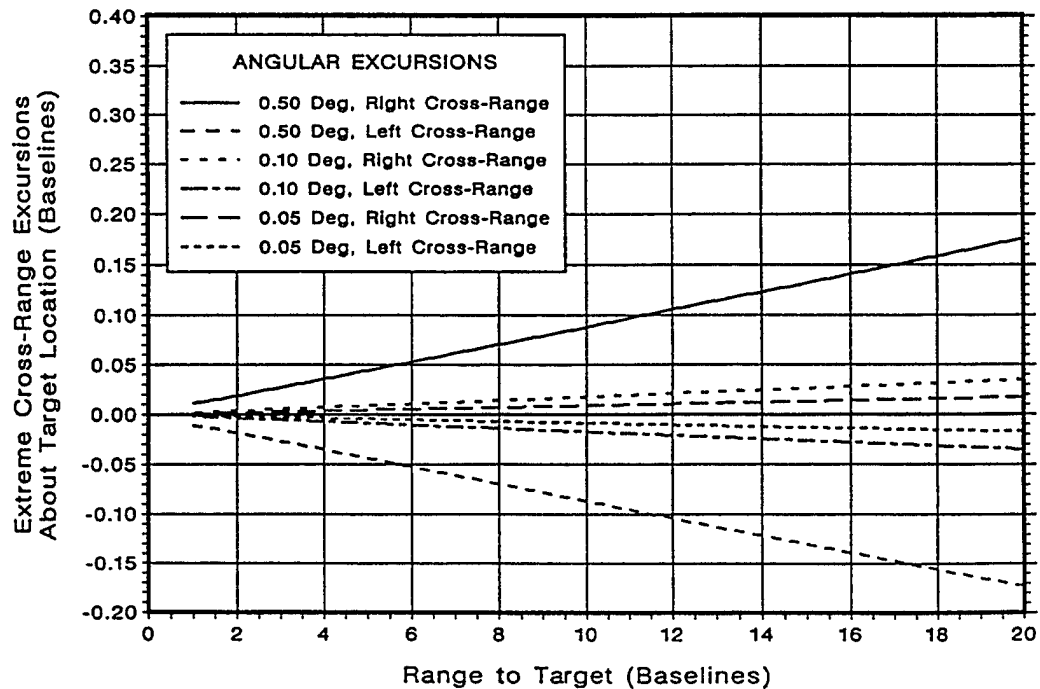
Figure 5.   Extreme Geometric Excursions for 0.05 to 0.50 Degree LOB Systems,
Target 40 Degrees Off-Boresight: (a) Range and (b) Cross-Range

9

the right most point (c) in the hatched area of Figure 2, and "Left Cross-Range" the left most point (d) in the hatched area of Figure 2.

Figure 4 shows an on-boresight zero-degree attack azimuth. In Figure 4a, if a range to target of 16 is selected, then the extreme range variations for angular variations of ±0.50° will be from ~ -3.4 to ~ +6.1 indicating that the target at range 16 (baselines) will appear at ranges anywhere between 12.6 and 22.1 baseline units. In Figure 4b, for a range to target of 16 baselines, the cross-range variation will be between -0.14 (left) to +0.14 (right) of the true target location.

Figure 5a shows an off-boresight 40° attack azimuth. Here, for the true target location of 16 meters mentioned previously, the target will appear anywhere from 4.3 meters closer to 9.2 meters further than its actual location. That is, the target located at 16 (baselines) will appear to be anywhere between 11.7 to 25.2 baselines distant. In Figure 5b, for a range to target of 16 baselines, the cross-range variation will be between -0.14 (left) to +0.14 (right) of the true target location. There is actually a slight shift of the cross-range variation (to the right) for this case, which does not show in the plot. When comparing these results with those from Figure 4, note that the off-boresight condition increases the extreme range excursions for a given range to target.

In some cases, the estimate of target location will be behind the baseline. This can be seen by considering the two lines of bearing to a distant target and visualizing a clockwise rotation of the right LOB line (the right dashed LOB line from S2 in Figure 2) and concurrently, a counterclockwise rotation of the left LOB line (the left dashed LOB line from S1 in Figure 2) such that these two lines no longer cross on the target side of the baseline, but at a point on the opposite side of the baseline. Increasing the angular excursions, decreasing the baseline separation of the sensors, or increasing the range-to-target distance can create conditions that cause the observed target location to appear to be behind the baseline. These effects are plotted in Figures 6 and 7 where the the extreme range and cross-range excursions are plotted as a function of range to target for increased angular excursions of 1°, 2°, and 3°.

In Figure 6a, note that at a range of about 9.5 baselines for an angular excursion of 3° (14.5 baselines for angular excursion of 2°), the extreme range excursions go from a large positive value to a large negative value. This indicates that the two LOB sensors' bearing lines are crossing behind the baseline, rather than in front of the baseline, resulting in a target that appears to be behind the baseline. Figure 6b shows the corresponding extreme cross-range variations.

Figure 7a is the plot for the 40° off-boresight attack azimuth. Here the target appears behind the baseline at about 7.4, and 10.9 baselines for angular excursions of 3° and 2° respectively. Figure 7b shows the corresponding extreme cross-range variations.

10

(a)

(b)
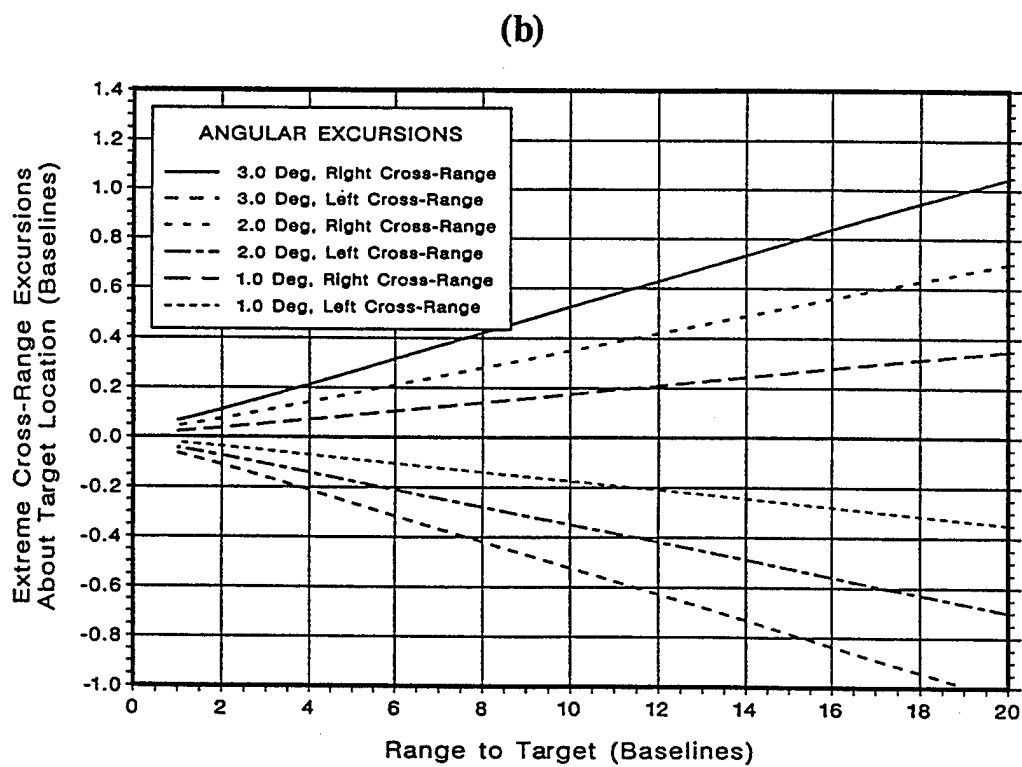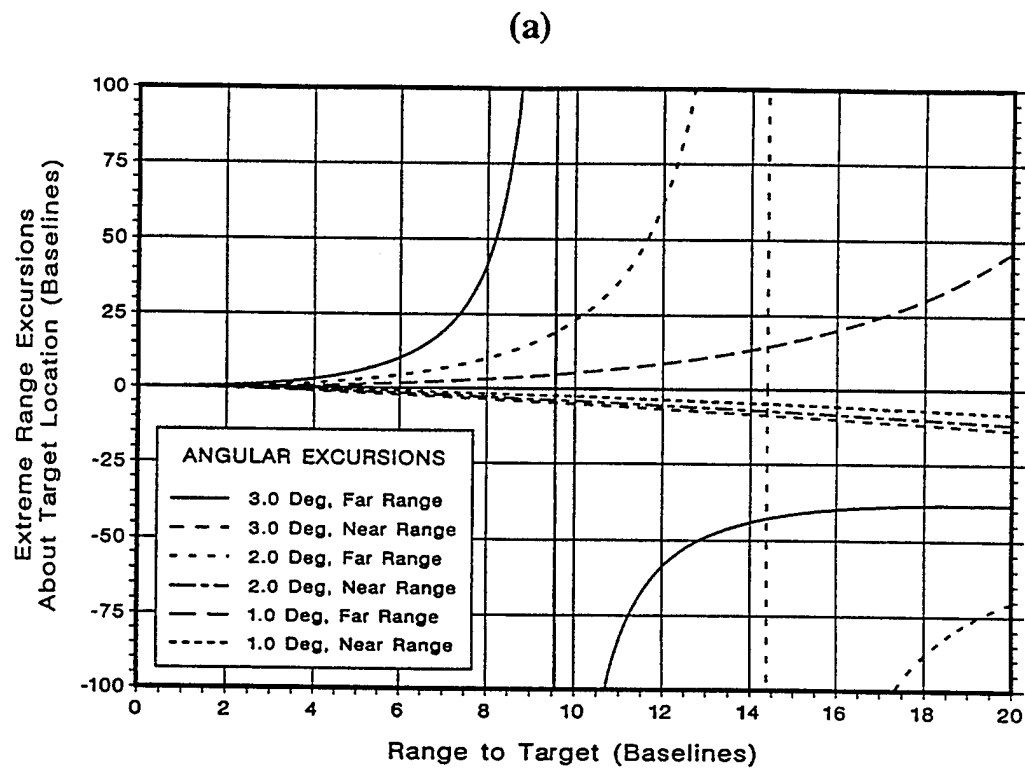
Figure 6.   Extreme Geometric Excursions for 1.0 to 3.0 Degree LOB Systems,
Target On-Boresight: (a) Range and (b) Cross-Range

11

(a)

(b)
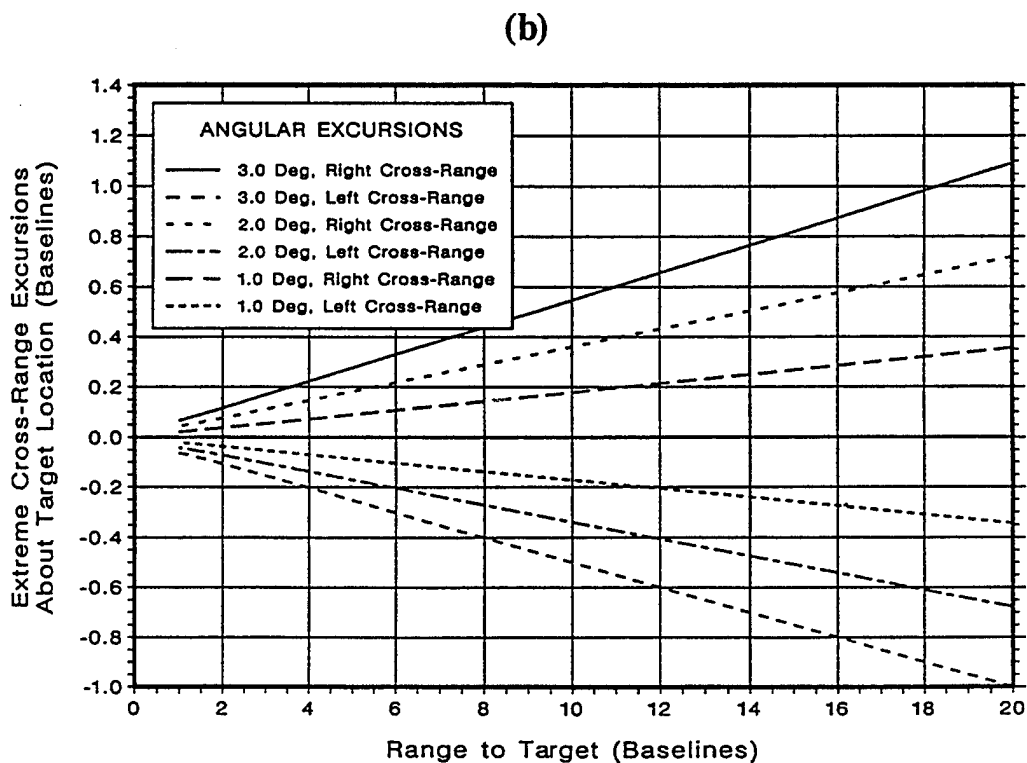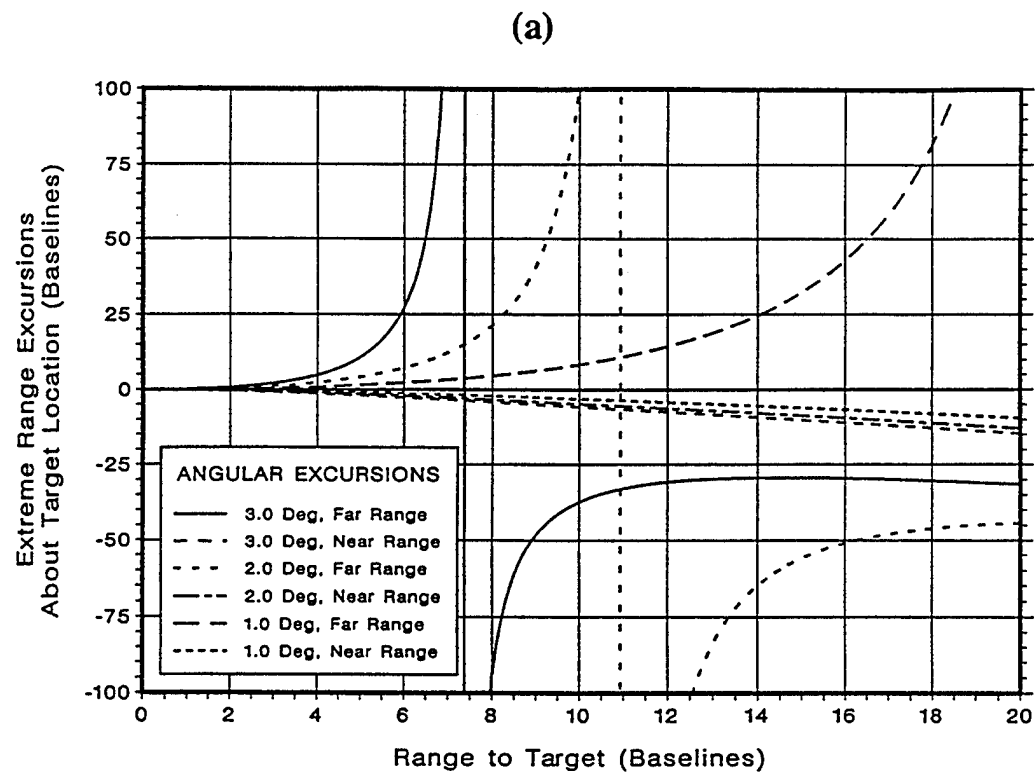
Figure 7. Extreme Geometric Range Excursions for 1.0 to 3.0 Degree LOB Systems, Target 40 Degrees Off-Boresight: (a) Range and (b) Cross-Range

12

Comparing Figure 7a with Figure 6a indicates that off-boresight attacks can cause the target to appear behind the baseline at shorter ranges.

From Figures 2 through 7, it is apparent that the LOB system geometry can result in errors in estimating both range and cross-range. However, the range estimates are most sensitive to geometry changes, such as range-to-baseline ratio and sensor angular variations. It can also be seen that small changes in the measurement errors can lead to implausible range location estimates (i.e., targets that appear behind the sensor baseline). Systems processing LOB information should be designed to consider and, if possible, ignore such cases. Measures for anticipating the occurrence of implausible observations in an LOB system are discussed in Thompson and Durfee (1993).

4. A SCENARIO OF INTEREST

Consider the following scenario as a two-dimensional problem to investigate. An incoming threat projectile (target) is approaching an armored vehicle at some attack azimuth at a constant speed. The threat projectile is first detected at short distances, say 30 meters or less. It is desired that a defeat mechanism intercept and destroy the incoming threat prior to impact, say at 10 meters. The defense tracking system's job is to track the threat from the detection point (~20 meters), continually make predictions as to WHEN and WHERE the threat will cross the 10-meter intercept line and, at some distance greater than the intercept distance (perhaps 11 meters), make a final decision as to WHEN and WHERE intercept will occur. To determine the WHEN and WHERE, one must have an estimate of the projectile's location, attack azimuth, and speed. In this section, it is assumed that only two LOB sensors are used to extract this information.

This scenario is depicted in Figure 8 where, for the sake of visual clarity, a geometry with a range-to-baseline ratio of approximately 2:1 and sensor angular variation of ±3.0° are presented. In Figure 8, S1 and S2 are the sensor locations, C-C is the projectile's trajectory, the "True Projectile Location" and "Intercept Line" are labeled, and the possible location area for the projectile is shown hatched. The problem is then one of determining the location, attack azimuth, and speed of the incoming projectile in order to predict its crossing point (the WHERE) and time of arrival (the WHEN) at the intercept line. Two possible estimates of the the projectile's location are shown as M1 and M2.

To simplify this problem and see the effects of LOB errors in only range estimates, assume that the projectile's speed and attack azimuth are exactly known. This reduces the problem to one of the defensive system's ability to estimate the projectile's range and cross-range location. In Figure 8, if the projectile's estimated location was at M1, then its trajectory will cause it to cross the intercept line at "a." Similarly, if the projectile's estimated location was at M2, then it will cross the intercept line at "b." Since the true intercept is at "x," it can be seen that, with the stated assumptions (known projectile speed

13
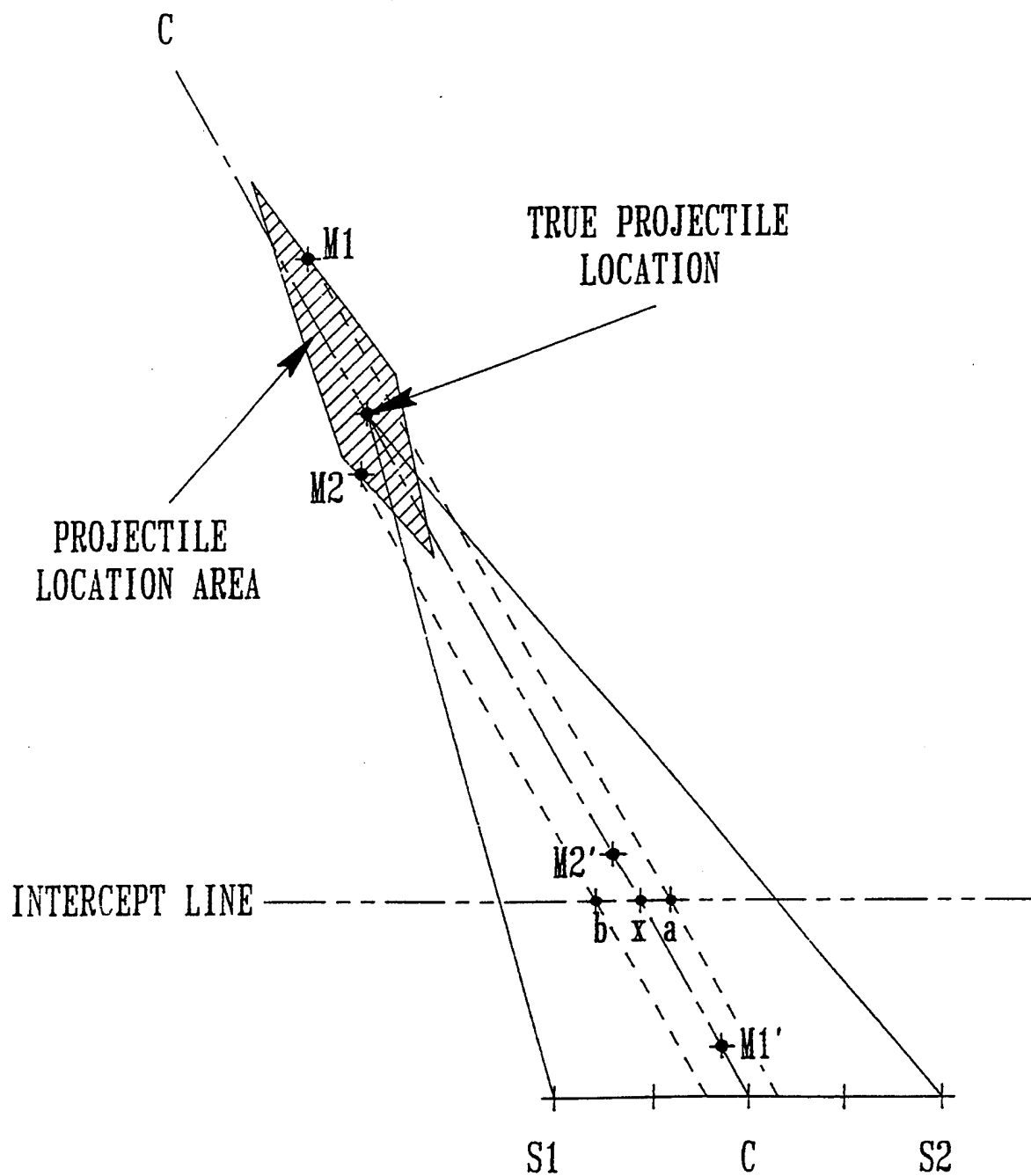
Figure 8. Two Dimensional Range Estimation Errors for LOB System with Known Projectile Speed and Angle-of-Attack

and attack azimuth), the error in WHERE the projectile will cross the intercept line is not large.

But WHEN will the projectile cross the intercept line? The much larger errors in estimating range will cause the true projectile location, apparently sighted at M1, to actually be at M1' (well past the intercept line) when time-of-flight predictions indicate it should be at "a" on the intercept line. Similarly, if the estimate of the true projectile location is at M2, then a time-of-flight prediction will indicate the projectile at "b" when it is actually at M2'(short of the intercept line). Estimates of range that are longer than the true range result in a projectile that has already crossed the intercept line at the time intercept is predicted (i.e., the projectile is closer than predicted and intercept has failed). Referring to the long "tail" (the long hatched area beyond the "true target location") in Figure 3, note that typically more range estimates will be long than will be short.

In this scenario, a defensive system that can exactly predict a projectile's speed and attack azimuth will give a reasonable estimate of WHERE the projectile will cross the intercept line, but will have considerable trouble in predicting WHEN it will cross the intercept line. Since a larger portion of the range estimates will be long, then much of the time the intercept solution will be late (i.e., the projectile will already have passed the intercept line).

Now consider a defensive system that is unable to exactly predict an incoming projectile's speed and attack azimuth but must determine these based on successive estimates of the projectile's location (i.e., at discrete time steps based on the system sampling rate). Such a two-dimensional system is shown in Figure 9 where the "True Projectile Location," the "Projectile Location Area," and the "Intercept Line" are labeled. In addition, M1, M2, and M3 are possible estimates of the projectile's location at some time step and P(t), P(t-1), P(t-2), P(t-3) are the true locations of the projectile at the current time step, the previous time step, two time steps ago, and three time steps ago respectively.

Consider that at the current time step "t" the projectile appears to be at M2 and at the previous time step "t-1" the projectile appeared to be at M1. Simply connecting M1 and M2 (dotted line) to determine the attack azimuth will result in the projectile appearing to intersect the "Intercept Line" at "a," to the left of the actual intercept location at "X." Also consider that if M2 was the current location estimate and M3 was the previous estimate, then the estimated projectile intercept will be much further to the left of the actual intercept "X." Finally, consider that if M3 was the current location estimate and M2 was the previous estimate, then the projectile will appear to be moving away from the intercept line. Less-accurate estimates further apart are better than more-accurate estimates close together.

To reduce the possible large variances in attack azimuth estimates and the possibility of a current location estimate at a range greater than the previous estimate, it is desirable

15
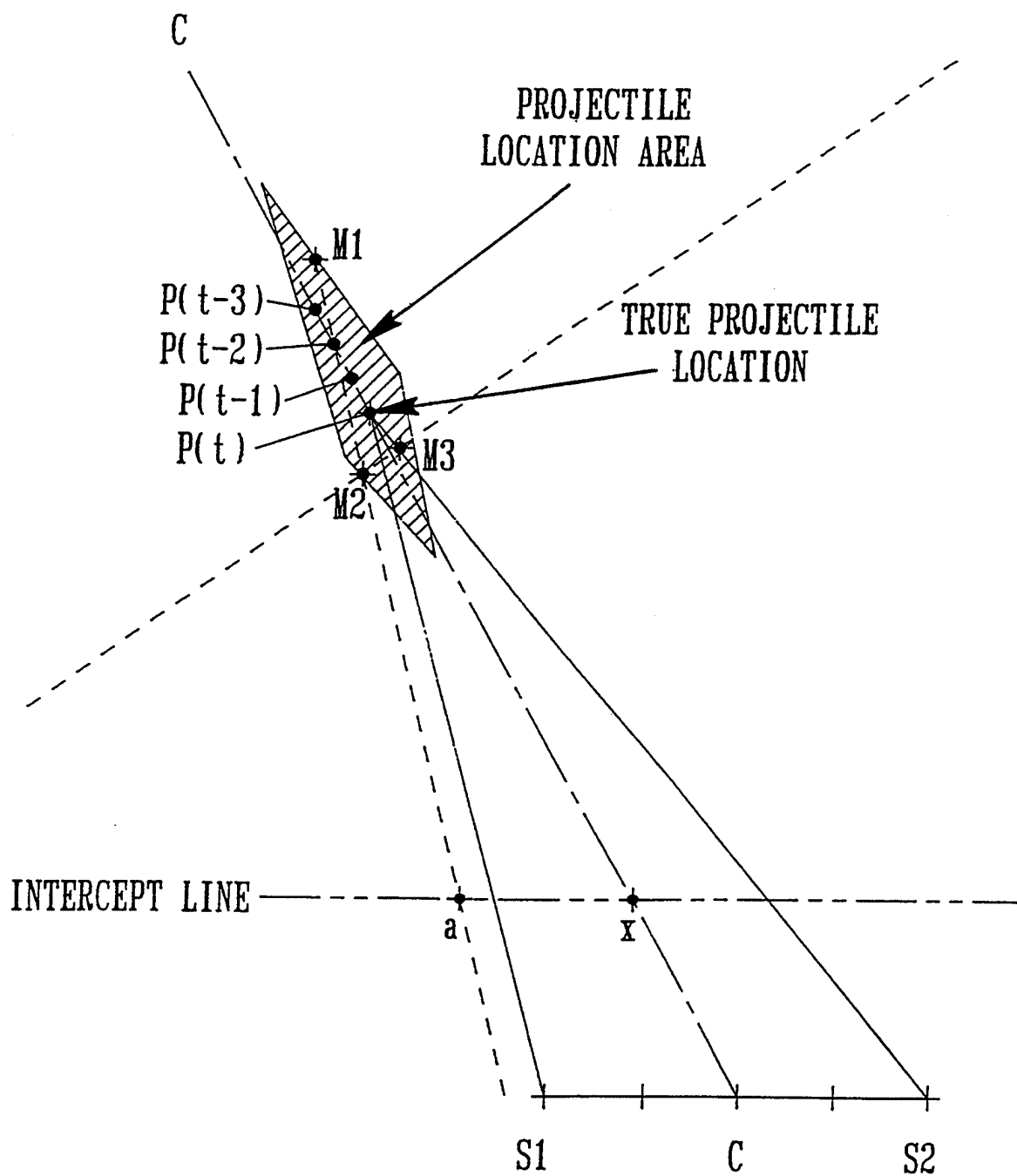
Figure 9. Two Dimensional Range, Speed, and Angle-of-Attack Estimation Errors for LOB System

to sample less frequently so that subsequent samples do not fall within the "Projectile Location Area" of the previous sample (i.e., connecting two estimates that are further apart is better than two that are close together when determining attack azimuth). However, this is not statistically practical. The geometry in Figure 9 is for a range-to-baseline ratio of 2:1 and, as was seen in Figure 3, increasing this ratio greatly increases the variations in range estimates (the length of the "Projectile Location Area" increases) causing overlap into previous "Projectile Location Areas." Therefore, if the sampling rate is decreased in order to reduce or eliminate overlapping "Projectile Location Areas," the result is that there are very few samples from which to make a prediction.

Another problem with the scenario depicted in Figure 9 is the difficulty in predicting the projectile's speed from successive location estimates. Again, if M2 is the current location estimate at time "t" and M1 is the previous estimate at time "t-1," and the sampling time step is known, then the projectile's speed is calculated based on the distance between M1 and M2, divided by the time step. However, as shown in Figure 9, the distance from M1 to M2 (estimated) is greater than the true distance traveled, P(t-1) to P(t). This causes large errors in estimating projectile speed that results in large errors in determining WHEN the projectile will cross the intercept line. High estimates of projectile speed will result in an estimated projectile arrival at the intercept line prior to the actual arrival.

To produce an effective system to determine both WHEN and WHERE a threat projectile crosses an intercept line, consider the choice of methods for making the location estimates and the way individual observations are combined to produce the desired predictions. A connect-the-dots method may result in large prediction errors in both intercept time and location. Some errors may be reduced by providing appropriate checks on individual location observations. For instance, if the observed target location is behind the sensor baseline, or at a range greater than the system's possible detection range, then the observations may be discarded. In addition, observations that resulted in estimated trajectories predicting projectile impacts well beyond either side of the target may also be discarded as outliers.

As shown in the geometry in Figures 8 and 9, simple combining of individual location observations can lead to large errors in trajectory estimation. In the simulation model discussed in the next section of this report, RLS, WLS, and Kalman estimation methods were used to combine target location observations, from various combinations of LOB, range, and velocity sensors, in an attempt to reduce trajectory estimation errors. In addition to types of processing, the effects of range sensors and velocity sensors are evaluated through the simulation.

17

5. LOB2D SYSTEM SIMULATION MODEL

In order to parametrically evaluate the scenario described in section 4, the two-dimensional Monte-Carlo system simulation model, LOB2D, was developed to provide estimates of WHEN and WHERE a projectile will cross a predetermined intercept line as a function of various input parameters. Some of these parameters relate to the projectile (speed, attack azimuth, detection range, aim point), the sensor (baseline location and separation, and the standard deviation for measurements of: angle, speed, and range), the geometry (intercept line location, decision line location), and sampling rate (time step).

In addition, LOB2D also allows for setting various cutoff parameters so that if an observation of the projectile's location is either too close (i.e., behind the sensor baseline) or too far (beyond possible detection range), or results in a predicted impact location too far to the left or right of the target to be a threat, or produces a projectile speed estimate that is unreasonably high, then the observation is discarded. This approach to data feasibility is referred to as gating. Acceptable location observations are combined using RLS, WLS, or Kalman filter estimation techniques (discussed in section 5.4) to predict the projectile's current location, speed, and direction.

5.1 LOB2D System Simulation Model Assumptions.
In the LOB2D simulation model, the following assumptions are made:

1) A two-dimensional model is used (i.e., threat projectile motion is limited to the x-y plane).

2) The origin of the x-y coordinate system used in the simulation is located on the baseline defined by the two angle-only sensors and is assumed to be at the center front edge of the armored vehicle.

3) The speed and direction of flight (angle of attack) of the threat projectile remain constant along its flight path (due to the short distances involved).

4) The threat projectile is always detected at the "detection line" and continually tracked thereafter.

5) The angle-only sensors observe an LOB to only the threat projectile of interest (i.e., there is only one projectile to track).

18

6) The velocity sensor observes the speed of only the threat projectile of interest. (Note that throughout this report a sensor that measures radial speed is referred to as a "velocity" sensor.)

7) The range sensor observes the range to only the threat projectile of interest.

8) All sensors have unrestricted fields of view.

9) The only noise in the simulation is applied to the angle-only, velocity, and range sensor's respective estimates as random Gaussian noise. This noise is uncorrelated.

5.2 LOB2D System Simulation Model Operation. The LOB2D simulation consists of a number of routines for processing flight information, checking sensor observations and estimates, performing tests on location and speed estimates, generating random numbers, bookkeeping, etc. Of primary interest are the routines that provide the "true" information (the "precision" routine) and the estimated sensor information (the "sensor" routines). There are six operational "sensor" routines as follows:

1) LOB with RLS estimation.

2) LOB and range with RLS estimation.

3) LOB with WLS estimation.

4) LOB and velocity with Kalman filter estimation.

5) LOB and range with WLS estimation.

6) LOB and velocity and range with Kalman filter estimation.

The sensor routine is selected by a program input number associated with the desired routine.

In the LOB2D simulation, the projectile is first flown in a "precision" routine from initial start position to baseline impact and all the true positional, angular, range, and intercept time and location information is recorded for each time step in the flight trajectory.

Next, a projectile flight commences (in the selected sensor routine) starting with the same initial conditions and with the "true" angular information provided for use in making the predictive calculations. For each time step in the flight, random noise is added to the true angular (and speed and range as appropriate) information and the projectile location is observed and the estimated intercept location and time-to-intercept are calculated. An estimation routine (described in section 5.4) is used to estimate projectile current location, speed, and attack azimuth. The projectile's observed location, estimated speed, and estimated impact location are tested by the cutoff parameters, and if they are acceptable, the process continues. However, if any are not acceptable, then the data for the current time step are discarded and the flight continues with the next time step.

The simulation continues stepping along the flight path until the projectile reaches a point where its *estimated* location is nearer than a specified distance (see further discussion in the first paragraph of section 6). This ends the flight and the final estimated intercept location and estimated time-to-intercept are recorded.

The estimated intercept location and time-to-intercept values are next compared with the "true" intercept location and time previously calculated (in the "precision" routine) and the differences are recorded.

Another flight is initiated with the same starting parameters but with different random noise applied to provide different angular (speed and range) variations. At the end of 500 such flights, the mean and standard deviations of the intercept location differences and time-to-intercept differences are recorded and output.

Finally, the simulation increments the attack azimuth, angular variation (and speed and range parameters as appropriate), and initiates another set of 500 flights. This continues until all the "loop" parameters have been satisfied.

An additional description of LOB2D can be found in Appendix E of Thompson and Durfee (1992) which includes a discussion of LOB2D inputs and outputs.

5.3   Sensors Investigated.   For these analyses, three types of sensors were modeled. The angle-only (or LOB), radial speed, and range sensors are discussed in the following sections.

5.3.1   Angle-Only (LOB) Sensors.   The LOB sensors are simulated simply as sensors with the ability to provide angular information (with random noise) equally well within a 180° field of view (to the front). The sensors, although located on the baseline (since they define the baseline), need not be symmetrically located about the center of the front edge of the armored vehicle. However, for the purposes of the examples in this report, the two sensors were placed equidistant on either side of the origin.

Random Gaussian noise is applied to the angular information (deviations about the true sensor LOB to projectile) for each time step along the projectile flight path. The 1σ value for the random number generator is specified as an input and applies to both sensors (although a different random variation draw is applied to each).

The intersection of the observed bearing line from both LOB sensors determines the observed projectile location at each time step. The LOB sensor observations may be processed by the RLS, WLS, or Kalman filter techniques.

5.3.2 Velocity Sensor. The velocity sensor has the ability to measure the radial speed (with random noise) of the incoming projectile. For convenience, the examples in this report had the velocity sensor co-located with the left LOB sensor.

Random Gaussian noise is applied to an input velocity sensor error (in meters/second). The program input "velocity error" is used as the 1σ value for the random number generator.

Radial speed observations are not suitable for processing by the RLS or WLS estimation techniques. Both of these techniques present implementation difficulties that can only be overcome by dramatically increasing the complexity of the filter. A Kalman filter implementation was used for velocity observations since the desired information (projectile location, speed, and angle of attack) is directly accessible at all times. This *desired information* is referred to as the *state* of the system. It was assumed that all velocity sensors supplied radial speed information.

The radial speed measured (dd) at the sensor is the product of the speed of the projectile and cosine of the angle, (θ), between the line connecting the sensor and the projectile and the actual path of the projectile. The relationship is described in the following equation where (x,y) is the projectile location and (dx,dy) is the projectile velocity.

$$dd = \cos(\theta) \, (\, dx^2 + dy^2)^{1/2} \, . \tag{1}$$

Using the law of cosines, the following relationship can be found:

$$\cos(\theta) = \frac{x \, dx + y \, dy}{(x^2 + y^2)^{1/2} \, (dx^2 + dy^2)^{1/2}} \, , \tag{2}$$

and so the actual radial speed is

$$dd = \frac{x \, dx + y \, dy}{(x^2 + y^2)^{1/2}} \, . \tag{3}$$

By taking partial derivatives of the expression for dd with respect to x, y, dx, and dy, a method for minimizing the overall error based on the state estimate and radial speed measurement can be achieved. The use of these ideas for the present circumstances is complicated because dx and dy are not directly observed. These values are estimated

21

from successive observations of x and y. This estimation process is sensitive, and easily derailed by heuristically tampering with the state covariance.

A method for using radial speed information that does not influence the estimate of the direction of the trajectory too much is described. First, find the inverse projection of radial speed onto the trajectory. Then estimate the actual speed and adjust the state estimates of the velocity. If possible, adjust the variance of the state so consideration is given to the measurement variance. If the variances of dx and dy are made small, then the location observations will not have much influence on the estimates of dx and dy; this, in fact, led to difficulties in several implementations.

5.3.3 Range Sensor.
The range sensor has the ability to measure the straight line distance (with random noise) from its location to the projectile's. For convenience, the examples in this report had the range sensor located at the origin of the coordinate system (on the baseline and equidistant between the two LOB sensors).

Random Gaussian noise is applied to the range sensor (as a fixed percent of true range to projectile) for each time step along the projectile flight path. The 1σ value for the random number generator is specified as a program input.

Range measurements modify the angle-only estimate of the projectile location by limiting the amount of range variation allowed in the estimate. This is shown geometrically in Figure 10, where $\pm 10\%$ range variation arcs are drawn from the range sensor location to bracket (± 0.4) the true projectile location at 4.0 baselines. Note that the range axis of the hatched area in Figure 10 has been dramatically reduced by the range bracket. Without the range information, the typical range (for the target at 4.0) extends from 2.5 to 7.9 baselines. With $\pm 10\%$ range information, the range axis extends from 3.6 to 4.4 baselines.

Range estimate information is used as follows in LOB2D. For a given range observation R, a range arc is drawn to intersect the LOB estimates from both angle-only sensors at A and B in Figure 11. Then the midpoint of the range arc C, between A and B, is selected as the observed target location, replacing the LOB sensors' location estimate. This method can lead to small increases in the cross-range error results as estimated locations can now appear outside the hatched area in Figure 10 (i.e., in the small triangular shaped areas bordered by the hatched area and the dashed LOB lines). For instance, in Figure 10, the projectile location can be estimated to be on the +10% range arc as far to the right as midway between the right-most LOB line (dashed-line from S1) and the hatched area to its left (i.e., outside the hatched area). In addition, there will always be some location error, even when there may be no LOB errors, whenever there is some range error. The new projectile location estimate may be processed by the RLS,

22
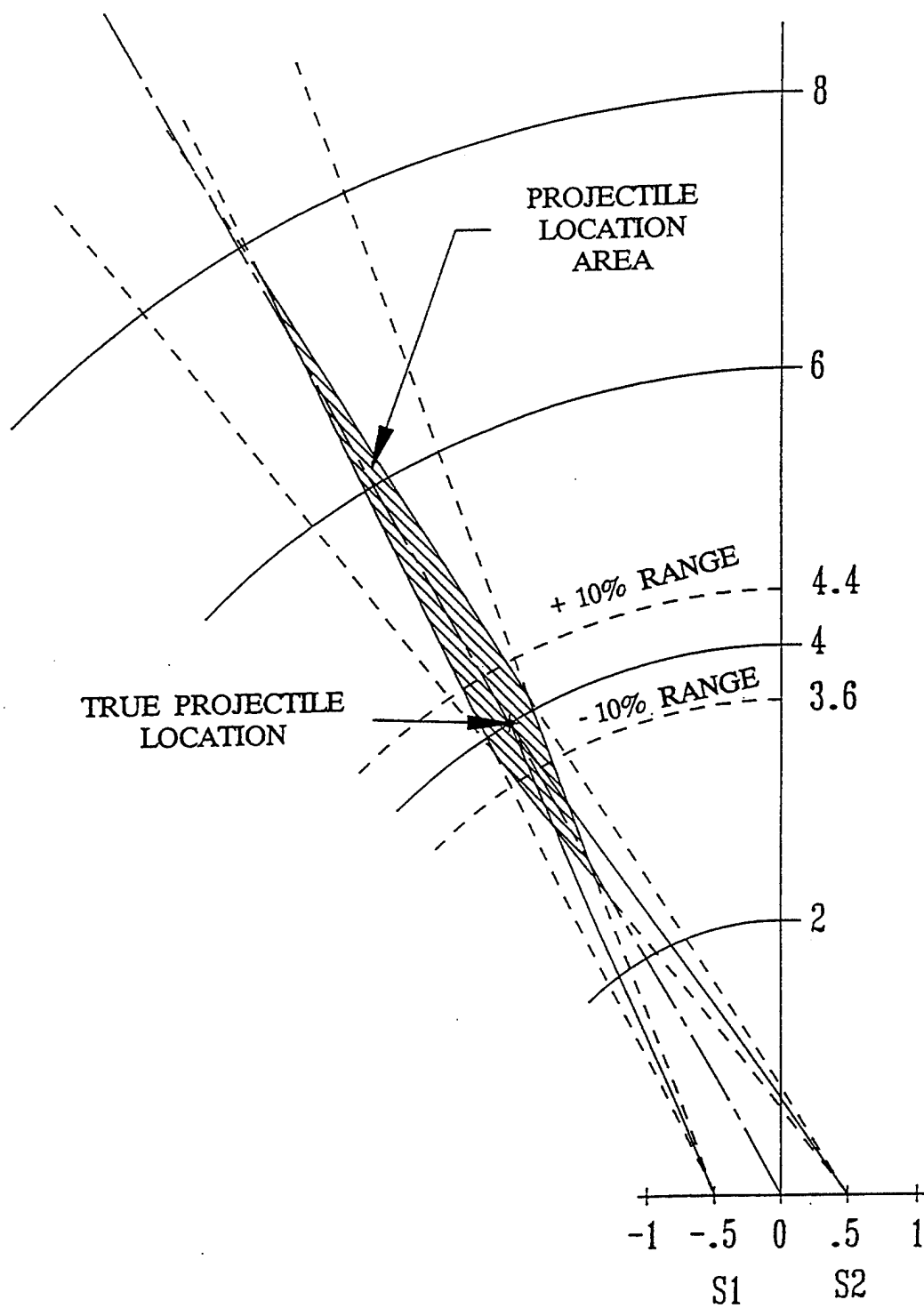
Figure 10. Geometry for Two LOB Sensor System with Range Sensor Trajectory Predicting System

23
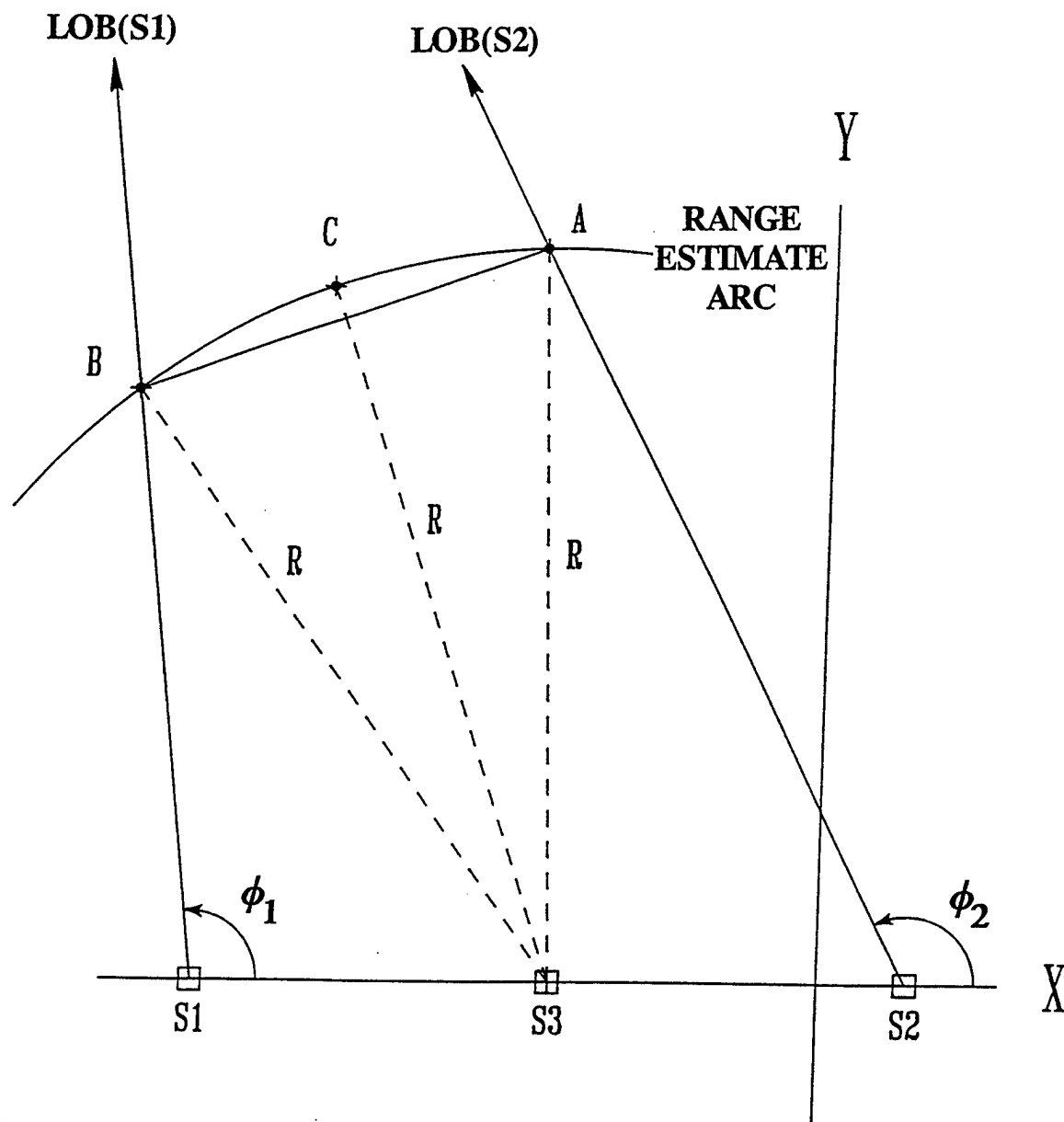
Figure 11. Range Interpolation Method used for Estimating Projectile Location

24

WLS, or Kalman filter estimation techniques. To find the covariance of a range LOB location estimate, the methods discussed in Thompson (1991b) were used.

Note that the range estimation method discussed in the previous paragraph (and Figures 10 and 11) turns out to be suboptimal in the sense that it is not a minimum variance estimate. This suboptimal solution is based on the assumption that the range error is always less than the range error from an LOB estimate. An optimal solution (one with a minimum variance unbiased estimator) can be developed based on the variances of both the range estimate and the range component of the LOB estimate. An optimal solution will discount the range observation when the LOB location estimate is more accurate. The effect of using this suboptimal solution manifests itself in the system simulation results by preventing the prediction error from going to zero as the LOB errors approach zero.

5.4 Estimation Techniques. The techniques used to predict a target trajectory are called estimators. Although there is only one unbiased minimum variance estimator, there may be many suboptimal estimators that perform almost as well and have an extra beneficial characteristic. For example, a technique that is almost as accurate as the optimal may be preferred because it is faster. When the observations have different amounts of confidence associated with them, the gain to associate with an observation is found by considering the covariances of the current estimate and the observation; this is discussed in Thompson (1991a). Models of the measurement error are used to estimate the covariance associated with a given observation. The performance of the estimator depends on these error models, since the influence of an observation and the covariance of the estimator are directly affected.

For most studies, closed form error models are used to model system errors. One such model, LOBCA, for LOB systems proposed by Dr. Charles Alexander, is discussed in Appendix A of Thompson and Durfee (1992). LOBCA develops a covariance model based on a trigonometric argument. Another closed form error model for range LOB systems is outlined in Thompson (1991b). This model is based on a linear algebra approach and is easily extended to predict three-dimensional covariances. One assumption of the closed form models is that nonlinearity is insignificant in the area of interest. This assumption allows higher ordered partial derivatives to be ignored when considering the effects of perturbations or errors on the true situation. When a Kalman filter or WLS estimate is used, the covariances to associate with observations are usually computed from closed form models. Potential problems with LOB covariances are discussed in Thompson and Durfee (1993).

Consider the estimation problem of a system that finds the path of an incoming projectile. One state representation of the projectile is its trajectory in the x and y dimensions. Assume that the sensor system gives estimates of the projectile's location at

each time step. If it is acceptable to assume a projectile travels at a constant velocity over the last portion of its path, the following two equations can be used to independently estimate the coordinates of the projectile at various times in its trajectory.

$$x = \alpha_1 + \alpha_2 t \ . \tag{4}$$

$$y = \beta_1 + \beta_2 t \ . \tag{5}$$

Note that independence means parallel computations are possible. Each of the previous equations can be solved using RLS processing. Improvements in the estimation are made by using recursive WLS estimation where the weights are based on estimates of the error in each dimension. To use all the information of the covariance structure of each location estimate, a Kalman filter using 6x6 matrices can be used; note that the full Kalman filter implementation precludes parallel processing. After evaluating the available techniques, a final decision can be based on concerns of computation speed and acceptable accuracy of the estimator.

The weight associated with a given observation is inversely proportional to its variance. For all cases considered in this study, the variance decreases as a function of range; thus the overall accuracy can be increased by processing closer observations. This effect will be shown in the results (section 8.1.3) when the data acquisition interval is increased by moving the decision point from 11 meters in to 6 meters.

5.4.1 Recursive Least Squares (RLS) Estimation.
Least squares estimators are optimal for identically distributed (i.e., the variances are the same for each observation), independent errors. In the cases where this is a poor assumption, either WLS or a Kalman filter can be used. With recursive processing, an estimate of the trajectory is always available; this is preferable to waiting to acquire all the data and then processing it in a batch operation. Acceptable location estimates are combined using an RLS estimation technique that estimates the projectile's start location, current location, speed, and attack azimuth. The least squares routine uses equal weights for all locations that are not discarded.

Recursive processing updates the estimate based on a pairwise combination of the current value and the new observation. The variance of the estimate is also updated during each estimate upgrade. Typically, the first observation is used to start the recursive process. In other cases, the process can be started by either a combination of the first several observations or by guessing the first value and associating low confidence with the guess. As each new observation becomes available for processing, a gradient is added to the current estimate; this result becomes the current estimate. The gradient consists of two components; first, the difference between the observation and the current estimate,

and second, the relative value of the observation. The value of the observation is based on the covariance of the current estimate and the covariance of the observation.

The notation for recursive estimation comes from control theory, not from statistics. To update the estimate, four pieces of information are needed:

1) The current estimate $X(-)$.

2) The covariance of the current estimate $P(-)$.

3) The current observation Z.

4) The covariance of the current observation R.

In formal discussions, recursive estimators are frequently discussed in terms of the updated estimate $X(+)$ and its covariance $P(+)$. They are calculated as follows:

$$X(+) = X(-) + P(-)(P(-) + R)^{-1}(Z - X(-)) \ . \tag{6}$$

$$P(+) = P(-) - P(-)(P(-) + R)^{-1}P(-) \ . \tag{7}$$

It can also be shown that for the RLS case formula (7) is the same as

$$P(+) = ((P(-))^{-1} + R^{-1})^{-1} \ . \tag{8}$$

If the errors are independent and identically distributed, the following formulation of RLS estimation is preferred:

$$A(+) = A(-) + H_i X_i \ . \tag{9}$$

$$P(+) = ((P(-))^{-1} + H_i H_i')^{-1} \ . \tag{10}$$

$$X(+) = P(+) A(+) \ . \tag{11}$$

In the previous equations, H_i is a vector of the values of the independent variables. $A(+)$ and $A(-)$ are intermediate results that measure the projection of the dependent variable onto the independent variables.

For the remainder of this section, the problem of estimating the trajectory of a projectile will be considered. It will be assumed that the time a fix is acquired is known without error; time is considered an independent variable. A quadratic trajectory can be modeled by including $t_i.ne2^2$ as an independent variable, but this is not pursued in this report. The assumptions made are as follows:

1) The trajectory is best described by a straight line.

2) The problem can be broken into two independent problems: the estimation of the projection of the trajectory onto the X axis, and the estimation of the projection of the trajectory onto the Y axis.

The following two equations are the models that will be used for the X and Y data.

$$X_i = \alpha_0 + \alpha_1 \, t_i \ . \tag{12}$$

$$Y_i = \beta_0 + \beta_1 \, t_i \ . \tag{13}$$

The time of the first observation, t_1, is taken to be 0; and each of the subsequent t_i's is the time duration from the initial observation. Each of the independent variables H_i will be $(\, 1, t_i)'$. The parameter sets, $\{\alpha_0, \alpha_1\}$ and $\{\beta_0, \beta_1\}$, will each have a covariance matrix of P, which can be found through the following relationships, where N is the number of observations.

$$P^{-1} = \sum_{i=1}^{N} H_i H_i' = \begin{bmatrix} N & \sum_{i=1}^{N} t_i \\ \sum_{i=1}^{N} t_i & \sum_{i=1}^{N} t_i^2 \end{bmatrix} . \tag{14}$$

In this two-dimensional problem, finding the inverse is not difficult; however, for higher order equations, the matrix inversion lemma can be used to reduce the computational load. For example, taking the inverse of a matrix is a n^2 operation, so using a 6x6 matrix to model location and speed in three dimensions takes on the order of 36 operations; however, using three 2x2 matrices takes on the order of 12 operations. Equations 9 through 11 give the most straightforward estimation technique for this situation. The assumption is that the observations are independent and identically distributed. The method described previously is sometimes referred to as information matrix processing. The next section modifies the above ideas for cases in which the covariance varies from observation to observation.

5.4.2 Weighted Least Squares (WLS) Estimation.
If the variance of the measurement noise varies from observation to observation, equations 9 through 11 can be generalized to the following:

$$A(+) = A(-) + H_i R^{-1}_i X_i \ . \tag{15}$$

$$P(+) = (\, (P(-)\,)^{-1} + H_i R^{-1}_i H_i')^{-1} \ . \tag{16}$$

$$X(+) = P(+) \, A(+) \ . \tag{17}$$

28

Assuming the observations are uncorrelated and that σ_{yi}^2 is the variance associated with the ith observation of the y location, then the variance of the parameters, (β_0, β_1), after N observations will be

$$P^{-1} = \sum_{i=1}^{N} H_i H_i' = \begin{bmatrix} \sum_{i=1}^{N} \sigma_{yi}^{-2} & \sum_{i=1}^{N} t_i \sigma_{yi}^{-2} \\ \sum_{i=1}^{N} t_i \sigma_{yi}^{-2} & \sum_{i=1}^{N} t_i^2 \sigma_{yi}^{-2} \end{bmatrix} . \tag{18}$$

The variance of the parameters associated with the motion along the X axis can be found by using the X measurement variance in place of those for Y in equation 18. Equations 14 or 18 can be used to define the optimal lower bound on system performance. Various techniques can be compared to these bounds to indicate how much more improvement is possible.

When the observations are correlated, more complex methods must be used if it is necessary for the estimator to consider the effects of the correlation. In this situation, the least squares criterion is not adequate. Methods include instrumental variables and approximate maximum likelihood. Adaptive filters are used when the parameters change over time; sometimes it is possible to include specific knowledge about a system's dynamics within the filter.

5.4.3 Kalman Filter Estimation.
The previous methods estimated the slope and intercepts of the trajectory in the XY plane. If the parameters of interest were the location and velocity, then the dynamics of the parameters must be incorporated into the estimator. Notationally, this is described by the equation

$$X_n(-) = \Phi \, X_{n-1}(+) \, , \tag{19}$$

where X is the vector of parameters and Φ is the state transition matrix. The state transition matrix captures the dynamics from one observation to the next. In the typical state space notation, the covariance of the state is represented by P rather than Σ. The transition of the covariance between time steps can be found through the following equation:

$$P_n(-) = \Phi \, P_{n-1}(+) \, \Phi^t \, . \tag{20}$$

The formula to update the state based on a new observation is

$$\hat{X}_{i+1}(+) = \Phi \hat{X}_i(+) + \Phi P_i(+) \Phi^t \, (\Phi P_i(+) \Phi^t + R_{Z_{i+1}})^{-1} \, (Z_{i+1} - \Phi \hat{X}_i(+)) \tag{21}$$

$$= \hat{X}_{i+1}(-) + P_{i+1}(-) \, (P_{i+1}(-) + R_{Z_{i+1}})^{-1} \, (Z_{i+1} - \hat{X}_{i+1}(-)) \, . \tag{22}$$

The covariance of the state after the observation has been processed is found as

$$P_{i+1}(+) = (\Phi P_i(+) \Phi^t + R_{Z_{i+1}})^{-1} \, . \tag{23}$$

29

Although the Kalman filter is more complex than RLS or WLS, it directly estimates the parameters of interest for a trajectory. In the situation where velocity information is available, the state values can be altered to reflect this new information. It was found that altering the covariance matrix to reflect a greater confidence in the current speed made the estimation process less sensitive to the effects of the location measurements on the slope of the trajectory; thus it is best not to alter the covariance matrix.

6. RESULTS

Consider again the scenario stated in the first paragraph of section 4. There is an incoming projectile approaching an armored vehicle at constant attack azimuth and a constant speed. The threat projectile can only be detected at close ranges. The problem is to track the threat from the detection point, continually make predictions as to WHEN and WHERE the threat will cross a predetermined intercept line, and at some distance prior to the projectile reaching the intercept line (to allow for the function of an appropriate intercept mechanism), make a final decision as to WHEN and WHERE intercept will occur. The geometry of this scenario is shown in Figure 12.

The LOB2D simulation model discussed in section 5 was exercised to provide information on the "along-intercept-line" position mean (bias) and standard deviation (the WHERE) and the "range-to-intercept line" position mean (bias) and standard deviation (the WHEN). In Figure 12, note that "along-intercept-line," which is parallel to the baseline, is equivalent to "cross-range" only when the attack azimuth equals zero. Also, since the model uses a "detection line" rather than a "detection range" arc, the true ranges for off-boresight attacks will be greater than the ranges for on-boresight attacks. Therefore, off-boresight attacks will not only have the apparent sensor baseline separation reduced (due to the attack azimuth angle), but will also have the range-to-projectile increased causing the range-to-baseline ratio to be greater than those of the on-boresight attacks.

Sample results were produced for a projectile approaching at a constant speed of 300 m/s with detection assumed at a range of 20 meters (i.e., Y = 20). The intercept line is located at 10 meters, the decision line is located at 11 meters, and there are two sensors separated by a baseline distance of 2 meters (Figure 12). The angle, speed, and range variations are based on a random draw from a normal distribution with 1σ values provided as program inputs.

For each flight, observations were taken every 0.0005 seconds (0.15 meter) along the projectile's straight line trajectory until its estimated position crossed the 11-meter decision line (Y = 11.0), at which time, the estimated time-to-intercept and intercept location were compared with the actual time-to-intercept and intercept location and the difference recorded. During a flight, any observed projectile location that was at a "Y" distance equal to or less than zero or greater than 40 meters was discarded as were
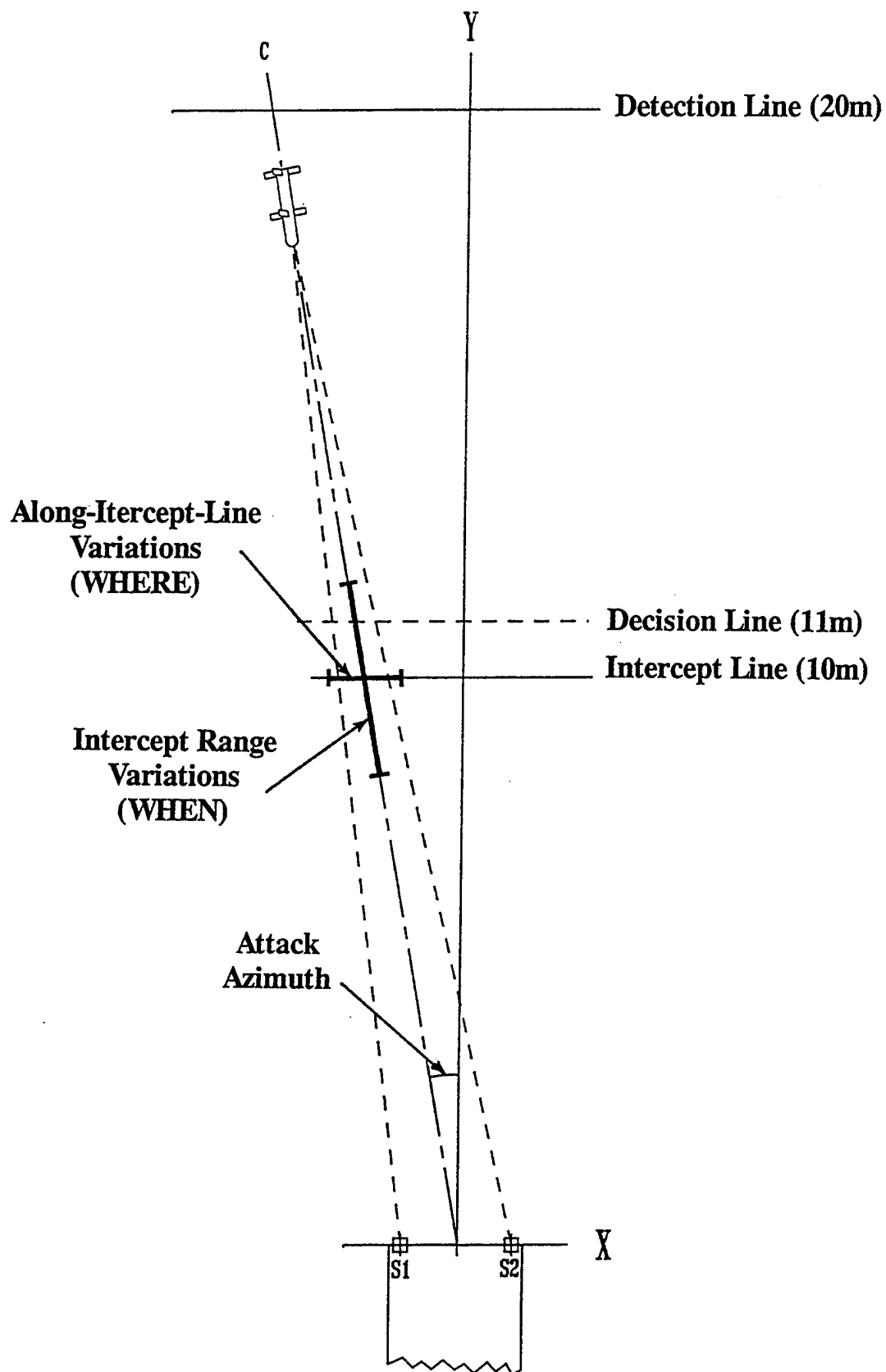
Figure 12. Typical Intercept Geometry for LOB2D Simulation Runs using a Two Meter Baseline (S1 to S2)

31

observations resulting in projectile speed estimates above 1500 m/s. Also, any estimated trajectory intercept location with the sensor baseline that was more than 20 meters to the right of the right sensor or more than 20 meters to the left of the left sensor was discarded. This process was repeated for 500 flights using different random number streams to generate gaussian LOB (and speed and range, as appropriate) errors. After the completion of 500 iterations, the time-to-intercept differences were combined to compute the mean and standard deviations. The intercept location differences were similarly combined. The time-to-intercept means and standard deviations, expressed in seconds, were multiplied by the true projectile speed to convert the results to range distances. Then the specified angular standard deviation was changed by 0.02° and the process (another 500 flights) repeated.

In the following sections, each of the six sensor/estimator combinations listed in section 5.2 are discussed. All the plots for cases 1 though 6 are located in Appendix A.

Note that an abnormality can be seen in several of the plots (i.e., A-5[c], A-6[c], A-11[c], A-12[c], B-6[c], and B-12[c]) as an increase in the projectile's along-intercept-line position bias when the LOB angular variations go from the smallest nonzero case to zero. This jump occurs due to a fix inserted in the model to remove divide-by-zero errors. The divide-by-zero error arises because the filtering methods use the reciprocal of the variance (angular variation) in finding the influence of an observation (X and Y observation error estimates). When the LOB angular variation is zero, the filter tries to give an observation infinite influence (resulting in a divide-by-zero error). To eliminate this problem, the variance was not used to compute X,Y observation errors, rather equal weights of 1.0 were assigned as the X,Y observation errors when the LOB angular variations were zero. This worked well for the LOB only case; however, when noisy range or speed observations are included, instead of being ignored, they are allowed to influence the estimate of the trajectory causing the abnormality. For these special instances, a more appropriate fixed weight for the X,Y observations' errors would have been some small number such as 0.0001, which would then allow the precise LOB observations to exert more influence over the less precise range and/or velocity values.

6.1 Case 1: LOB (Angle-Only Sensors) System, RLS Estimation, 10-Meter Intercept.

For this case, angular variations are based on a random draw from a normal distribution with 1σ values ranging from 0.0° to 3.0° in 0.02° steps. An RLS estimation technique (see section 5.4.1) was used to predict projectile trajectory. Velocity and range sensors were not used. Intercept was at 10 meters.

Figure A-1(a) shows the intercept range bias (mean) in meters as a function of sensor angular variations from 0° to 3° (1σ) for five attack azimuths (0°, 10°, 20°, 30°, and 40°). Note that an attack azimuth of 0° is a head-on (or on-boresight) attack, a 20° attack azimuth comes from the direction 20° left of center, etc. For attack azimuths of 0°

to 20°, the range biases are similar and settle to values between ±1.0 meter for angular variations of ±2.3° or less. For the 30° and 40° attack azimuth, the range biases are much larger and, for 40°, don't settle between ±1.0 meter until the angular variations are less than ±1.5°. A positive range bias indicates an average location estimate that is closer to the intercept line than the true projectile location, and a negative range bias indicates a location estimate that is further from the intercept line than the true projectile location. Overestimated projectile speeds and/or underestimated projectile ranges can cause the range bias to be positive. Underestimates of projectile speeds and/or overestimates of projectile ranges can cause the range bias to be negative. In addition, the discarding of unacceptable locations (discussed in the fourth paragraph of section 6) (i.e., those outside the specified cutoff ranges) may affect the range bias.

Figure A-1(b) is a plot of the intercept range standard deviations (i.e., the computed standard deviation about the means plotted in Figure A-1[a]). In Figure A-1(b), the standard deviations for all attack azimuths exhibit some random variations. The standard deviations for 0°, 10°, 20°, and 30° attack azimuths tend to settle below 1.0 meter for angular variations less that 1.1°, while the standard deviations for the 40° attack azimuth do not settle below 1.0 meter until angular variations are less than 0.7°.

Figures A-1(c) and (d) show the "along-intercept-line" results for 1σ angular errors from 0° to 3.0°. Figure A-1(c) shows the "along-intercept-line" position bias to be less than ±0.1 meter (all attack azimuths) for angular variations less than 3.0°. Figure A-1(d) shows the standard deviations (all attack azimuths) below 0.5 meter for angular variations less than 3.0°. Clearly, "along-intercept-line" biases and standard deviations are significantly smaller than the "range" biases and standard deviations shown in Figures A-1(a) and (b). Note that the Y-axes of Figures A-1(c) and (d) are plotted on different scales than those of Figures A-1(a) and (b).

Figure A-2 is a plot of the same data used in Figure A-1 with different scales for the axes so that the results for angular variations below 1.0° are more readable. In Figure A-2(a), note that the intercept range bias is between ±0.1 meter for all attack azimuths when angular variations are less than 0.6°. In Figure A-2(b), all azimuths have an intercept range standard deviation less than 0.5 meter when angular variations are less than 0.3°.

Figures A-2(c) and (d) show the "along-intercept-line" results for 1σ angular errors from 0° to 1.0°. Figure A-2(c) shows the "along-intercept-line" position bias is less than ±0.01 meter (all attack azimuths) for angular variations less than 1.0°. Figure A-2(d) shows that the corresponding standard deviations are less than 0.08 meter (all attack azimuths) for angular variations below 1.0°. From Figure A-2, it is clear that the "along-intercept-line" biases and standard deviations are significantly smaller than those for "intercept range."

6.2 Case 2: LOB (Angle-Only Sensors) System, WLS Estimation, 10-Meter Intercept. For this case, angular variations are based on a random draw from a normal distribution with 1σ values ranging from 0.0° to 3.0° in 0.02° steps. A WLS estimation technique (see section 5.4.2) was used to predict projectile trajectory. Velocity and range sensors were not used. Intercept was at 10 meters.

Figures A-3(a) and (b) show the intercept range bias and standard deviation as a function of sensor angular variations. Figure A-3(a) shows the intercept range bias (mean) in meters as a function of sensor angular variations. For attack azimuths of 0° to 20°, the range biases are similar and settle to values between ±1.0 meter for angular variations of ±1.5° or less. For the 30° and 40° attack azimuth, the range biases are much larger and, for 40°, do not settle between ±1.0 meter until the angular variations are less than ±1.1°.

Figure A-3(b) is a plot of the intercept range standard deviations (i.e., the computed standard deviation about the means plotted in Figure A-3[a]). In Figure A-3(b), the standard deviations for all attack azimuths exhibit large random variations. The standard deviations for 0°, 10°, 20°, and 30° attack azimuths are below 1.0 meter for angular variations less that 1.0°, while the standard deviations for the 40° attack azimuth do not settle below 1.0 meter until angular variations are less than 0.7°.

Figures A-3(c) and (d) show the "along-intercept-line" position bias and standard deviation as a function of sensor angular variations. Figure A-3(c) shows the "along-intercept-line" position bias to be less than ±0.1 meter (all attack azimuths) for angular variations less than 2.3°. Figure A-3(d) shows the standard deviations (all attack azimuths) below 0.5 meter for angular variations less than 1.2°. Note that the "along-intercept-line" biases and standard deviations are significantly smaller than the "range" biases and standard deviations shown in Figures A-3(a) and (b). However, although they are lower in amplitude, they are still quite noisy for angular variation above 1.0°. Note that Y-axes of Figures A-3(c) and (d) are plotted on different scales than those of Figures A-3(a) and (b).

Figure A-4 is a plot of the same data used in Figure A-3 with different scales for the axes so that the results for angular variation below 1.0° are more readable. In Figure A-4(a), note that the intercept range bias is between ±0.1 meter for all attack azimuths when the angular variations are below 0.2°. In Figure A-4(b), all azimuths have an intercept range standard deviation less than 0.5 meter when the angular variation are less than 0.38°.

Figures A-4(c) and (d) show the "along-intercept-line" results for 1σ errors from 0° to 1.0°. Figure A-4(c) shows the "along-intercept-line" position bias is less than ±0.01 meter (all attack azimuths) for angular variations less than 0.84°. Figure A-4(d) shows that the corresponding standard deviations are less than 0.08 meter (all attack

34

azimuths) for angular variations below 0.76°. From Figure A-4, it is clear that the "along-intercept-line" biases and standard deviations are significantly smaller than those for "intercept range."

6.3   Case 3: LOB System With Velocity Sensor, Kalman Estimation, 10-Meter Intercept.   For this case, angular variations are based on a random draw from a normal distribution with 1σ values ranging from 0.0° to 3.0° in 0.02° steps. Velocity variations were based on a random draw from a normal distribution with 5 meters per second as the 1σ value. A Kalman filter estimation (see section 5.4.3) was used to predict projectile trajectory. Range sensors were not used. Intercept was at 10 meters.

Figures A-5(a) and (b) show the intercept range bias and standard deviation as a function of sensor angular variations. Figure A-5(a) shows the intercept range bias (mean) in meters as a function of sensor angular variations. For attack azimuths of 0° to 20°, the range biases are similar and settle to values between ±1.0 meter for angular variations of about ±2.0° or less. For the 30° and 40° attack azimuth, the range biases are much larger and, for 40°, do not settle between ±1.0 meter until the angular variations are less than ±1.3°.

Figure A-5(b) is a plot of the intercept range standard deviations (i.e., the computed standard deviation about the means plotted in Figure A-5[a]). In Figure A-5(b), the standard deviations for all attack azimuths exhibit some random variations. The standard deviations for 0°, 10°, 20°, and 30° attack azimuths tend to settle down below 1.0 meter for angular variations less that 1.2°, while the standard deviations for the 40° attack azimuth settle below 1.0 meter for angular variations below 0.8°.

Figures A-5(c) and (d) show the "along-intercept-line" position bias and standard deviation as a function of sensor angular variations. Figure A-5(c) shows the "along-intercept-line" position bias to be less than ±0.1 meter (all attack azimuths) for angular variations less than 1.0°. Figure A-5(d) shows the standard deviations (all attack azimuths) below 0.5 meter for angular variations less than 3.0°. It is clear that the "along-intercept-line" biases and standard deviations are significantly smaller than the "range" biases and standard deviations shown in Figures A-5(a) and (b). Note that the Y-axes of Figures A-5(c) and (d) are plotted on different scales than those of Figures A-5(a) and (b).

Figure A-6 is a plot of the same data used in Figure A-5 with different scales for the axes so that the results for angular variation below 1.0° are more readable. In Figure A-6(a), note that the intercept range bias is between ±0.1 meter for all attack azimuths when the angular variations are below 0.36°. In Figure A-6(b), all azimuths have an intercept range standard deviation less than 0.5 meter when the angular variations are less than 0.65°.

35

Figures A-6(c) and (d) show the "along-intercept-line" results for 1σ angular errors from 0° to 1.0°. Figure A-6(c) shows that the "along-intercept-line" position bias is less than ±0.01 meter (all attack azimuths) for angular variations less than 0.5°. Figure A-6(d) shows that the corresponding standard deviations are less than 0.08 meter (all attack azimuths) for angular variations below 0.74°. From Figure A-6, it is clear that the "along-intercept-line" biases and standard deviations are significantly smaller than those for "intercept range."

Note that in Figures A-5(c) and A-6(c) there is an abnormality in the "along-intercept-line" position bias as LOB angular variations decrease from some small value to zero. A possible cause for this abnormality was discussed in the last paragraph of section 6.

6.4 Case 4: LOB System With Range Sensor, RLS Estimation, 10-Meter Intercept.

For this case, angular variations are based on a random draw from a normal distribution with 1σ values ranging from 0.0° to 3.0° in 0.02° steps. Range variations were based on a random draw from a normal distribution with 1σ values input as 5% of true range from range sensor to projectile. Velocity sensors were not used. An RLS estimation technique (see section 5.4.1) was used to predict projectile trajectory. Intercept was at 10 meters.

Figures A-7(a) and (b) show the intercept range bias and standard deviation as a function of sensor angular variations. Figure A-7(a) shows the intercept range bias (mean) in meters as a function of sensor angular variations. For attack azimuths of 0° to 40°, the range biases are all less than ±0.1 meter for angular variations out to ±3.0°.

Figure A-7(b) is a plot of the intercept range standard deviations (i.e., the computed standard deviation about the means plotted in Figure A-7[a]). In Figure A-7(b), the standard deviations for all attack azimuths remain below 0.3 meter at angular variations out to 3.0°. When the angular variation is reduced to 0.0°, the range standard deviations approach 0.2 meter, and not zero. This is caused by the range variations that were fixed, for these evaluations, at 5% of true range. So, although the angular variations went to zero, there were still variations in the range observations weighting the estimation routine. This was discussed in the last paragraph of section 5.3.3.

Figures A-7(c) and (d) show the "along-intercept-line" position bias and standard deviation as a function of sensor angular variations. Figure A-7(c) shows the "along-intercept-line" position bias to be less than ±0.05 meter (all attack azimuths) for angular variations less than 3.0°. Figure A-7(d) shows the standard deviations (all attack azimuths) below 0.3 meter for angular variations less than 3.0°. Note that the "along-intercept-line" biases are smaller than the "range" biases shown in Figure A-7(a). However, at angular variations around 3.0°, the "along-intercept-line" position standard deviations are similar to those in Figure A-7(b), but decrease to zero as the angular

variation approaches zero. Note that the Y-axes of Figures A-7(c) and (d) are plotted on different scales than those of Figures A-7(a) and (b).

Figure A-8 is a plot of the same data used in Figure A-7 with different scales for the axes so that the results for angular variation below 1.0° are more readable. In Figure A-8(a), note that the intercept range bias is between ±0.03 meter for all attack azimuths for all angular variations. In Figure A-8(b), all azimuths have an intercept range standard deviation less than 0.25 meter for all angular variations.

Figures A-8(c) and (d) show the "along-intercept-line" results for 1σ angular errors from 0° to 1.0°. Figure A-2(c) shows the "along-intercept-line" position bias is less than ±0.01 meter (all attack azimuths) for angular variations less than 1.0°. Figure A-2(d) shows that the corresponding standard deviations are less than 0.08 meter (all attack azimuths) for angular variations below 1.0°. From Figure A-8, it is clear that the "along-intercept-line" biases and standard deviations are significantly smaller than those for "intercept range."

6.5 Case 5: LOB System With Range Sensor, WLS Estimation, 10-Meter Intercept.

For this case, angular variations are based on a random draw from a normal distribution with 1σ values ranging from 0.0° to 3.0° in 0.02° steps. Range variations were based on a random draw from a normal distribution with 1σ values input as 5% of true range from range sensor to projectile. Velocity sensors were not used. A WLS estimation technique (see section 5.4.2) was used to predict projectile trajectory. Intercept was at 10 meters.

Figures A-9(a) and (b) show the intercept range bias and standard deviation as a function of sensor angular variations. Figure A-9(a) shows the intercept range bias (mean) in meters. For attack azimuths of 0° to 40°, the range biases are all less than ±0.1 meter for angular variations out to ±3.0°.

Figure A-9(b) is a plot of the intercept range standard deviations (i.e., the computed standard deviation about the means plotted in Figure A-9[a]). In Figure A-9(b), the standard deviations for all attack azimuths remain below 0.3 meter at angular variations out to 3.0°. When the angular variation is reduced to 0.0°, the range standard deviations approach 0.2 meter, and not zero. This is caused by the range variations that were fixed, for these evaluations, at 5% of true range. So, although the angular variations went to zero, there were still variations in the range observations weighting the estimation routine. This was discussed in the last paragraph of section 5.3.3.

Figures A-9(c) and (d) show the "along-intercept-line" position bias and standard deviation as a function of sensor angular variations. Figure A-9(c) shows the "along-intercept-line" position bias to be less than ±0.05 meter (all attack azimuths) for angular variations less than 3.0°. Figure A-9(d) shows the standard deviations (all attack azimuths) below 0.3 meter for angular variations less than 3.0°. Note that the "along-

intercept-line" biases are smaller than the "range" biases shown in Figure A-9(a). However, at angular variations around 3.0°, the "along-intercept-line" position standard deviations are close to those in Figure A-9(b) but decrease to zero as the angular variation approaches zero. Note that the Y-axes of Figures A-9(c) and (d) are plotted on different scales than those of Figures A-9(a) and (b).

Figure A-10 is a plot of the same data used in Figure A-9 with different scales for the axes so that the results for angular variation below 1.0° are more readable. In Figure A-10(a), note that the intercept range bias is between ±0.04 meter for all attack azimuths for all angular variations. In Figure A-10(b) all azimuths have an intercept range standard deviation less than 0.24 meter for all angular variations.

Figures A-10(c) and (d) show the "along-intercept-line" results for 1σ angular errors from 0° to 1.0°. Figure A-10(c) shows the "along-intercept-line" position bias is less than ±0.01 meter (all attack azimuths) for angular variations less than 1.0°. Figure A-10(d) shows that the corresponding standard deviations are less than 0.08 meter (all attack azimuths) for angular variations below 1.0°. From Figure A-10, it is clear that the "along-intercept-line" biases and standard deviations are significantly smaller than those for "intercept range."

6.6 Case 6: LOB System With Velocity and Range Sensors, Kalman Estimation, 10-Meter Intercept.

For this case, angular variations are based on a random draw from a normal distribution with 1σ values ranging from 0.0° to 3.0° in 0.02° steps. Velocity variations were based on a random draw from a normal distribution with 5 meters per second as the 1σ value. Range variations were based on a random draw from a normal distribution with 1σ values input as 5% of true range from range sensor to projectile. A Kalman filter estimation (see section 5.4.3) was used to predict projectile trajectory. Intercept was at 10 meters.

Figures A-11(a) and (b) show the intercept range bias and standard deviation as a function of sensor angular variations. Figure A-11(a) shows the intercept range bias (mean) in meters as a function of sensor angular variations. For attack azimuths of 0° to 40°, the range biases are all less than ±0.1 meter for angular variations out to ±3.0°.

Figure A-11(b) is a plot of the intercept range standard deviations (i.e., the computed standard deviation about the means plotted in Figure A-11[a]). In Figure A-11(b), the standard deviations for all attack azimuths remain below 0.2 meter at angular variations out to 3.0°. When the angular variation is reduced to 0.0°, the range standard deviations approach 0.15 meter, and not zero. This is caused by the range variations that were fixed, for these evaluations, at 5% of true range. So, although the angular variations went to zero, there were still variations in the range observations weighting the estimation routine. This was discussed in the last paragraph of section 5.3.3.

38

Figures A-11(c) and (d) show the "along-intercept-line" position bias and standard deviation as a function of sensor angular variations. Figure A-11(c) shows the "along-intercept-line" position bias to be less than ±0.05 meter (all attack azimuths) for angular variations less than 3.0°. Figure A-11(d) shows the standard deviations (all attack azimuths) below 0.3 meter for angular variations less than 3.0°. However, at angular variations around 3.0°, the "along-intercept-line" position standard deviations are similar to those in Figure A-11(b), but decrease to zero as the angular variation approaches zero. Note that the Y-axes of Figures A-11(c) and (d) are plotted on different scales than those of Figures A-11(a) and (b).

Figure A-12 is a plot of the same data used in Figure A-11 with different scales for the axes so that the results for angular variation below 1.0° are more readable. In Figure A-12(a), note that the intercept range bias is between ±0.03 meter for all attack azimuths for all angular variations. In Figure A-12(b), all azimuths have an intercept range standard deviation less than 0.18 meter for all angular variations.

Figures A-12(c) and (d) show the "along-intercept-line" results for 1σ angular errors from 0° to 1.0°. Figure A-12(c) shows the "along-intercept-line" position bias is less than ±0.02 meter (all attack azimuths) for angular variations less than 1.0°. Figure A-12(d) shows that the corresponding standard deviations are less than 0.08 meter (all attack azimuths) for angular variations below 1.0°. From Figure A-12, it is clear that the "along-intercept-line" biases and standard deviations are smaller than those for "intercept range."

Note that in Figures A-11(c) and A-12(c) there is an abnormality in the "along-intercept-line" position bias as LOB angular variations decrease from some small value to zero. A possible cause for this abnormality was discussed in the last paragraph of section 6.

7. ADDITIONAL RESULTS, CASES 1 THROUGH 6 REVISITED, 5-METER INTERCEPT

To provide some additional insight on the applicability of the various estimation routines for scenarios with differing geometries, Cases 1 through 6 (sections 6.1 through 6.6) were rerun under the same conditions described in section 6, except that the decision line was moved from 11 to 6 meters and the intercept line was moved from 10 to 5 meters (see Figure 12). This has the effect of providing approximately 55% more observations from which to make an intercept decision. Also, since the added observations (those from 11 to 6 meters) were closer to the sensors, they are more accurate and thus exert greater influence on the estimate.

The results of reducing the intercept range from 10 to 5 meters for Cases 1 through 6 are plotted in Figures B-1 through B-12. These runs were made with random number streams identical to those used in Cases 1 through 6.

As with the results for Cases 1 through 6, a positive range bias indicates an average location estimate that is closer to the intercept line than the true projectile location and a negative range bias indicates a location estimate that is further from the intercept line than the true projectile location. Overestimated projectile speeds and/or underestimated projectile ranges can cause the range bias to be positive. Underestimates of projectile speeds and/or overestimates of projectile ranges can cause the range bias to be negative. In addition, the discarding of unacceptable locations (discussed in the fourth paragraph of section 6) (i.e., those outside the input cutoff ranges) affect the range bias.

All plots for Cases 1a though 6a are located in Appendix B.

7.1 Case 1a: LOB (Angle-Only Sensors) System, RLS Estimation, 5-Meter Intercept.

For this case, angular variations are based on a random draw from a normal distribution with 1σ values ranging from 0.0° to 3.0° in 0.02° steps. An RLS estimation technique (see section 5.4.1) was used to predict projectile trajectory. Velocity and range sensors were not used. Intercept was at 5 meters.

Figure B-1(a) shows the intercept range bias (mean) in meters as a function of sensor angular variations from 0° to 3° (1σ) for five attack azimuths (0°, 10°, 20°, 30°, and 40°). For attack azimuths of 0° to 40°, the range biases are smaller than ±1.0 meter for angular variations of 3.0° or less. As before, positive range bias indicates an average location estimate that is closer to the intercept line than the true projectile location and a negative range bias indicates a location estimate that is further from the intercept line than the true projectile location. Overestimated projectile speeds and/or underestimated projectile ranges can cause the range bias to be positive. Underestimates of projectile speeds and/or overestimates of projectile ranges can cause the range bias to be negative. In addition, the discarding of unacceptable locations (discussed in the fourth paragraph of section 6) (i.e., those outside the specified cutoff ranges) may affect the range bias.

Figure B-1(b) is a plot of the intercept range standard deviations (i.e., the computed standard deviation about the means plotted in Figure B-1[a]). In Figure B-1(b), the standard deviations for all attack azimuths exhibit some random variations. The standard deviations for 0°, 10°, 20°, and 30° attack azimuths tend to settle below 1.0 meter for angular variations less that 3.0°, while the standard deviations for the 40° attack azimuth do not settle below 1.0 meter until angular variations are less than 2.5°.

Figures B-1(c) and (d) show the "along-intercept-line" results for 1σ angular errors from 0° to 3.0°. Figure B-1(c) shows the "along-intercept-line" position bias to be less than ±0.05 meter (all attack azimuths) for angular variations less than 3.0°. Figure B-1(d) shows the standard deviations (all attack azimuths) below 0.18 meter for angular variations less than 3.0°. Note that the Y-axes of Figures B-1(c) and (d) are plotted on different scales than those of Figures B-1(a) and (b).

Figure B-2 is a plot of the same data used in Figure B-1 with different scales for the axes so that the results for angular variation below 1.0° are more readable. In Figure B-2(a), note that the intercept range bias is between ±0.1 meter for all attack azimuths when angular variations less than 0.36°. In Figure B-2(b), all azimuths have an intercept range standard deviation less than 0.5 meter when angular variation are less than 0.50°.

Figures B-2(c) and (d) show the "along-intercept-line" results for 1σ angular errors from 0° to 1.0°. Figure B-2(c) shows the "along-intercept-line" position bias is less than ±0.01 meter (all attack azimuths) for angular variations less than 1.0°. Figure B-2(d) shows that the corresponding standard deviations are less than 0.05 meter (all attack azimuths) for angular variations below 1.0°.

7.2. Case 2a: LOB (Angle-Only Sensors) System, WLS Estimation, 5-Meter Intercept.

For this case, angular variations are based on a random draw from a normal distribution with 1σ values ranging from 0.0° to 3.0° in 0.02° steps. A WLS estimation technique (see section 5.4.3) was used to predict projectile trajectory. Velocity and range sensors were not used. Intercept was at 5 meters.

Figures B-3(a) and (b) show the intercept range bias and standard deviation as a function of sensor angular variations. Figure B-3(a) shows the intercept range bias (mean) in meters as a function of sensor angular variations. For attack azimuths of 0° to 20°, the range biases are similar and settle to values between ±1.0 meter for angular variations of ±1.7° or less. For the 30° and 40° attack azimuth, the range biases are larger and, for 40°, do not settle between ±1.0 meter until the angular variations are less than ±1.2°.

Figure B-3(b) is a plot of the intercept range standard deviations (i.e., the computed standard deviation about the means plotted in Figure B-3[a]). In Figure B-3(b), the standard deviations for all attack azimuths exhibit large random variations when angular variations are above 1.5°. The deviations for all attack azimuths are below 1.0 meter for angular variations less that 1.0°.

Figures B-3(c) and (d) show the "along-intercept-line" position bias and standard deviation as a function of sensor angular variations. Figure B-3(c) shows the "along-intercept-line" position bias to be less than ±0.1 meter (all attack azimuths) for angular variations less than 1.3°. Figure B-3(d) shows the standard deviations (all attack azimuths) below 0.5 meter for angular variations less than 1.0°. Note that the "along-intercept-line" biases and standard deviations are smaller than the "range" biases and standard deviations shown in Figures B-3(a) and (b). However, although they are lower in amplitude, they are still quite noisy for angular variation above 1.0°.

Figure B-4 is a plot of the same data used in Figure B-3 with different scales for the axes so that the results for angular variation below 1.0° are more readable. In

41

Figure B-4(a), note that the intercept range bias is between ±0.1 meter for all attack azimuths when the angular variations are below 0.7°. In Figure B-4(b), all azimuths have an intercept range standard deviation less than 0.5 meter when the angular variation are less than 0.98°.

Figures B-4(c) and (d) show the "along-intercept-line" results for 1σ angular errors from 0° to 1.0°. Figure B-4(c) shows the "along-intercept-line" position bias is less than ±0.01 meter (all attack azimuths) for angular variations less than 1.0°. Figure B-4(d) shows that the corresponding standard deviations are less than 0.05 meter (all attack azimuths) for angular variations below 1.0°.

7.3. Case 3a: LOB System With Velocity Sensor, Kalman Estimation, 5-Meter Intercept.
For this case, angular variations are based on a random draw from a normal distribution with 1σ values ranging from 0.0° to 3.0° in 0.02° steps. Velocity variations were based on a random draw from a normal distribution with 5 meters per second as the 1σ value. A Kalman filter estimation (see section 5.4.3) was used to predict projectile trajectory. Range sensors were not used. Intercept was at 5 meters.

Figures B-5(a) and (b) show the intercept range bias and standard deviation as a function of sensor angular variations. Figure B-5(a) shows the intercept range bias (mean) in meters as a function of sensor angular variations. For attack azimuths of 0° to 40°, the range biases are between ±0.6 meter for angular variations of ±3.0° or less.

Figure B-5(b) is a plot of the intercept range standard deviations (i.e., the computed standard deviation about the means plotted in Figure B-5[a]). The standard deviations for 0°, 10°, 20°, and 30° attack azimuths tend to settle down below 1.0 meter for angular variations less that 2.8°, while the standard deviations for the 40° attack azimuth settle below 1.0 meter for angular variations below 2.2°.

Figures B-5(c) and (d) show the "along-intercept-line" position bias and standard deviation as a function of sensor angular variations. Figure B-5(c) shows the "along-intercept-line" position bias to be less than ±0.1 meter (all attack azimuths) for angular variations less than 1.7°. Figure B-5(d) shows the standard deviations (all attack azimuths) below 0.3 meter for angular variations less than 3.0°. Note that the Y-axes of Figures B-5(c) and (d) are plotted on different scales than those of Figures B-5(a) and (b).

Figure B-6 is a plot of the same data used in Figure B-5 with different scales for the axes so that the results for angular variation below 1.0° are more readable. In Figure B-6(a), note that the intercept range bias is between ±0.1 meter for all attack azimuths when the angular variations are below 0.7°. In Figure B-6(b), all azimuths have an intercept range standard deviation less than 0.26 meter when the angular variations are less than 1.0°.

Figures B-6(c) and (d) show the "along-intercept-line" results for 1σ angular errors from 0° to 1.0°. Figure B-6(c) shows the "along-intercept-line" position bias is less than

±0.01 meter (all attack azimuths) for angular variations less than 0.7°. Figure B-6(d) shows that the corresponding standard deviations are less than 0.05 meter (all attack azimuths) for angular variations below 1.0°.

Note that in Figure B-6(c) there is an abnormality in the "along-intercept-line" position bias as LOB angular variations decrease from some small value to zero. A possible cause for this abnormality was discussed in the last paragraph of section 6.

7.4   Case 4a: LOB System With Range Sensor, RLS Estimation, 5-Meter Intercept.

For this case, angular variations are based on a random draw from a normal distribution with 1σ values ranging from 0.0° to 3.0° in 0.02° steps. Range variations were based on a random draw from a normal distribution with 1σ values input as 5% of true range from range sensor to projectile. Velocity sensors were not used. An RLS estimation technique (see section 5.4.1) was used to predict projectile trajectory. Intercept was at 5 meters.

Figures B-7(a) and (b) show the intercept range bias and standard deviation as a function of sensor angular variations. Figure B-7(a) shows the intercept range bias (mean) in meters. For attack azimuths of 0° to 40°, the range biases are all less than ±0.1 meter for angular variations out to ±3.0°.

Figure B-7(b) is a plot of the intercept range standard deviations (i.e., the computed standard deviation about the means plotted in Figure B-7[a]). In Figure B-7(b), the standard deviations for all attack azimuths remain below 0.2 meter at angular variations out to 3.0°. When the angular variation is reduced to 0.0°, the range standard deviations approach 0.15 meter, and not zero. This is caused by the range variations that were fixed, for these evaluations, at 5% of true range. So, although the angular variations went to zero, there were still variations in the range observations weighting the estimation routine. This was discussed in the last paragraph of section 5.3.3.

Figures B-7(c) and (d) show the "along-intercept-line" position bias and standard deviation as a function of sensor angular variations. Figure B-7(c) shows the "along-intercept-line" position bias to be less than ±0.05 meter (all attack azimuths) for angular variations less than 3.0°. Figure B-7(d) shows the standard deviations (all attack azimuths) below 0.16 meter for angular variations less than 3.0°. Note that the "along-intercept-line" biases are smaller than the "range" biases shown in Figure B-7(a). However, at angular variations around 3.0°, the "along-intercept-line" position standard deviations are similar to those in Figure B-7(b), but decrease to zero as the angular variation approaches zero. Note that the Y-axes of Figures B-7(c) and (d) are plotted on different scales than those of Figures B-7(a) and (b).

Figure B-8 is a plot of the same data used in Figure B-7 with different scales for the axes so that the results for angular variation below 1.0° are more readable. In Figure B-8(a), note that the intercept range bias is between ±0.03 meter for all attack

azimuths for all angular variations. In Figure B-8(b), all azimuths have an intercept range standard deviation less than 0.15 meter for all angular variations.

Figures B-8(c) and (d) show the "along-intercept-line" results for 1σ angular errors from 0° to 1.0°. Figure B-8(c) shows the "along-intercept-line" position bias is less than ±0.01 meter (all attack azimuths) for angular variations less than 1.0°. Figure B-8(d) shows that the corresponding standard deviations are less than 0.05 meter (all attack azimuths) for angular variations below 1.0°.

7.5 Case 5a: LOB System With Range Sensor, WLS Estimation, 5-Meter Intercept.

For this case, angular variations are based on a random draw from a normal distribution with 1σ values ranging from 0.0° to 3.0° in 0.02° steps. Range variations were based on a random draw from a normal distribution with 1σ values input as 5% of true range from range sensor to projectile. Velocity sensors were not used. A WLS estimation technique (see section 5.4.2) was used to predict projectile trajectory. Intercept was at 5 meters.

Figures B-9(a) and (b) show the intercept range bias and standard deviation as a function of sensor angular variations. Figure B-9(a) shows the intercept range bias (mean) in meters. For attack azimuths of 0° to 40°, the range biases are all less than±0.1 meter for angular variations out to ±3.0°.

Figure B-9(b) is a plot of the intercept range standard deviations (i.e., the computed standard deviation about the means plotted in Figure B-9[a]). In Figure B-9(b), the standard deviations for all attack azimuths remain below 0.2 meter at angular variations out to 3.0°. When the angular variation is reduced to 0.0°, the range standard deviations approach 0.1 meter, and not zero. This is caused by the range variations that were fixed, for these evaluations, at 5% of true range. So, although the angular variations went to zero, there were still variations in the range observations weighting the estimation routine. This was discussed in the last paragraph of section 5.3.3.

Figures B-9(c) and (d) show the "along-intercept-line" position bias and standard deviation as a function of sensor angular variations. Figure B-9(c) shows the "along-intercept-line" position bias to be less than ±0.03 meter (all attack azimuths) for angular variations less than 3.0°. Figure B-9(d) shows the standard deviations (all attack azimuths) below 0.12 meter for angular variations less than 3.0°. Note that the "along-intercept-line" biases are smaller than the "range" biases shown in Figure B-9(a). However, at angular variations around 3.0°, the "along-intercept-line" position standard deviations are close to those in Figure B-9(b), but decrease to zero as the angular variation approaches zero. Note that the Y-axes of Figures B-9(c) and (d) are plotted on different scales than those of Figures B-9(a) and (b).

Figure B-10 is a plot of the same data used in Figure B-9 with different scales for the axes so that the results for angular variation below 1.0° are more readable. In

44

Figure B-10(a), note that the intercept range bias is between ±0.03 meter for all attack azimuths for all angular variations. In Figure B-10(b), all azimuths have an intercept range standard deviation less than 0.14 meter for all angular variations.

Figures B-10(c) and (d) show the "along-intercept-line" results for 1σ angular errors from 0° to 1.0°. Figure B-10(c) shows the "along-intercept-line" position bias is less than ±0.01 meter (all attack azimuths) for angular variations less than 1.0°. Figure B-10(d) shows that the corresponding standard deviations are less than 0.04 meter (all attack azimuths) for angular variations below 1.0°.

Note that there is an anomaly in Figures B-9(d) and B-10(d) where the standard deviation for the 10°, and possibly the 20°, attack azimuths begins to rise as the LOB angular variations approach zero. This anomaly was only observed in this particular sensor/estimation-routine combination for the 5-meter intercept case. The cause of this anomaly has not been determined, however, the random number stream problems have been ruled out as a cause. This anomaly is still under investigation.

7.6   Case 6a: LOB System With Velocity and Range Sensors, Kalman Estimation, 5-Meter Intercept. For this case, angular variations are based on a random draw from a normal distribution with 1σ values ranging from 0.0° to 3.0° in 0.02° steps. Velocity variations were based on a random draw from a normal distribution with 5 meters per second as the 1σ value. Range variations were based on a random draw from a normal distribution with 1σ values input as 5% of true range from range sensor to projectile. A Kalman filter estimation (see section 5.4.3) was used to predict projectile trajectory. Intercept was at 5 meters.

Figures B-11(a) and (b) show the intercept range bias and standard deviation as a function of sensor angular variations. Figure B-11(a) shows the intercept range bias (mean) in meters as a function of sensor angular variations. For attack azimuths of 0° to 40°, the range biases are all less than ±0.1 meter for angular variations out to ±3.0°.

Figure B-11(b) is a plot of the intercept range standard deviations (i.e., the computed standard deviation about the means plotted in Figure B-11[a]). In Figure B-11(b), the standard deviations for all attack azimuths remain below 0.15 meter at angular variations out to 3.0°. When the angular variation is reduced to 0.0°, the range standard deviations approach 0.10 meter, and not zero. This is caused by the range variations that were fixed, for these evaluations, at 5% of true range. So, although the angular variations went to zero, there were still variations in the range observations weighting the estimation routine. This was discussed in the last paragraph of section 5.3.3.

Figures B-11(c) and (d) show the "along-intercept-line" position bias and standard deviation as a function of sensor angular variations. Figure B-11(c) shows the "along-intercept-line" position bias to be less than ±0.02 meter (all attack azimuths) for angular variations less than 3.0°. Figure B-11(d) shows the standard deviations (all attack

azimuths) below 0.12 meter for angular variations less than 3.0°. Note that the "along-intercept-line" biases appear smaller than the "range" biases shown in Figure B-11(a). However, at angular variations around 3.0°, the "along-intercept-line" position standard deviations are similar to those in Figure B-11(b), but decrease to zero as the angular variation approaches zero. Note that the Y-axes of Figures B-11(c) and (d) are plotted on different scales than those of Figures B-11(a) and (b).

Figure B-12 is a plot of the same data used in Figure B-11 with different scales for the axes so that the results for angular variations below 1.0° are more readable. In Figure B-12(a), note that the intercept range bias is between ±0.02 meter for all attack azimuths for angular variations less than 1.0°. In Figure B-12(b), all azimuths have an intercept range standard deviation less than 0.08 meter for angular variations less than 1.0°.

Figures B-12(c) and (d) show the "along-intercept-line" results for 1σ angular errors from 0° to 1.0°. Figure B-12(c) shows that the "along-intercept-line" position bias is less than ±0.01 meter (all attack azimuths) for angular variations less than 1.0°. Figure B-12(d) shows that the corresponding standard deviations are less than 0.04 meter (all attack azimuths) for angular variations below 1.0°.

Note that in Figure B-12(c) there is an abnormality in the "along-intercept-line" position bias as LOB angular variations decrease from some small value to zero. A possible cause for this abnormality was discussed in the last paragraph of section 6.

8. COMPARISONS

This section will compare the results (provided in sections 6 and 7) for the various sensor and estimation technique combinations. Comparisons can be made by studying the the figures in Appendices A and B. Appendix A results were discussed in section 6 and Appendix B results were discussed in section 7. Each figure in the Appendices contains four plots:

1) Intercept range bias as a function of angular variation.

2) Intercept range standard variation as a function of angular variation.

3) Along-intercept-line position bias as a function of angular variation.

4) Along-intercept-line position standard deviation as a function of angular variation.

46

In an effort to summarize the information from the many plots in Appendices A and B, Tables 1 through 4 have been provided. These tables were generated by reading information from the plots in Appendices A and B.

Table 1 shows the magnitude of the intercept range (I-Rng) bias and standard deviation (I-Rng Std Dev) and the magnitude of the along-intercept-line bias (AIL Bias) and standard deviation (AIL Std Dev) for the 10-meter intercept case. In Table 1, the results are grouped by sensor/filter case and show biases and standard deviations for seven selected angular variations. Each angular variation value includes all angular variations at or below the one listed above each column in the table. That is, the values listed under the ≤ 1.5° column heading include the "worst" bias and standard deviation (from the appropriate plot) for all angular variations ≤ 1.5°. This value may not necessarily be the actual bias or standard deviation value at 1.5°. The "worst" result was normally, but not necessarily, the result for the 40° attack azimuth. In some instances, the bias or standard deviation value exceeded the scale of the plot and this was noted with an asterisk (*). The absolute value, or magnitude, of all biases is shown in the table. The LOB-RLS (at 10-meter intercept range) case is considered the "Base Case" against which the other cases are compared. The last column in the table shows the figures from which the data were extracted. The shaded cells indicate instances where the results were worse than those of the base case. Conversely, the unshaded cells indicate instances where the results were as good as or better than the base case.

Table 2 shows the results of comparing various sensor/estimation systems with the "Base Case" (LOB-RLS) system. In Table 2, the actual values for the "Base Case" (LOB-RLS system with 10-meter intercept) are listed in the LOB-RLS section. All the following sections (such as, LOB-WLS, LOB/VELOC-Kalman, etc.) in Table 3 show the differences between the corresponding values for that particular system and the "Base Case" system. In this table, negative values indicate a system that is better than the "Base Case" system by the numeric value indicated.

Table 3 shows the results for the 5-meter intercept distance condition and is set up the same as Table 1. Note that the intercept-range-bias plots (Appendices A and B) are not symmetric (for plots that range out to 3.0° angular variation) (i.e., Y-axes range from -2.0 m to +8.0 m). This can cause some confusion in comparing Tables 1 and 3 LOB-WLS values where Table 1 shows some values at > 8.0 and Table 3 shows some values at > 2.0. From the plots (Appendices A and B), it is not clear that the > 2.0 biases are better than the > 8.0 biases. The last column in the table shows the figures from which the data were extracted. The shaded cells indicate instances where the results were worse than those of the corresponding 10-meter intercept case. Conversely, the unshaded cells indicate instances where the results were as good as or better than the corresponding 10-meter intercept case.

47

Table 1. System Prediction Summary for 10-Meter Intercept Range and Worst-Case Attack Azimuth

BASE CASE LOB-RLS	LOB Angular Variations (Degrees)							Figure
	≤ 0.1	≤ 0.5	≤ 1.0	≤ 1.5	≤ 2.0	≤ 2.5	≤ 3.0	
I I-Rng Bias I (m)	≤ 0.02	≤ 0.1	≤ 0.28	≤ 0.8	≤ 3.5	≤ 5.8	≤ 7.6	A-1,2
I-Rng Std Dev (m)	< 0.6	< 0.86	< 1.2	< 2.8	< 4.3	> 5.0 *	> 5.0 *	A-1,2
I AIL Bias I (m)	~ 0.0	≤ 0.01	≤ 0.01	≤ 0.01	≤ 0.04	≤ 0.07	≤ 0.09	A-1,2
AIL Std Dev (m)	< 0.01	< 0.04	< 0.08	< 0.14	< 0.24	< 0.36	< 0.52	A-1,2
LOB-WLS								
I I-Rng Bias I (m)	≤ 0.02	≤ 0.6	≤ 0.6	≤ 6.1	> 8.0 *	> 8.0 *	> 8.0 *	A-3,4
I-Rng Std Dev (m)	< 0.13	< 0.61	< 3.5	> 5.0 *	> 5.0 *	> 5.0 *	> 5.0 *	A-3,4
I AIL Bias I (m)	~ 0.0	≤ 0.005	≤ 0.015	≤ 0.055	≤ 0.09	≤ 0.11	≤ 0.14	A-3,4
AIL Std Dev (m)	< 0.01	< 0.04	< 0.13	> 0.8 *	> 0.8 *	> 0.8 *	> 0.8 *	A-3,4
LOB/VELOC-Kalman								
I I-Rng Bias I (m)	~ 0.0	≤ 0.18	≤ 0.4	≤ 3.5	> 8.0 *	> 8.0 *	> 8.0 *	A-5,6
I-Rng Std Dev (m)	< 0.09	< 0.4	< 1.2	> 5.0 *	> 5.0 *	> 5.0 *	> 5.0 *	A-5,6
I AIL Bias I (m)	~ 0.0 **	≤ 0.025	≤ 0.013	≤ 0.2	≤ 0.2	≤ 0.2	≤ 0.2	A-5,6
AIL Std Dev (m)	< 0.01	< 0.04	< 0.13	< 0.22	< 0.34	< 0.42	< 0.5	A-5,6
LOB/RANGE-RLS								
I I-Rng Bias I (m)	≤ 0.04	≤ 0.04	≤ 0.04	≤ 0.04	≤ 0.04	≤ 0.04	≤ 0.04	A-7,8
I-Rng Std Dev (m)	< 0.24	< 0.24	< 0.25	< 0.25	< 0.26	< 0.26	< 0.26	A-7,8
I AIL Bias I (m)	≤ 0.005	≤ 0.005	≤ 0.005	≤ 0.03	≤ 0.04	≤ 0.04	≤ 0.05	A-7,8
AIL Std Dev (m)	< 0.01	< 0.04	< 0.08	< 0.12	< 0.18	< 0.22	< 0.28	A-7,8
LOB/RANGE-WLS								
I I-Rng Bias I (m)	≤ 0.04	≤ 0.04	≤ 0.04	≤ 0.04	≤ 0.04	≤ 0.04	≤ 0.04	A-9,10
I-Rng Std Dev (m)	< 0.25	< 0.25	< 0.25	< 0.25	< 0.25	< 0.30	< 0.30	A-9,10
I AIL Bias I (m)	~ 0.0	≤ 0.005	≤ 0.005	≤ 0.01	≤ 0.02	≤ 0.03	≤ 0.04	A-9,10
AIL Std Dev (m)	< 0.01	< 0.04	< 0.075	< 0.12	< 0.16	< 0.2	< 0.25	A-9,10
LOB/VELOC/RANGE-KALMAN								
I I-Rng Bias I (m)	≤ 0.03	≤ 0.03	≤ 0.03	≤ 0.03	≤ 0.03	≤ 0.03	≤ 0.03	A-11,12
I-Rng Std Dev (m)	< 0.16	< 0.17	< 0.18	< 0.18	< 0.2	< 0.2	< 0.2	A-11,12
I AIL Bias I (m)	≤ 0.005**	≤ 0.01	≤ 0.02	≤ 0.03	≤ 0.04	≤ 0.05	≤ 0.06	A-11,12
AIL Std Dev (m)	< 0.01	< 0.035	< 0.075	< 0.12	< 0.14	< 0.18	< 0.22	A-11,12

Notes:

LOB = 2 Line-of-Bearing Sensors

VELOC = 1 Velocity Sensor

RANGE = 1 Range Sensor

RLS = Recursive Least Squares Processing Filter

WLS = Weighted Least Squares Processing Filter

KALMAN = Kalman Processing Filter

▨ = Worse than Base Case

I I-Rng Bias I = Magnitude of Intercept Range Bias

I-Rng Std Dev = Intercept Range Standard Deviation

I AIL Bias I = Magnitude of Along-Intercept-Line Bias

AIL Std Dev = Along-Intercept-Line Standard Deviation

* Exceeded Maximum + or - Value on Plot

** Anomaly near 0.0 degrees ignored (see the discussion in the last paragraph of section 6)

Table 2. System Prediction Changes From Base Case (LOB-RLS) for 10-Meter Intercept Range

BASE CASE (Actual Values) LOB-RLS	LOB Angular Variations (Degrees)							Figure
	≤ 0.1	≤ 0.5	≤ 1.0	≤ 1.5	≤ 2.0	≤ 2.5	≤ 3.0	
I-Rng Bias I (m)	≤ 0.02	≤ 0.1	≤ 0.28	≤ 0.8	≤ 3.5	≤ 5.8	≤ 7.6	A-1,2
I-Rng Std Dev (m)	< 0.6	< 0.86	< 1.2	< 2.8	< 4.3	> 5.0 *	> 5.0 *	A-1,2
I AIL Bias I (m)	~ 0.0	≤ 0.01	≤ 0.01	≤ 0.01	≤ 0.04	≤ 0.07	≤ 0.09	A-1,2
AIL Std Dev (m)	< 0.01	< 0.04	< 0.08	< 0.14	< 0.24	< 0.36	< 0.52	A-1,2
LOB-WLS								
I I-Rng Bias I (m)	0.0	+0.5	+0.32	+5.3	> +4.5 *	> +2.2 *	> +0.4 *	A-3,4
I-Rng Std Dev (m)	-0.47	-0.25	+2.3	> +2.2 *	> +0.7 *	0.0 *	0.0 *	A-3,4
I AIL Bias I (m)	0.0	-0.005	+0.005	+0.045	+0.05	+0.04	+0.05	A-3,4
AIL Std Dev (m)	0.0	0.0	+0.5	+0.66 *	+0.56 *	+0.46 *	+0.28 *	A-3,4
LOB/VELOC- Kalman								
I I-Rng Bias I (m)	-0.02	+0.08	+0.12	+2.7	> +4.5 *	> +2.2 *	> +0.4 *	A-5,6
I-Rng Std Dev (m)	-0.51	-0.46	0.0	+2.2 *	+0.7 *	0.0 *	0.0 *	A-5,6
I AIL Bias I (m)	0.0 **	+0.015	+0.003	+0.1	+0.16	+0.13	+0.11	A-5,6
AIL Std Dev (m)	0.0	0.0	+0.05	+0.08	+0.1	+0.06	-0.02	A-5,6
LOB/RANGE- RLS								
I I-Rng Bias I (m)	+0.02	-0.06	-0.24	-0.76	-3.46	-5.76	-7.56	A-7,8
I-Rng Std Dev (m)	-0.36	-0.62	-0.95	-2.55	-4.04	-4.74	-4.74	A-7,8
I AIL Bias I (m)	+0.005	-0.005	-0.005	+0.02	0.0	-0.03	-0.04	A-7,8
AIL Std Dev (m)	0.0	0.0	0.0	-0.02	-0.06	-0.14	-0.24	A-7,8
LOB/RANGE- WLS								
I I-Rng Bias I (m)	+0.02	-0.06	-0.24	-0.76	-3.46	-5.76	-7.56	A-9,10
I-Rng Std Dev (m)	-0.35	-0.61	-0.95	-2.55	-4.05	-4.7	-4.7	A-9,10
I AIL Bias I (m)	0.0	-0.005	-0.005	0.0	-0.02	-0.04	-0.05	A-9,10
AIL Std Dev (m)	0.0	0.0	-0.005	-0.02	-0.08	-0.16	-0.27	A-9,10
LOB/VELOC/RANGE- KALMAN								
I I-Rng Bias I (m)	+0.01	-0.07	-0.25	-0.77	-3.47	-5.77	-7.57	A-11,12
I-Rng Std Dev (m)	-0.44	-0.69	-1.02	-2.62	-4.1	-4.8	-4.8	A-11,12
I AIL Bias I (m)	+0.005**	0.0	+0.01	+0.02	0.0	-0.02	-0.03	A-11,12
AIL Std Dev (m)	0.0	-0.005	-0.005	-0.02	-0.1	-0.18	-0.3	A-11,12

Notes:

LOB = 2 Line-of-Bearing Sensors	I I-Rng Bias I = Magnitude of Intercept Range Bias
VELOC = 1 Velocity Sensor	I-Rng Std Dev = Intercept Range Standard Deviation
RANGE = 1 Range Sensor	I AIL Bias I = Magnitude of Along-Intercept-Line Bias
RLS = Recursive Least Squares Processing Filter	AIL Std Dev = Along-Intercept-Line Standard Deviation
WLS = Weighted Least Squares Processing Filter	* Exceeded Maximum + or - Value on Plot
KALMAN = Kalman Processing Filter	** Anomaly near 0.0 degrees ignored (see the discussion in the last paragraph of section 6)

Table 3. System Prediction Summary for 5-Meter Intercept Range and Worst-Case Attack Azimuth

	LOB Angular Variations (Degrees)							Figure
LOB-RLS	≤ 0.1	≤ 0.5	≤ 1.0	≤ 1.5	≤ 2.0	≤ 2.5	≤ 3.0	
I-Rng Bias I (m)	≤ 0.01	≤ 0.22	≤ 0.23	≤ 0.7	≤ 0.8	≤ 0.8	≤ 0.8	B-1,2
I-Rng Std Dev (m)	< 0.1	< 0.52	< 0.8	< 0.8	< 0.9	> 1.2	> 1.6	B-1,2
I AIL Bias I (m)	~ 0.0	≤ 0.0025	≤ 0.0075	≤ 0.02	≤ 0.03	≤ 0.03	≤ 0.04	B-1,2
AIL Std Dev (m)	< 0.005	< 0.025	< 0.045	< 0.07	< 0.09	< 0.11	< 0.17	B-1,2
LOB-WLS								
I I-Rng Bias I (m)	~ 0.0	≤ 0.02	≤ 0.345	> 2.0 *	> 2.0 *	> 2.0 *	> 2.0 *	B-3,4
I-Rng Std Dev (m)	< 0.05	< 0.24	< 0.54	> 5.0 *	> 5.0 *	> 5.0 *	> 5.0 *	B-3,4
I AIL Bias I (m)	~ 0.0	≤ 0.005	≤ 0.01	≤ 0.02	> 0.2 *	> 0.2 *	> 0.2 *	B-3,4
AIL Std Dev (m)	< 0.005	< 0.02	< 0.045	> 0.8 *	> 0.8 *	> 0.8 *	> 0.8 *	B-3,4
LOB/VELOC-Kalman								
I I-Rng Bias I (m)	~ 0.0	≤ 0.06	≤ 0.22	≤ 0.4	< 0.6	< 0.6	< 0.6	B-5,6
I-Rng Std Dev (m)	< 0.04	< 0.13	< 0.26	< 0.4	< 1.0	< 2.5	< 4.2	B-5,6
I AIL Bias I (m)	~ 0.0 **	≤ 0.005	≤ 0.03	≤ 0.08	≤ 0.16	> 0.2 *	> 0.2 *	B-5,6
AIL Std Dev (m)	< 0.005	< 0.025	< 0.05	< 0.1	< 0.16	< 0.24	< 0.31	B-5,6
LOB/RANGE-RLS								
I I-Rng Bias I (m)	≤ 0.0025	≤ 0.005	≤ 0.005	≤ 0.005	≤ 0.005	≤ 0.005	≤ 0.005	B-7,8
I-Rng Std Dev (m)	< 0.15	< 0.15	< 0.15	< 0.15	< 0.15	< 0.2	< 0.2	B-7,8
I AIL Bias I (m)	~ 0.0	~ 0.0	≤ 0.005	≤ 0.01	≤ 0.02	≤ 0.025	≤ 0.04	B-7,8
AIL Std Dev (m)	< 0.005	< 0.025	< 0.045	< 0.08	< 0.1	< 0.12	< 0.145	B-7,8
LOB/RANGE-WLS								
I I-Rng Bias I (m)	≤ 0.0025	≤ 0.0025	≤ 0.0025	≤ 0.0025	≤ 0.0025	≤ 0.0025	≤ 0.0025	B-9,10
I-Rng Std Dev (m)	< 0.12 **	< 0.12	< 0.12	< 0.12	< 0.12	< 0.15	< 0.15	B-9,10
I AIL Bias I (m)	~ 0.0	~ 0.0	≤ 0.005	≤ 0.005	≤ 0.01	≤ 0.01	≤ 0.03	B-9,10
AIL Std Dev (m)	< 0.005 **	< 0.02	< 0.04	< 0.06	< 0.08	< 0.1	< 0.12	B-9,10
LOB/VELOC/RANGE-KALMAN								
I I-Rng Bias I (m)	≤ 0.0025	≤ 0.0025	≤ 0.0025	≤ 0.0025	≤ 0.0025	≤ 0.0025	≤ 0.0025	B-11,12
I-Rng Std Dev (m)	< 0.08	< 0.08	< 0.08	< 0.1	< 0.1	< 0.1	< 0.1	B-11,12
I AIL Bias I (m)	≤ 0.0025	≤ 0.0025	≤ 0.05	≤ 0.1	≤ 0.15	≤ 0.2	≤ 0.2	B-11,12
AIL Std Dev (m)	< 0.005***	< 0.02	< 0.04	< 0.06	< 0.08	< 0.09	< 0.11	B-11,12

Notes:

LOB	= 2 Line-of-Bearing Sensors	I I-Rng Bias I	= Magnitude of Intercept Range Bias
VELOC	= 1 Velocity Sensor	I-Rng Std Dev	= Intercept Range Standard Deviation
RANGE	= 1 Range Sensor	I AIL Bias I	= Magnitude of Along-Intercept-Line Bias
RLS	= Recursive Least Squares Processing Filter	AIL Std Dev	= Along-Intercept-Line Standard Deviation
WLS	= Weighted Least Squares Processing Filter	*	Exceeded Maximum + or - Value on Plot
KALMAN	= Kalman Processing Filter	**	Anomaly near 0.0 degrees ignored (see the discussion in
▨	= Worse than 10 meter Case		the last paragraph of section 6)
		***	Anomaly below 0.1 degrees ingnored (see the discussion
			in the sixth paragraph of section 7.5)

Table 4 shows the differences between the 10-meter and 5-meter intercepts. Table 4 is in essence a cell-by-cell subtraction of Table 1 from Table 3. In Table 4, negative values indicate instances where the 5-meter intercept was better (by the numeric value indicated) than the 10-meter intercept for the corresponding sensor/estimation combination.

Throughout this section on comparisons, terms like "slight," "moderate," "significant," and "dramatic" will be used along with some numeric examples from Tables 1 through 4. These terms are used as cues to the reader as to areas that might warrant further attention. It is left to the reader to investigate the tables (and associated plots) to determine if the actual numeric improvements (or degradations) are in fact "slight," "moderate," "significant," or "dramatic" for specific systems of interest. In addition, most of the discussion will be on the intercept range biases and standard deviations, as these are the two parameters that are the most difficult to predict with a short baseline LOB system. Therefore, although an along-intercept-bias (or standard deviation) may improve from 0.005 to 0.0025 m (a 100% improvement), this type improvement will be discounted since the errors are so small (as compared to the intercept range errors).

8.1 Sensor/Filter Base Case, Table 1.

LOB-RLS: The angle-only LOB sensor system with RLS estimation and a 10-meter intercept distance provided the base case against which the other sensor/estimation combinations were compared. Table 1 shows that the along-intercept-line (AIL) biases and standard deviations were generally very small compared to the intercept range (I-Rng) values for the LOB-RLS baseline case. Intercept range biases and standard deviations varied from 0.02 to 7.6 meters and 0.6 to > 5.0 meters, respectively, while along-intercept-line biases and standard deviations varied from 0.0 to 0.09 meter and 0.01 to 0.52 meter respectively. For the LOB-WLS, and LOB/VELOC-Kalman cases, the AIL biases and standard deviations were also generally very small compared to the I-Rng values. For the three RANGE cases, the along-intercept-line biases and standard deviations were only slightly smaller than the corresponding intercept-range biases and standard deviations. The shaded cells indicate instances where the results were worse than those of the base case. Conversely, the unshaded cells indicate instances where the results were as good as or better than the base case.

8.2 Variations From Base Case for Other Sensors/Filter Combinations, Table 2.

Table 2 compares the results of Table 1 for various sensor/estimation combinations (i.e., LOB-WLS, LOB/VELOC-Kalman, etc.) with the "Base Case" (LOB-RLS). Table 2 shows the differences between the indicated case and the "Base Case."

Table 4. System Prediction Changes From 10-Meter to 5-Meter Intercept Range

LOB-RLS	LOB Angular Variations (Degrees)							Figure
	≤ 0.1	≤ 0.5	≤ 1.0	≤ 1.5	≤ 2.0	≤ 2.5	≤ 3.0	
I I-Rng Bias I (m)	-0.01	+0.12	-0.05	-0.1	-2.7	-5.0	-6.8	A&B(1,2)
I-Rng Std Dev (m)	-0.5	-0.34	-0.4	-2.0	-3.4	-3.8	-3.4	A&B(1,2)
I AIL Bias I (m)	0.0	-0.0075	-0.0025	+0.01	-0.01	-0.04	-0.05	A&B(1,2)
AIL Std Dev (m)	-0.005	-0.015	-0.035	-0.07	-0.15	-0.25	-0.35	A&B(1,2)
LOB-WLS								
I I-Rng Bias I (m)	-0.02	-0.58	-0.255	-4.1 *	-6.0 *	-6.0 *	-6.0 *	A&B(3,4)
I-Rng Std Dev (m)	-0.08	-0.37	-2.96	0.0 *	0.0 *	0.0 *	0.0 *	A&B(3,4)
I AIL Bias I (m)	0.0	0.0	-0.005	-0.035	+0.11 *	+0.09 *	+0.06 *	A&B(3,4)
AIL Std Dev (m)	-0.005	-0.02	-0.085	0.0 *	0.0 *	0.0 *	0.0 *	A&B(3,4)
LOB/VELOC-Kalman								
I I-Rng Bias I (m)	0.0	-0.12	-0.18	-3.1	-7.4	-7.4	-7.4	A&B(5,6)
I-Rng Std Dev (m)	-0.05	-0.27	-0.94	-4.6	-4.0	-2.5	-0.8	A&B(5,6)
I AIL Bias I (m)	0.0 **	-0.02	+0.017	-0.12	-0.04	0.0 *	0.0 *	A&B(5,6)
AIL Std Dev (m)	-0.005	-0.015	-0.08	-0.12	-0.18	-0.18	-0.19	A&B(5,6)
LOB/RANGE-RLS								
I I-Rng Bias I (m)	-0.0375	-0.035	-0.035	-0.035	-0.035	-0.035	-0.035	A&B(7,8)
I-Rng Std Dev (m)	-0.09	-0.09	-0.1	-0.1	-0.11	-0.06	-0.06	A&B(7,8)
I AIL Bias I (m)	-0.005	-0.005	0.0	-0.02	-0.02	-0.015	-0.01	A&B(7,8)
AIL Std Dev (m)	-0.005	-0.015	-0.035	-0.04	-0.08	-0.1	-0.135	A&B(7,8)
LOB/RANGE-WLS								
I I-Rng Bias I (m)	-0.0375	-0.0375	-0.0375	-0.0375	-0.0375	-0.0375	-0.0375	A&B(9,10)
I-Rng Std Dev (m)	-0.13 **	-0.13	-0.13	-0.13	-0.13	-0.15	-0.15	A&B(9,10)
I AIL Bias I (m)	0.0	-0.005	0.0	-0.005	-0.01	-0.02	-0.01	A&B(9,10)
AIL Std Dev (m)	-0.005 **	-0.02	-0.035	-0.06	-0.08	-0.1	-0.13	A&B(9,10)
LOB/VELOC/RANGE-KALMAN								
I I-Rng Bias I (m)	-0.0275	-0.0275	-0.0275	-0.0275	-0.0275	-0.0275	-0.0275	A&B(11,12)
I-Rng Std Dev (m)	-0.08	-0.09	-0.1	-0.08	-0.1	-0.1	-0.1	A&B(11,12)
I AIL Bias I (m)	-0.0025**	-0.0075	+0.03	+0.07	+.11	+0.15	+0.14	A&B(11,12)
AIL Std Dev (m)	-0.005***	-0.015	-0.035	-0.06	-0.06	-0.09	-0.11	A&B(11,12)

Notes:

LOB = 2 Line-of-Bearing Sensors

VELOC = 1 Velocity Sensor

RANGE = 1 Range Sensor

RLS = Recursive Least Squares Processing Filter

WLS = Weighted Least Squares Processing Filter

KALMAN = KALMAN Processing Filter

I I-Rng Bias I = Magnitude of Intercept Range Bias

I-Rng Std Dev = Intercept Range Standard Deviation

I AIL Bias I = Magnitude of Along-Intercept-Line Bias

AIL Std Dev = Along-Intercept-Line Standard Deviation

* Exceeded Maximum + or - Value on Plot

** Anomaly near 0.0 degrees ignored (see the discussion in the last paragraph of section 6)

*** Anomaly below 0.1 degrees ingnored (see the discussion in the sixth paragraph of section 7.5)

Negative values in Table 2 indicate cases where the results were better than those of the LOB-RLS "Base Case."

LOB-WLS: Comparing with the LOB-RLS "Base Case," the WLS estimation resulted in a moderate improvement (reductions of 0.25 and 0.47 meter) in intercept range standard deviations for angular variations $\leq 0.5°$. However, most intercept range results were worse, especially for angular variations above 0.5°. Results for along-intercept-line standard deviations were worse for angular variations $> 0.5°$. Intercept range biases and standard deviations varied from 0.02 to > 8.0 meters and 0.13 to > 5.0 meters, respectively, while along-intercept-line biases and standard deviations varied from 0.0 to 0.14 meter and 0.01 to > 0.8 meter respectively (see Table 1).

LOB/VELOC-Kalman: The addition of a velocity sensor and Kalman filter resulted in significant improvement, over the LOB-RLS case, in the intercept range standard deviation (reductions in excess of 0.46 meter) for angular variations $\leq 0.5°$. For angular variations above 0.5°, these standard deviations were generally worse. Results for the along-intercept-line biases increased up to 0.19 meter, while the standard deviations increased up to 0.1 meter from the base case. Intercept range biases and standard deviations varied from 0.0 to > 8.0 meters and 0.09 to > 5.0 meters, respectively, while along-intercept-line biases and standard deviations varied from 0.0 to 0.2 meter and 0.01 to 0.5 meter, respectively (see Table 1).

LOB/RANGE-RLS: Adding a range sensor to the LOB sensors (w/RLS estimation) results in a dramatic improvement, over the LOB-RLS case, in intercept range bias and standard deviation. These biases showed significant reductions ranging from 0.24 to 7.56 meters for angular variations $\geq 1.0°$, and the standard deviations had reductions ranging from 0.36 to 4.74 meters for all angular variations. Results for the along-intercept-line standard deviations showed some improvement for angular variations $> 2.0°$ (reductions of 0.14 and 0.24 meter). Intercept range biases were constant at 0.04 meter, and the standard deviations varied from 0.24 to 0.26 meter, while along-intercept-line biases and standard deviations varied from 0.005 to 0.05 meter and 0.01 to 0.28 meter, respectively (see Table 1).

LOB/RANGE-WLS: Adding a range sensor and WLS estimation to the base case LOB sensors resulted in a dramatic improvement, over the LOB-RLS case, in intercept range bias and standard deviation. These biases showed reductions ranging from 0.24 to 7.56 meters for angular variations $\geq 1.0°$, and the standard deviations

h. reductions ranging from 0.35 to 4.7 meters for all angular variations. Results for the along-intercept-line standard deviation showed some improvement, over the base case, for angular variations $\geq 2.0°$ (reductions of 0.08, 0.16, and 0.27 meter). Intercept range biases were constant at 0.04 meter, and the standard deviations varied from 0.25 to 0.3 meter, while along-intercept-line biases and standard deviations varied from 0.0 to 0.04 meter and 0.01 to 0.25 meter, respectively. These results are almost identical with the LOB/RANGE-RLS results (see Table 1).

LOB/VELOC/RANGE-KALMAN: Adding a velocity sensor, range sensor, and Kalman filtering to the base case results in dramatic improvement, over the LOB-RLS case, in intercept range bias and standard deviation. These biases showed significant reductions ranging from 0.25 to 7.57 meters for angular variations $\geq 1.0°$, and the standard deviations had reductions ranging from 0.44 to 4.8 meters for all angular variations. Results for the along-intercept-line standard deviation showed some improvement, over the base case, for angular variations $\geq 2.0°$ (reductions of 0.1, 0.18, and 0.3 meter). Intercept range biases were constant at 0.03 meter and the standard deviations varied from 0.16 to 0.2 meter while along-intercept-line biases and standard deviations varied from 0.005 to 0.06 meter and 0.01 to 0.22 meter, respectively (see Table 1). These results are slightly better than those of the LOB/R..NGE-RLS and LOB/RANGE-WLS cases.

If one were interested in reducing the intercept range standard deviation of an LOB-RLS (Base Case) system and considered a 0.1-meter reduction significant, then Table 2 shows that either the LOB-WLS or the LOB/VELOC-Kalman system provides this improvement for angular variations $\leq 0.5°$. The required improvements is also be achieved with: an LOB/RANGE-RLS or an LOB/RANGE-RLS or an LOB/VELOC/RANGE-Kalman system for all angular variations $\leq 3.0°$.

From Table 2, it can be seen that inclusion of a range measuring sensor provided the the greatest improvements to intercept range standard deviations at all LOB angular variations. The LOB/VELOC/RANGE-Kalman provided the best improvements of the range sensor systems. The LOB-WLS and LOB/VELOC-Kalman systems showed degraded performance (intercept range standard deviations) for many LOB angular variations.

8.3 Effects of Reducing Intercept Range From 10 to 5 Meters, Tables 3 and 4.

Table 3 shows the results of reducing the intercept range from 10 to 5 meters (Table 1 showed these results for 10-meter intercept). Each cell in Table 3 can be compared with the corresponding cell in Table 1 to see the effects of reducing the intercept distance. The shaded cells in Table 3 indicate instances where the results were worse than those of the

corresponding 10-meter intercept case. Conversely, the unshaded cells indicate instances where the results were as good as or better than the corresponding 10-meter intercept case.

Table 4 compares the 10-meter cases in Table 1 with the 5-meter cases in Table 3 and shows the differences between the two tables. Negative values in Table 4 indicate cases where the 5-meter intercept results were better than the 10-meter results. In this table, only like cases are compared (e.g, LOB-RLS at 10-meter vs. 5-meter intercept).

LOB-RLS: Reducing the intercept range from 10 to 5 meters results in a significant to dramatic improvement in intercept range biases for angular variations $\geq 1.5°$ and improvement to the standard deviations for all angular variations. Intercept range biases showed reductions ranging from 0.1 to 6.8 meters, and the standard deviation reductions ranged from 0.5 to 3.4 meters. All the along-intercept-line standard deviations were moderately improved for angular variations $\geq 2.0°$, with reductions ranging from 0.15 to 0.35 meter. Intercept range biases and standard deviations varied from 0.01 to 0.8 meter and 0.1 to 1.6 meters, respectively, while along-intercept-line biases and standard deviations varied from 0.0 to 0.04 meter and 0.005 to 0.17 meter, respectively (see Table 3). Studies not presented here indicate that these improvements are primarily due to the improved quality of the observations obtained closer to the LOB sensors as the threat projectile is allowed to move closer (i.e., the decision line is reduced from 11 to 6 meters range). Additional observations added at increased ranges, by increasing the sensor detection range, do not improve the results in the dramatic way that adding "close-in" observations do.

LOB-WLS: Reducing the intercept range from 10 to 5 meters results in a dramatic improvement in intercept range biases for angular variations $\geq 0.5°$, and intercept range standard deviations for angular variations $\leq 1.0°$. Intercept biases showed reductions ranging from 0.255 to 6.0 meters and the standard deviation reductions ranged from 0.37 to 2.96 meters. However, due to the asymmetric axes used for the intercept range bias plots, it is not clear if there is any improvement for angular variations above 1.0°. The along-intercept-line biases increased as much as 0.11 meter for angular variations $\geq 2.0°$. Intercept range biases and standard deviations varied from 0.00 to > 2.0 meters and 0.05 to > 5.0 meters, respectively, while along-intercept-line biases and standard deviations varied from 0.0 to > 0.2 meter and 0.005 to > 0.8 meter, respectively (see Table 3).

LOB/VELOC-Kalman: Reducing the intercept range from 10 to 5 meters results in a significant to dramatic improvement in intercept range biases and

standard deviations for angular variations of $\geq 0.5°$. Intercept range biases showed reductions ranging from 0.12 to 7.4 meters, and the standard deviation reductions ranged from 0.27 to 4.6 meters. The along-intercept-line standard deviations were improved for angular variations $\geq 1.5°$. Intercept range biases and standard deviations varied from 0.00 to > 0.6 meter and 0.04 to 4.2 meters, respectively, while along-intercept-line biases and standard deviations varied from 0.0 to > 0.2 meter and 0.005 to 0.31 meter, respectively (see Table 3).

LOB/RANGE-RLS: Reducing the intercept range from 10 to 5 meters results in a slight improvement in intercept range biases and standard deviations for all angular variations. Intercept range biases showed reductions of 0.035 meter, and the standard deviation reductions ranged from 0.06 to 0.11 meter. The along-intercept-line standard deviations were slightly improved for all angular variations. Intercept range biases and standard deviations varied from 0.0025 to 0.005 meter and 0.15 to 0.2 meter, respectively, while along-intercept-line biases and standard deviations varied from 0.0 to 0.04 meter and 0.005 to 0.145 meter, respectively (see Table 3).

LOB/RANGE-WLS: Reducing the intercept range from 10 to 5 meters results in some improvement in the intercept range standard deviations for all angular variations. Intercept range biases showed reductions of 0.0375 meter, and the standard deviation reductions ranged from 0.13 to 0.15 meter. The along-intercept-line standard deviations were improved for angular variations $\geq 2.5°$. Intercept range biases were constant at 0.0025 meter, while the standard deviations varied from 0.12 to 0.15 meter (see Table 3). The along-intercept-line biases and standard deviations varied from 0.0 to 0.03 meter and 0.005 to 0.12 meter, respectively (see Table 3).

LOB/VELOC/RANGE-Kalman: Reducing the intercept range from 10 to 5 meters results in very slight improvement in the intercept range standard deviations for all angular variations. Intercept range biases showed reductions of 0.0275 meter, and the standard deviation reductions ranged from 0.08 to 0.1 meter. The along-intercept-line standard deviations were slightly better for all angular variations. Intercept range biases were constant at 0.0025 meter, while the standard deviations varied from 0.08 to 0.1 meter (Table 3). The along-intercept-line biases and standard deviations varied from 0.0025 to 0.15 meter and 0.005 to 0.11 meter, respectively (Table 3).

If one were interested in reducing the intercept range standard deviation of an LOB-RLS (Base Case) system and considered a 0.1-meter reduction significant, then moving

the intercept line from 10 to 5 meters can provide some improvements. Table 4 shows 0.1 meter or better improvements to intercept range standard deviations for all LOB angular variations for the LOB-RLS and LOB/RANGE-WLS systems. Improvements of 0.1 meter or better can also be achieved with an LOB-WLS system with angular variations between 0.5° and 1.0°, an LOB/VELOC-Kalman system with angular variations between 0.5° and 3.0°, an LOB/RANGE-RLS system with angular variations between 1.0 and 2.0 meters, or an LOB/VELOC/RANGE-Kalman system for most angular variations between 1.0 and 3.0 meters.

From Table 4, it can be seen that reducing the intercept range from 10 to 5 meters can result in some very dramatic improvements in the intercept range biases and standard deviations for the LOB-RLS, LOB-WLS, and LOB/VELOC-Kalman systems. These improvements are much less dramatic in the systems already improved by the inclusion of range sensors.

9. CONCLUSIONS

The results presented in this report lead to the following conclusions:

1) The accuracy of short baseline LOB subsystem for estimation of a projectile trajectory over the terminal portion of its flight is determined using the methods suggested by this report. These subsystems consist of a method for processing information, a method for sensing information, and an accuracy for individual sensors.

2) Estimated range biases and standard deviations were worse than cross-range results due to the short baseline LOB sensor triangulation geometry that results in large range variations from small sensor angular variations.

3) Off-axis attack azimuths provided results that were worse than on-axis attacks. This was due to the fact that off-axis attacks resulted in an effective reduction in the sensor baseline. In addition, due to the specific geometry implementation (range lines parallel to baseline rather than range arcs) used in these simulations, the range was increased as the attack azimuth moved off-axis.

4) For LOB sensor systems with bad angular variations ($\geq 1.0°$), the addition of a range sensor (with the ability to measure range to within 5%) provides significant reductions in range bias and standard deviation.

57

5) For LOB sensor systems with very good angle sensors ($< 0.1°$ angular variation), range information can degrade results. Note that the range estimation method implemented for these studies was suboptimal in the sense that it is not a minimum variance estimate. This suboptimal solution is based on the assumption that the range error is always less than the range error from an LOB estimate. For accurate LOB systems, an optimal solution based on the variances of both the range estimate and the range component of the LOB estimate is required. An optimal solution discounts the range observation when the LOB location estimate is more accurate.

6) Reducing the intercept range from 10 to 5 meters produces better results for all sensor/estimator combinations. This is primarily due to the better 'quality' of observations closer to the LOB sensor baseline. The addition of observations at greater ranges did not improve trajectory estimation.

7) It has been shown that, for the scenario discussed, the greatest reduction in time-of-arrival (range) errors is accomplished by the addition of a range sensor (in this case with 5% variation) with simple LOB position adjusting algorithm for LOB systems with angular variations greater than $±0.4°$. For LOB sensor systems with angular variations less than $±0.4°$, one of the other sensor/processing method combinations is better: for angular variations less than $±0.10°$, an LOB tracker system with RLS processing; for angular variations less than $±0.22°$, an LOB tracker system with WLS processing; for angular variations below $±0.36°$, an LOB tracker system with velocity sensor and Kalman filter processing.

8) Note that, although the Kalman filter processing produced the best results below angular variations of $±0.36°$, this processing method is the most complex to implement in a system. The WLS is less complex with the RLS processing being the easiest to implement. Therefore, careful consideration must be given to both the sensor mix and the processing schemes and their impact upon the computational speed, accuracy, and complexity of the entire system.

10. SUMMARY

This report investigated methods for analyzing and improving the tracking ability of line-of-bearing (LOB) systems. Of particular interest were systems with short distances between the LOB sensors (short baseline), such as a conceptual system that places LOB sensor on an armored vehicle in order to track an incoming threat and make an accurate prediction to the threat's future location at some time so that an appropriate reaction can

be initiated. The LOB2D sensor tracking system simulation model was used to make these investigations.

The methods presented in this report allow the prediction of a short baseline, LOB tracking system's ideal performance for several system configurations. These configurations included six combinations of sensor/estimation types: LOB with recursive least squares estimation, LOB sensors with weighted least squares estimation, LOB and velocity sensors with Kalman filter estimation, LOB and range sensors with recursive least squares estimation, LOB and range sensors with weighted least squares estimation, and LOB with velocity and range sensors and Kalman filter estimation. Five attack azimuths (0°, 10°, 20°, 30°, and 40°) were used for all cases. In addition, two tracking length scenarios were investigated by varying the LOB2D inputs that specify how close the threat projectile is allowed to approach its target before data acquisition stops.

It was shown that the inherent geometry of a short-baseline LOB system leads to large errors in the system's ability to determine range, whereas cross-range determinations are not so affected by the geometry. Range sensors can greatly improve the performance of inherently bad LOB sensors, however, care must be taken in properly formulating the LOB/range sensor estimation routines so as not to bias the results. In the cases presented in this report, it was pointed out that the nonoptimal range solutions selected to improve very bad LOB sensors resulted in penalizing very good LOB sensors.

It was also shown that it is important to allow the incoming threat projectile to approach as close as is feasible to improve the quality of the LOB observations and thus the overall estimation. This was shown by reducing the intercept range, an input to the LOB2D simulation, from 10 to 5 meters.

This study represented only a small portion of the possible system configurations and scenario variations that are of interest. Using the tools and methods described herein, it will be possible to investigate the performance of other notional short-baseline, short-range, projectile tracking systems.

INTENTIONALLY LEFT BLANK

11. REFERENCES

Alexander, Charles. "Techniques to Evaluate the Performance of Tactical Airbourne Geolocation Systems." NSA-TR-R56/01/80, National Security Agency, 1980.

Thompson, A. A., and Durfee, G. L.. "A Study of Line of Bearing Errors." ARL-TR-209, U.S. Army Research Laboratory, 1993.

Thompson, A. A. "Data Fusion for Least Squares." BRL-TR-3303, U.S. Army Ballistic Research Laboratory, 1991a.

Thompson, A. A., and Durfee, G. L. "Techniques for Evaluating Line of Bearing Systems." BRL-TR-3390, U.S. Army Ballistic Research Laboratory, 1992.

Thompson, A. A. "A Model of a Range-Angle of Arrival Sensor System for an Active Protection System." BRL-TR-3243, U.S. Army Ballistic Research Laboratory, 1991b.

INTENTIONALLY LEFT BLANK

APPENDIX A:

SIMULATION RESULTS FOR 10-METER INTERCEPT RANGE

INTENTIONALLY LEFT BLANK

This appendix provides plotted results from the LOB2D simulation model (discussed in section 5) for the discussions provided in section 6 of the report. Each figure in this appendix contains four plots:

a) Intercept range bias as a function of angular variation.

b) Intercept range standard variation as a function of angular variation.

c) Along-intercept-line position bias as a function of angular variation.

d) Along-intercept-line position standard deviation as a function of angular variation.

There are two figures (eight plots) for each of the six cases discussed in section 6:

a) Figures A-1 and A-2: LOB (angle-only sensors) system, recursive least squares estimation.

b) Figures A-3 and A-4: LOB (angle-only sensors) system, weighted least squares estimation.

c) Figures A-5 and A-6: LOB system with velocity sensor, Kalman estimation.

d) Figures A-7 and A-8: LOB system with range sensor, recursive least squares estimation.

e) Figures A-9 and A-10: LOB system with range sensor, weighted least squares estimation.

f) Figures A-11 and A-12: LOB system with velocity and range sensors, Kalman estimation.

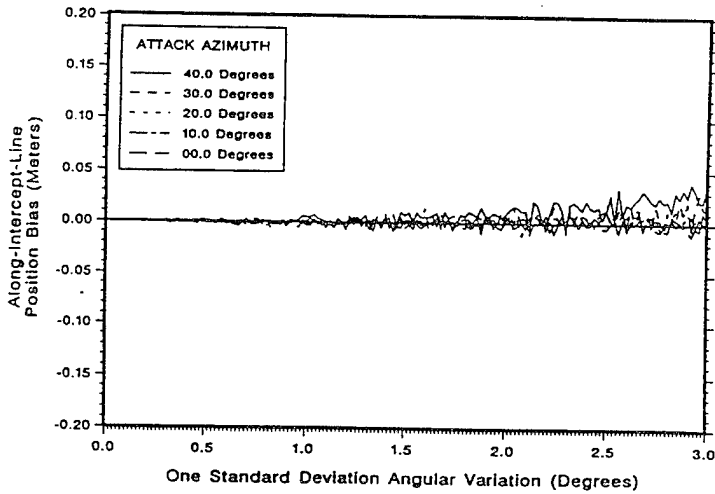## LOB Sensors with Recursive
Least Squares Estimation

(a)
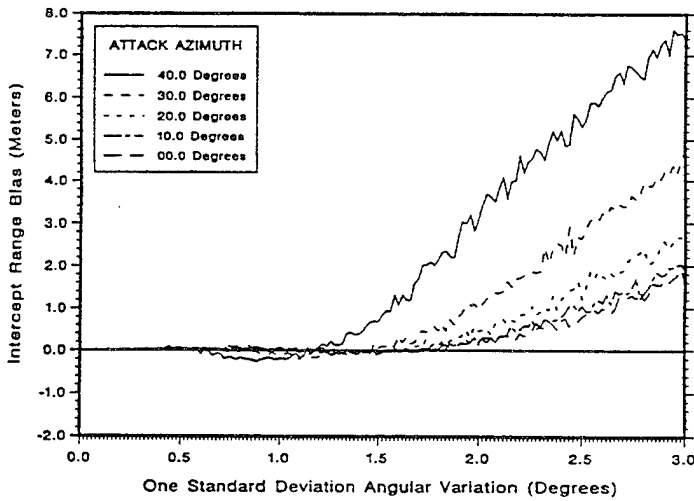
(b)
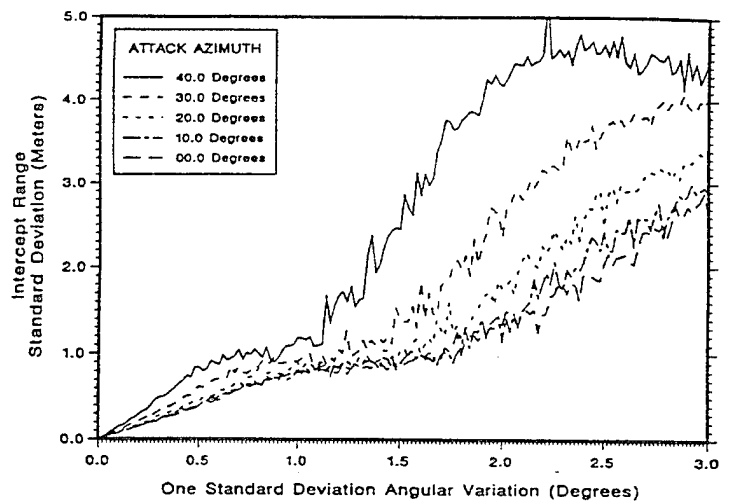
(c)
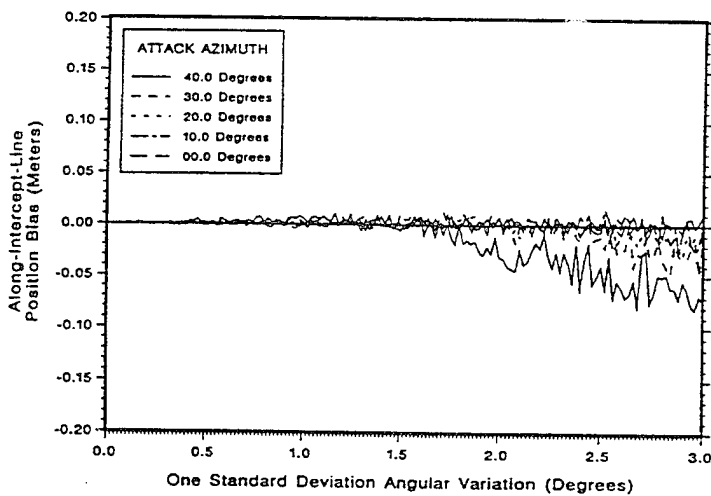
(d)
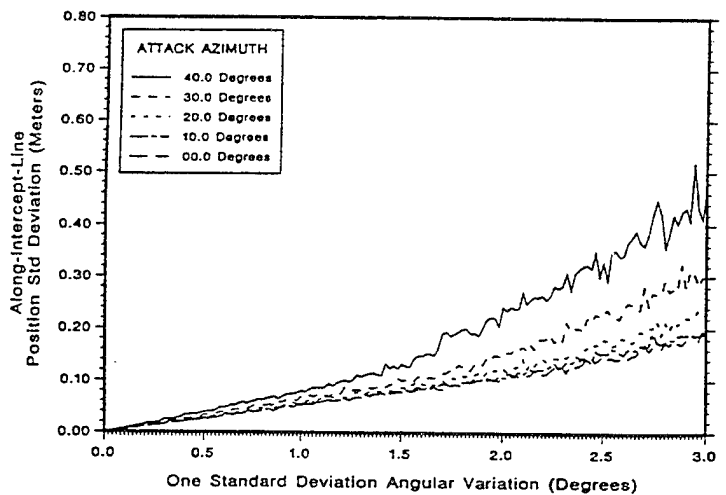
Figure A-1.   LOB Tracker with 0.0 to 3.0 Degree Angular Variations, Recursive
Least-Squares Estimation, 10 Meter Intercept: (a) Intercept Range
Bias, (b) Intercept Range Standard Deviation, (c) Along-Intercept-Line
Position Bias, and (d) Along-Intercept-Line Position Standard Deviation

LOB Sensors with Recursive
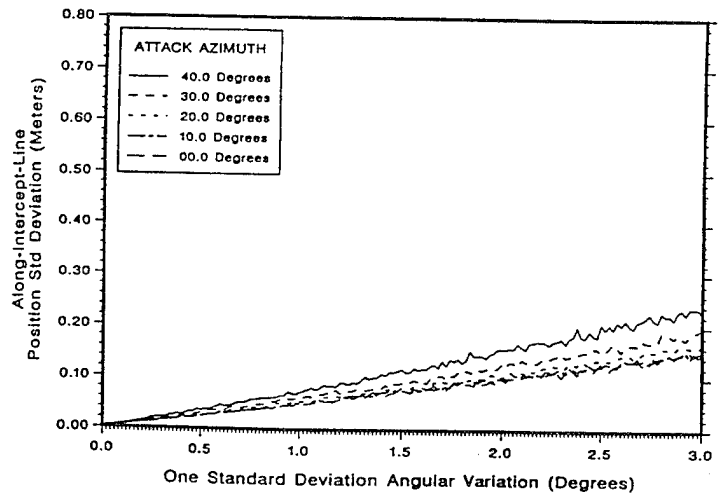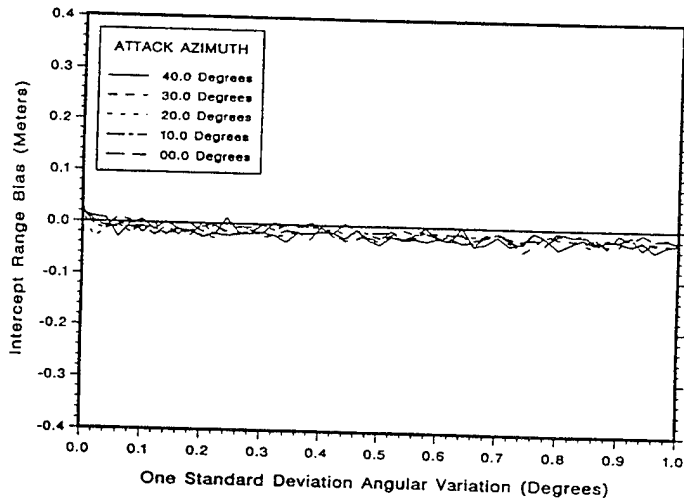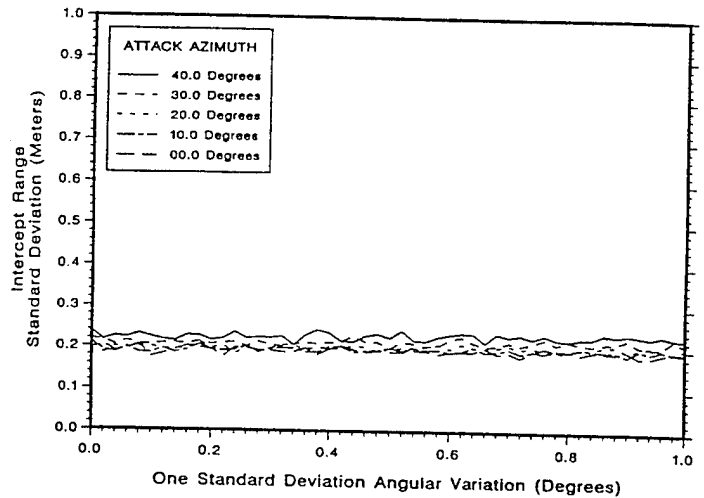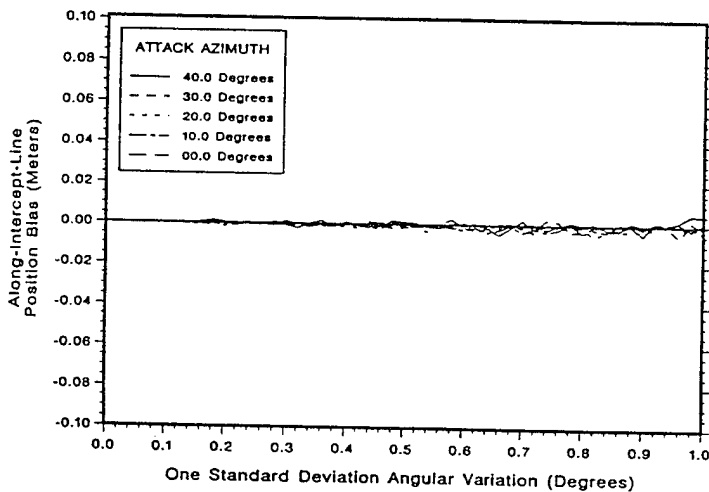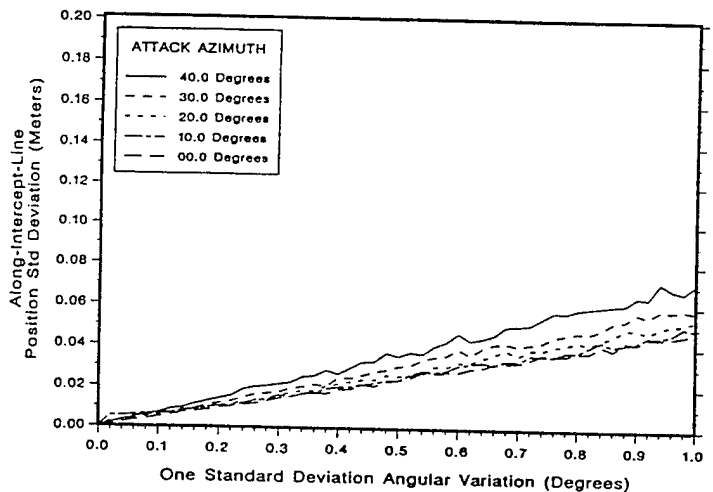# Least Squares Estimation

(a)

(b)

(c)

(d)
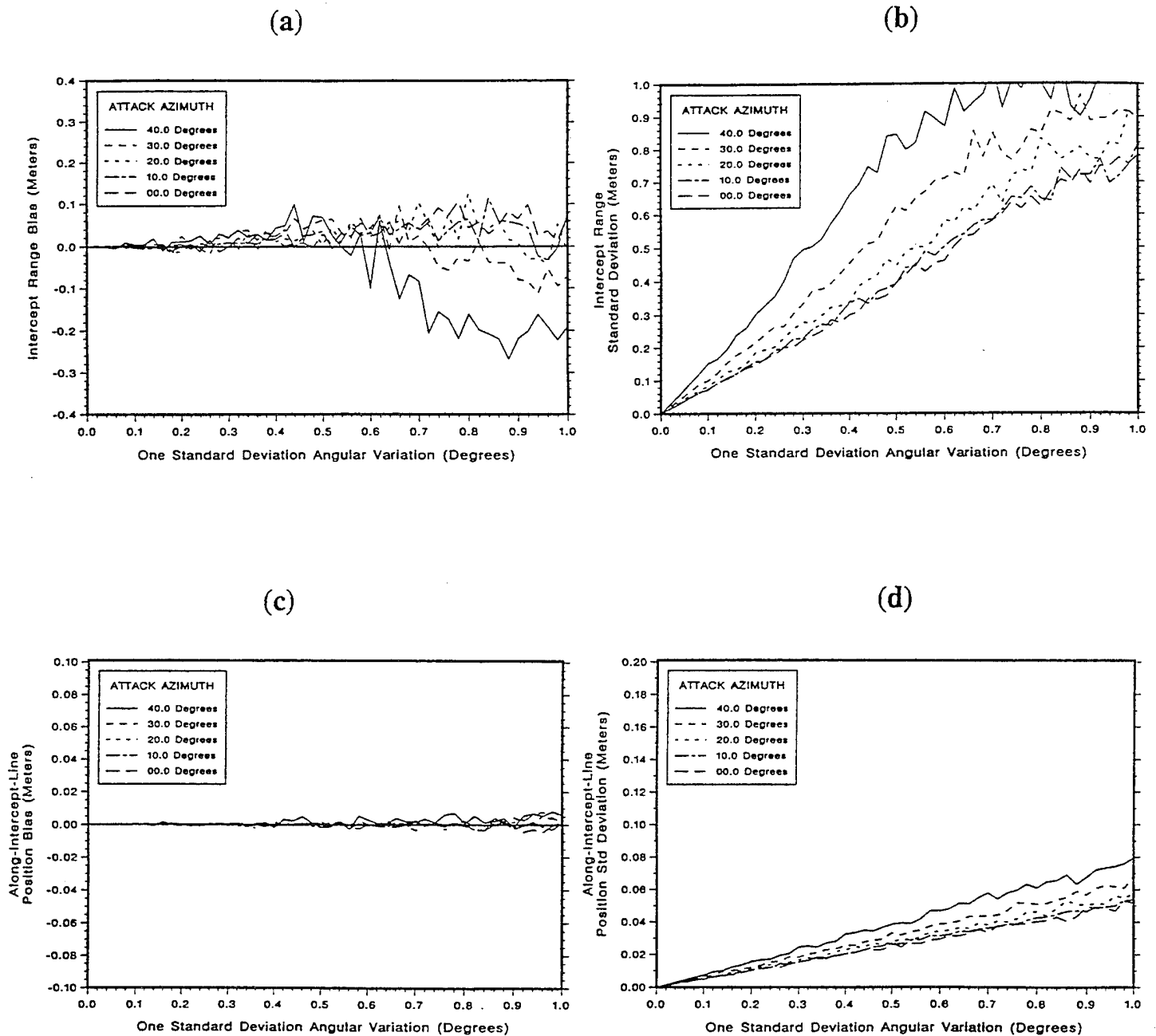
Figure A-2. LOB Tracker with 0.0 to 1.0 Degree Angular Variations, Recursive Least-Squares Estimation, 10 Meter Intercept: (a) Intercept Range Bias, (b) Intercept Range Standard Deviation, (c) Along-Intercept-Line Position Bias, and (d) Along-Intercept-Line Position Standard Deviation

67

LOB Sensors with Weighted
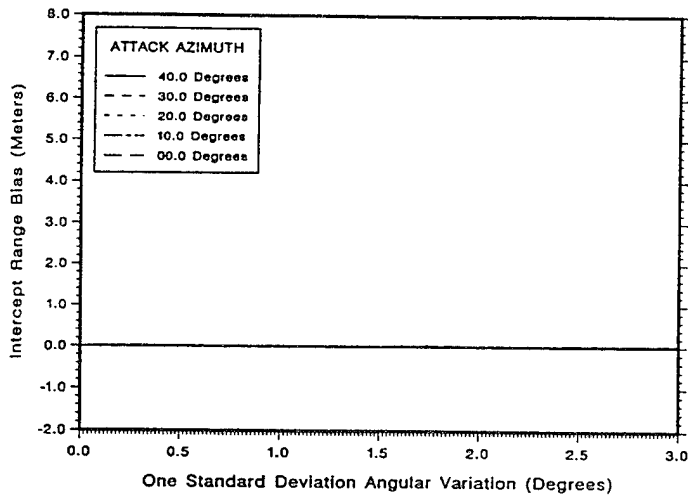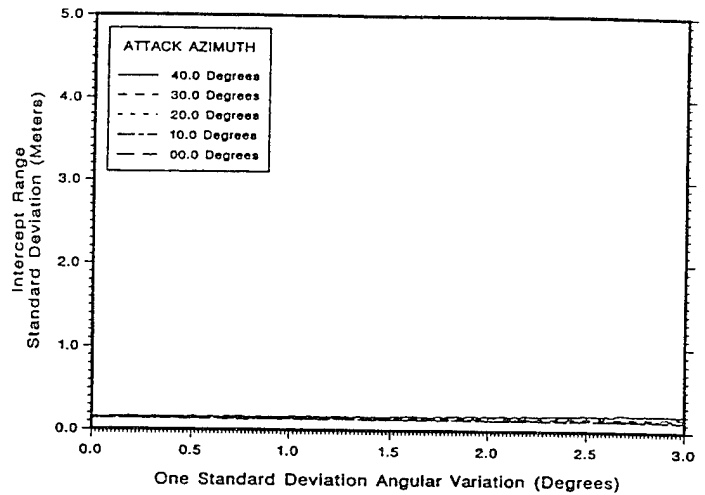## Least Squares Estimation

(a)
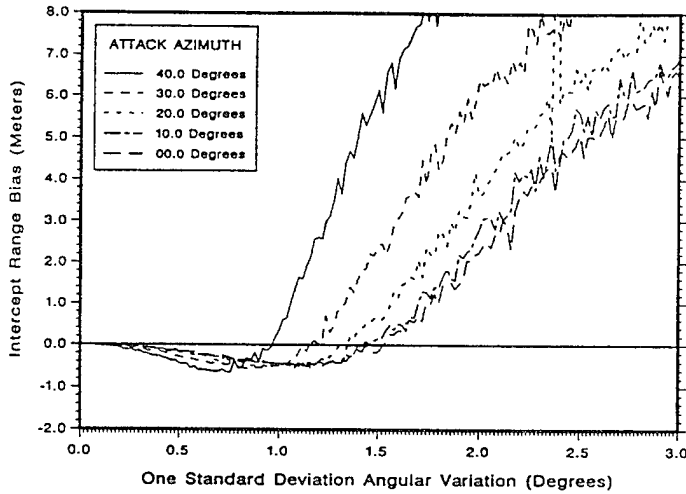
(b)
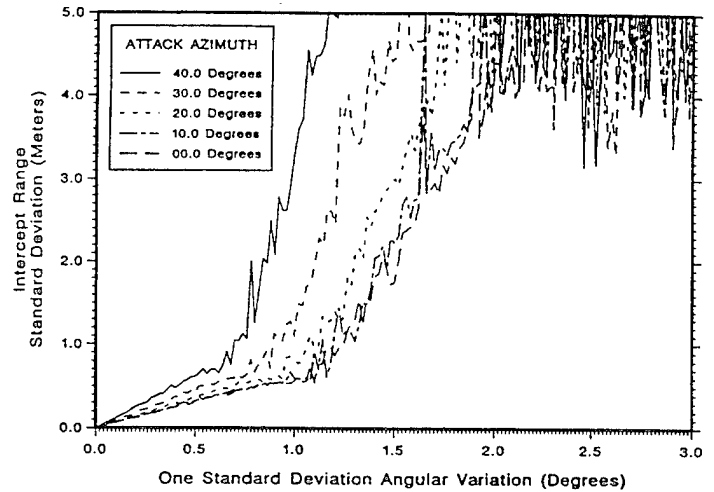
(c)
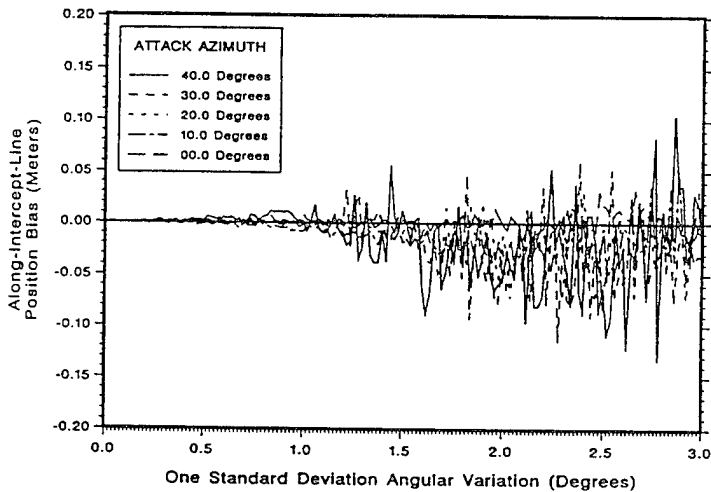
(d)
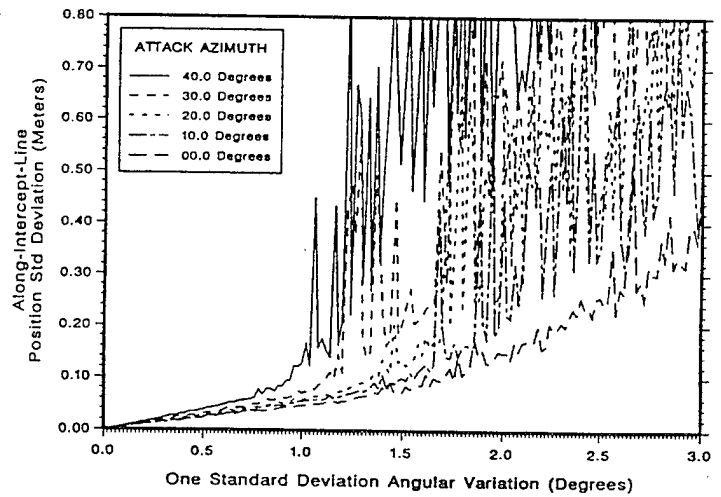
Figure A-3.   LOB Tracker with 0.0 to 3.0 Degree Angular Variations, Weighted Estimation, 10 Meter Intercept: (a) Intercept Range Bias, (b) Intercept Range Standard Deviation, (c) Along-Intercept-Line Position Bias, and (d) Along-Intercept-Line Position Standard Deviation

68

LOB Sensors with Weighted
Least Squares Estimation

(a)

(b)

(c)

(d)
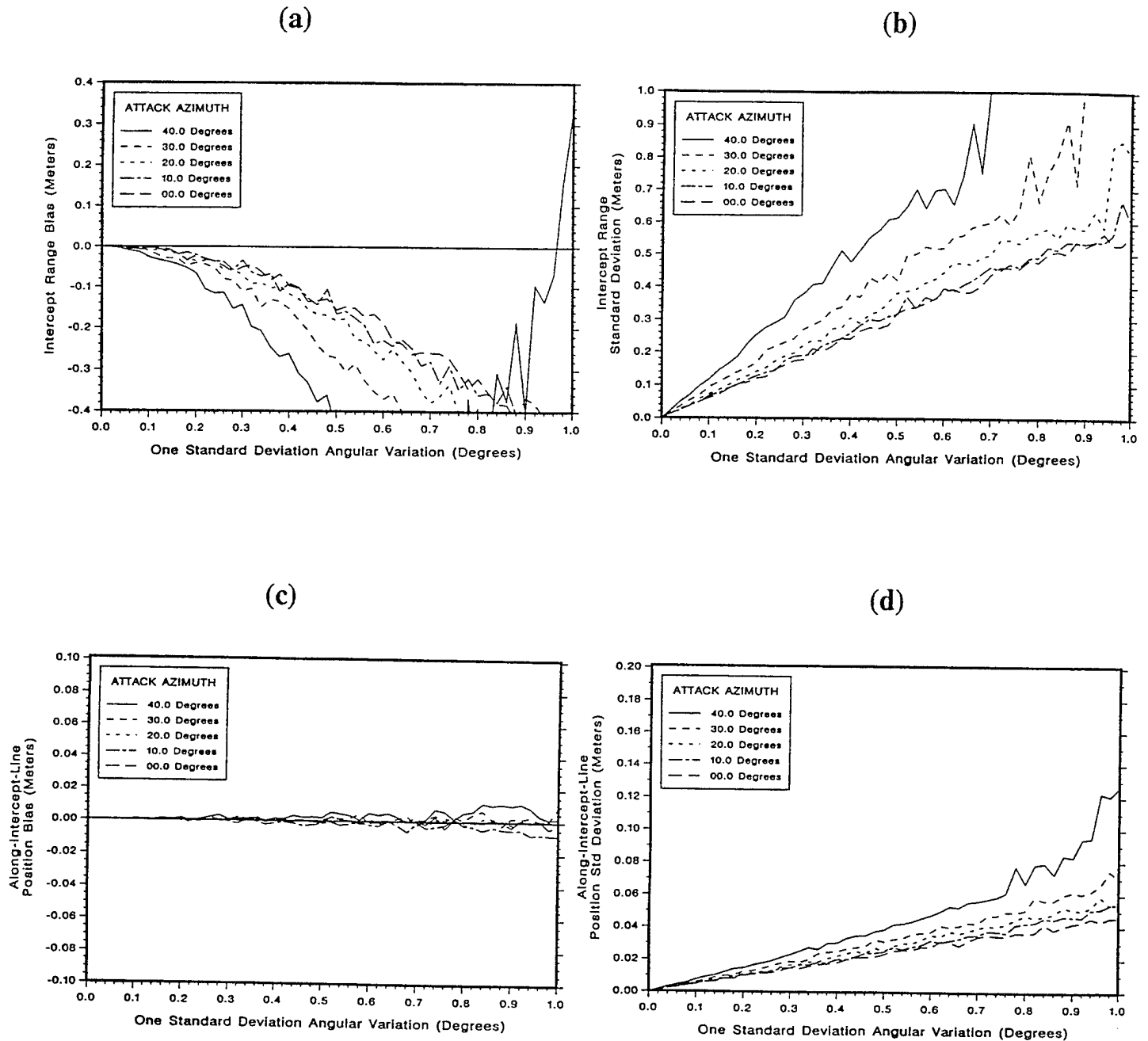
Figure A-4. LOB Tracker with 0.0 to 1.0 Degree Angular Variations, Weighted Estimation, 10 Meter Intercept: (a) Intercept Range Bias, (b) Intercept Range Standard Deviation, (c) Along-Intercept-Line Position Bias, and (d) Along-Intercept-Line Position Standard Deviation

69

LOB and Velocity Sensors
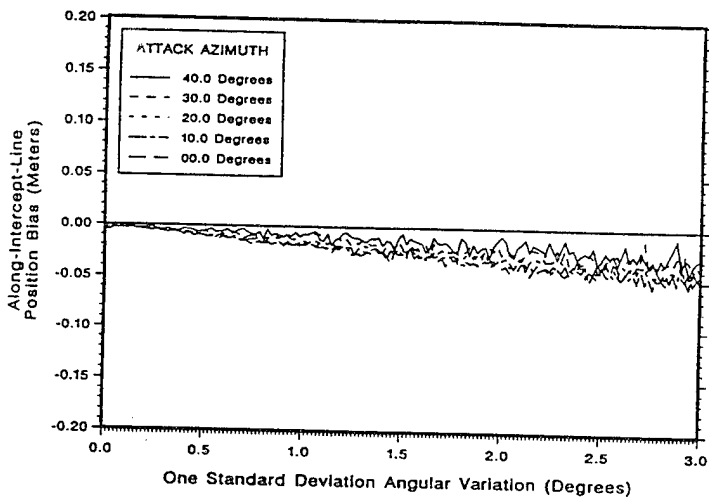## with Kalman Estimation

(a)
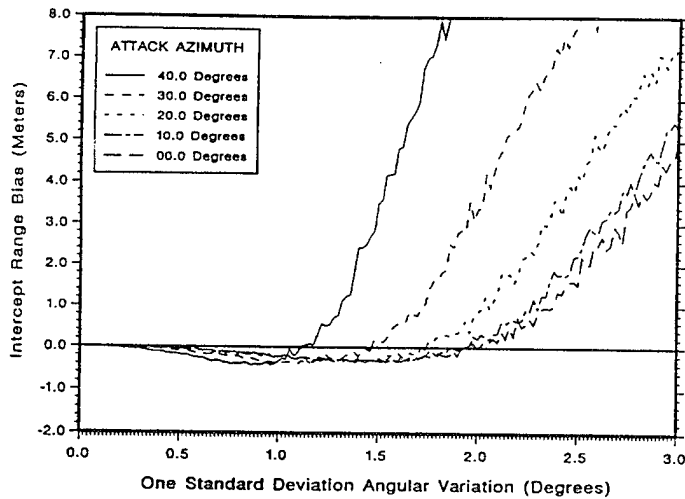
(b)
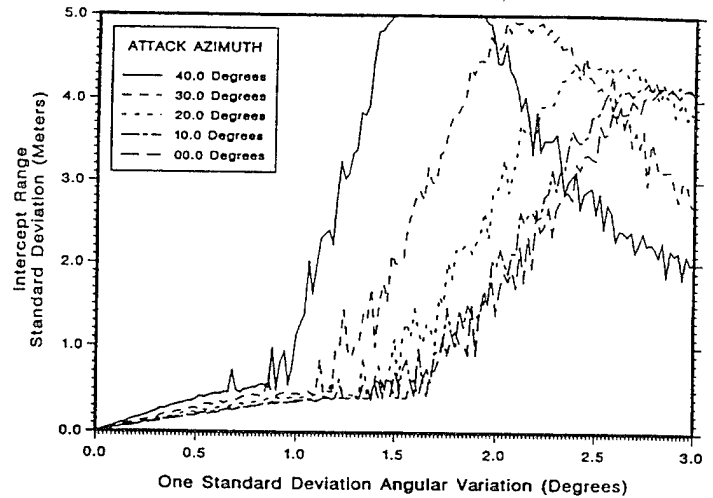
(c)
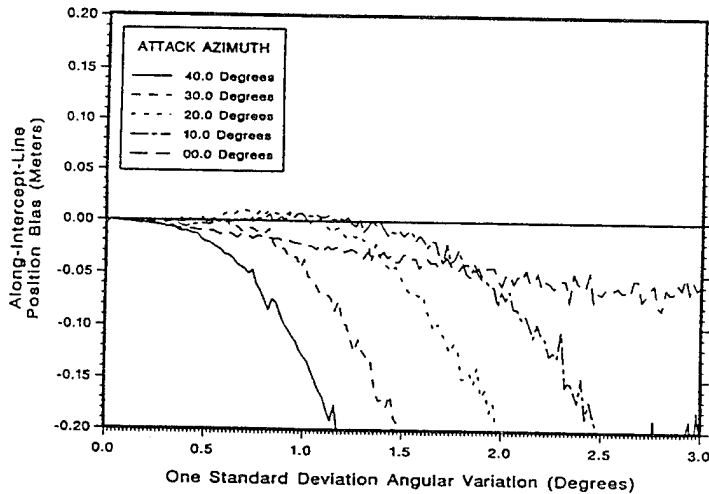
(d)
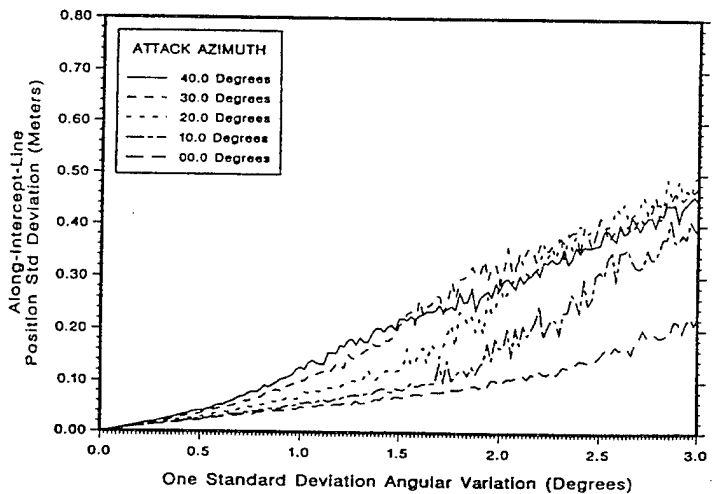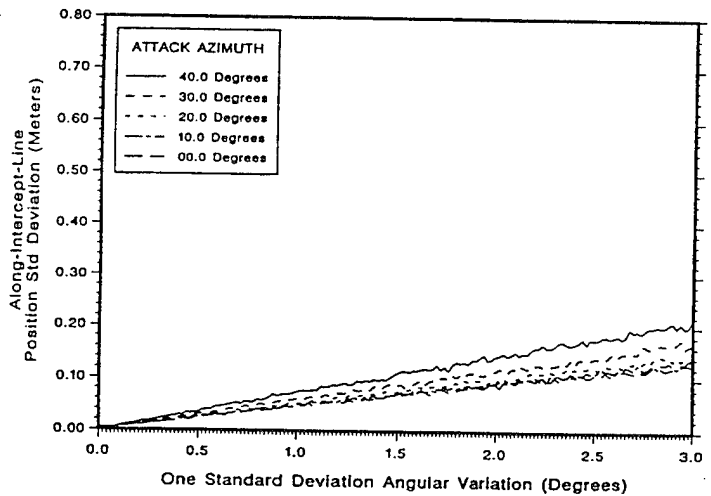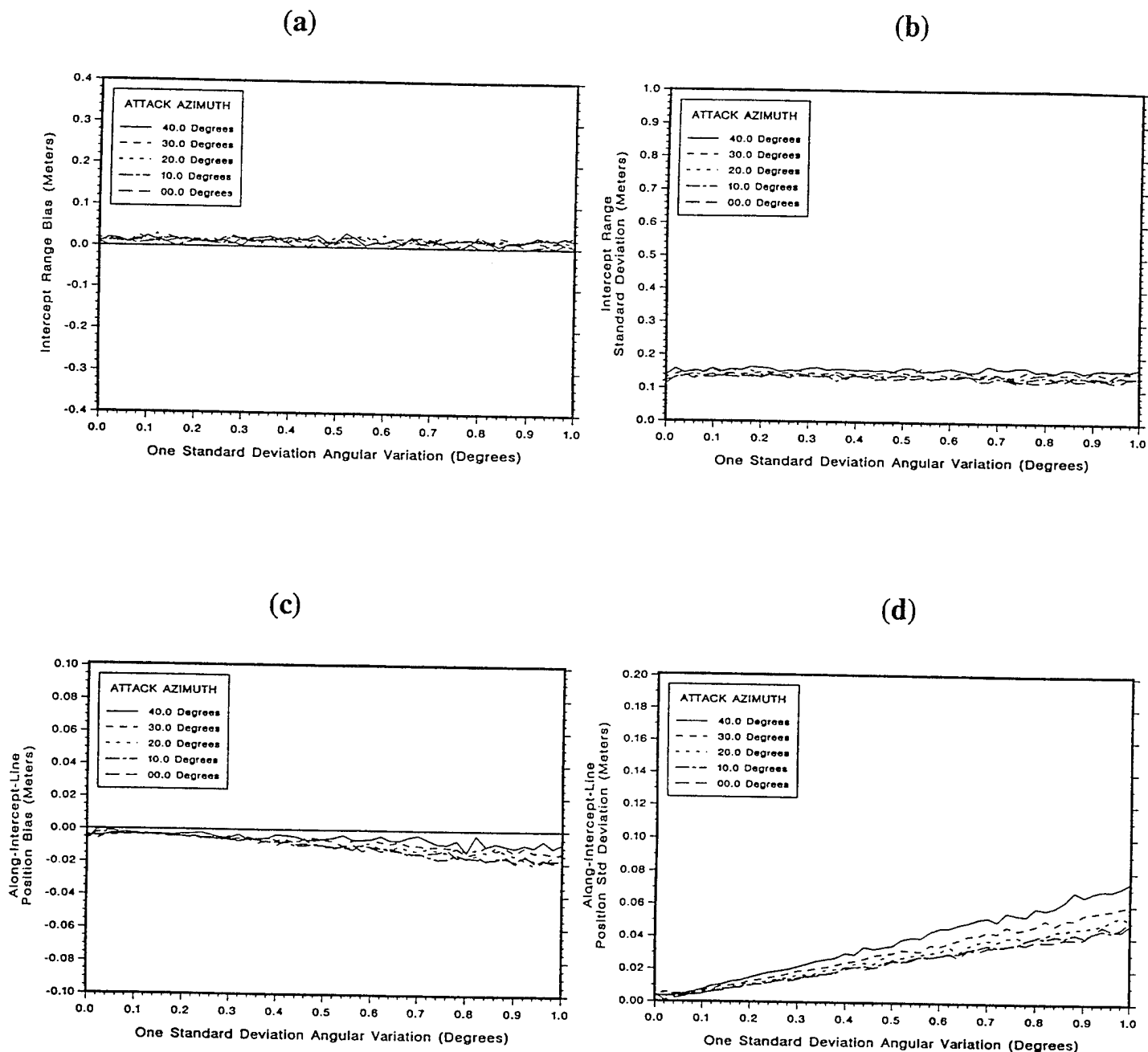

Figure A-5. LOB Tracker with 0.0 to 3.0 Degree Angular Variations, Includes Velocity
Sensor, Kalman Estimation, 10 Meter Intercept: (a) Intercept Range Bias,
(b) Intercept Range Standard Deviation, (c) Along-Intercept-Line Position
Bias, and (d) Along-Intercept-Line Position Standard Deviation

LOB and Velocity Sensors
with Kalman Estimation

(a)
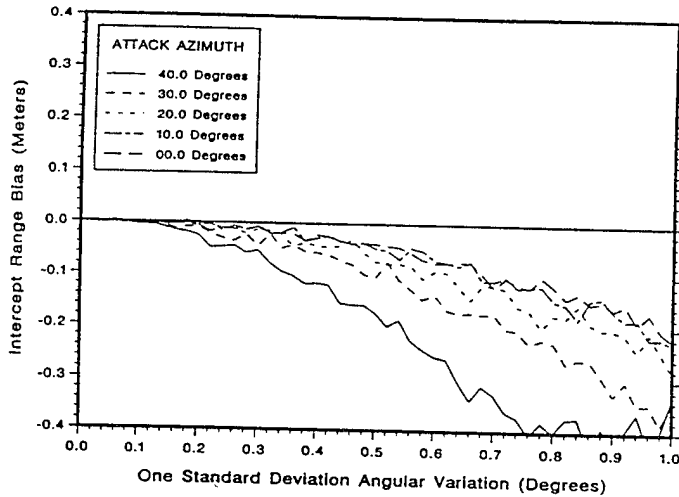
(b)
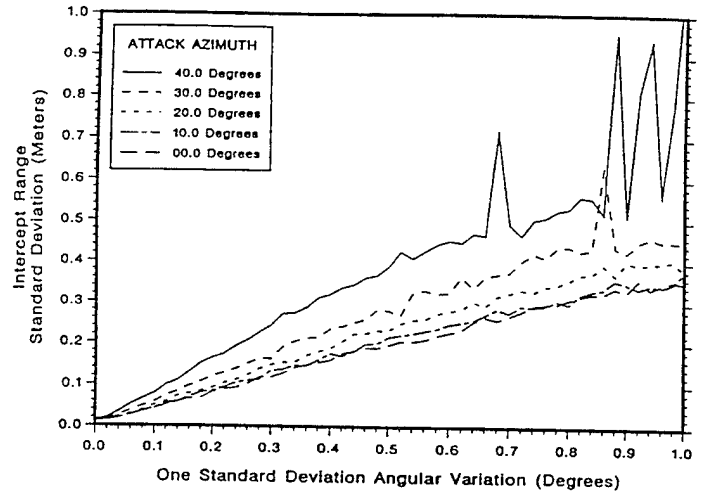
(c)
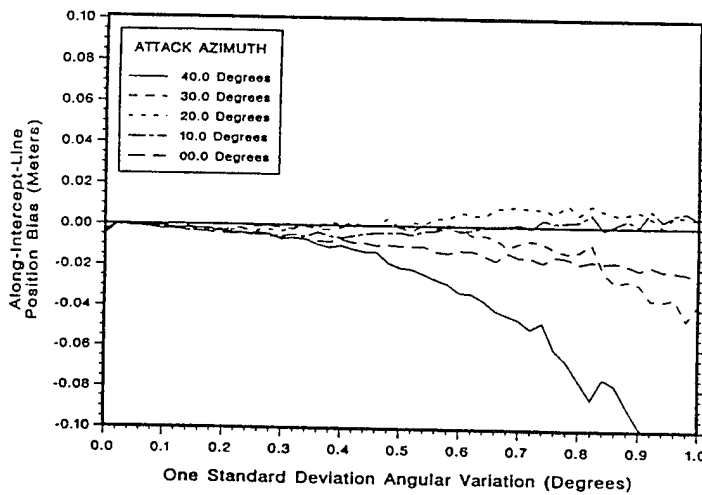
(d)
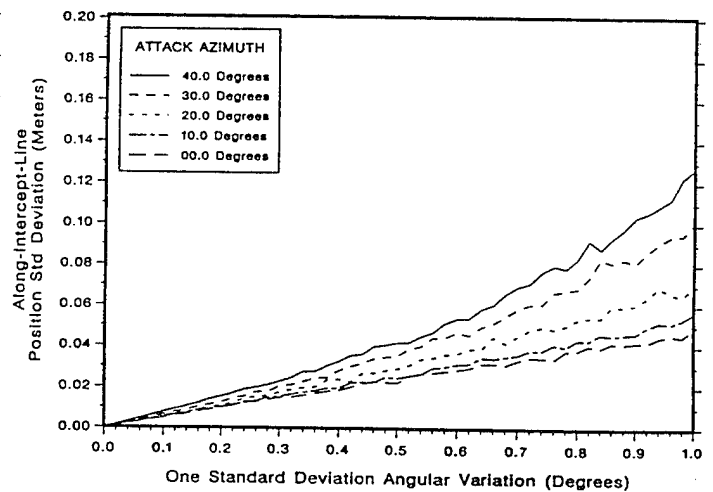
Figure A-6. LOB Tracker with 0.0 to 1.0 Degree Angular Variations, Includes Velocity Sensor, Kalman Estimation, 10 Meter Intercept: (a) Intercept Range Bias, (b) Intercept Range Standard Deviation, (c) Along-Intercept-Line Position Bias, and (d) Along-Intercept-Line Position Standard Deviation

71

LOB and Range Sensors with Recursive
Least Squares Estimation

(a)
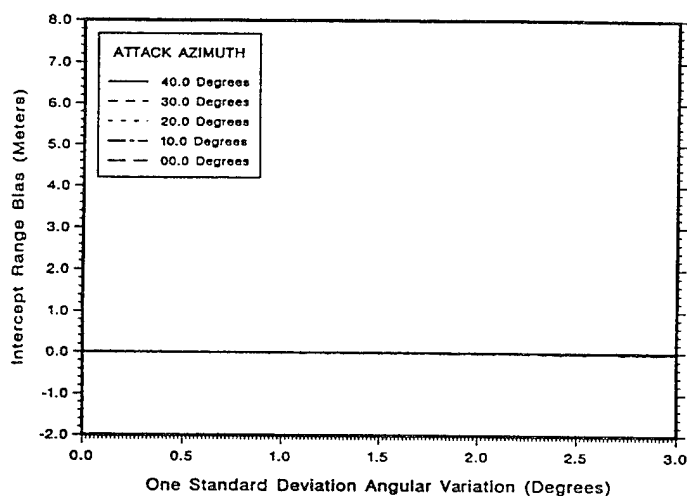
(b)
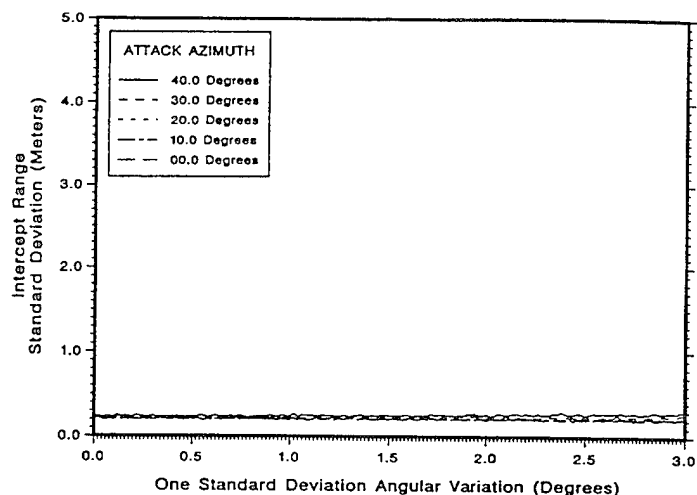
(c)
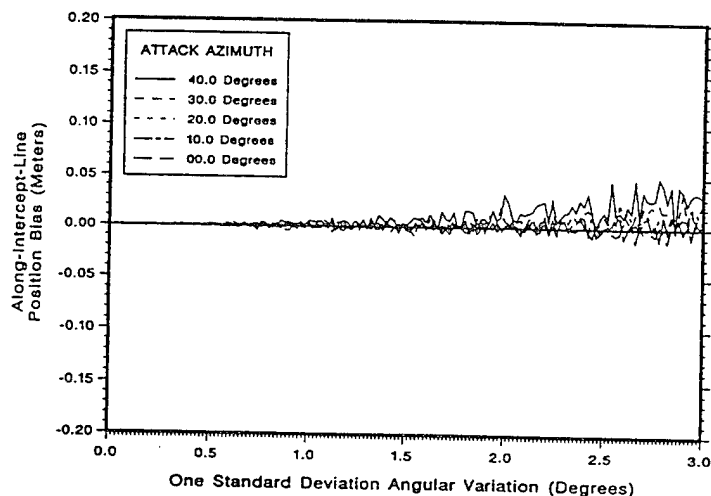
(d)
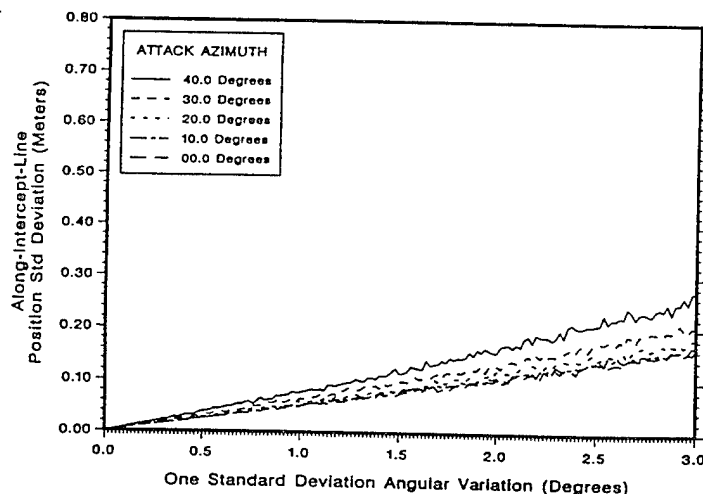
Figure A-7. LOB Tracker with 0.0 to 3.0 Degree Angular Variations, Includes Range Sensor, Recursive Least-Squares Estimation, 10 Meter Intercept: (a) Intercept Range Bias, (b) Intercept Range Standard Deviation, (c) Along-Intercept-Line Position Bias, and (d) Along-Intercept-Line Position Standard Deviation

LOB and Range Sensors with Recursive
Least Squares Estimation

(a)

(b)

(c)

(d)
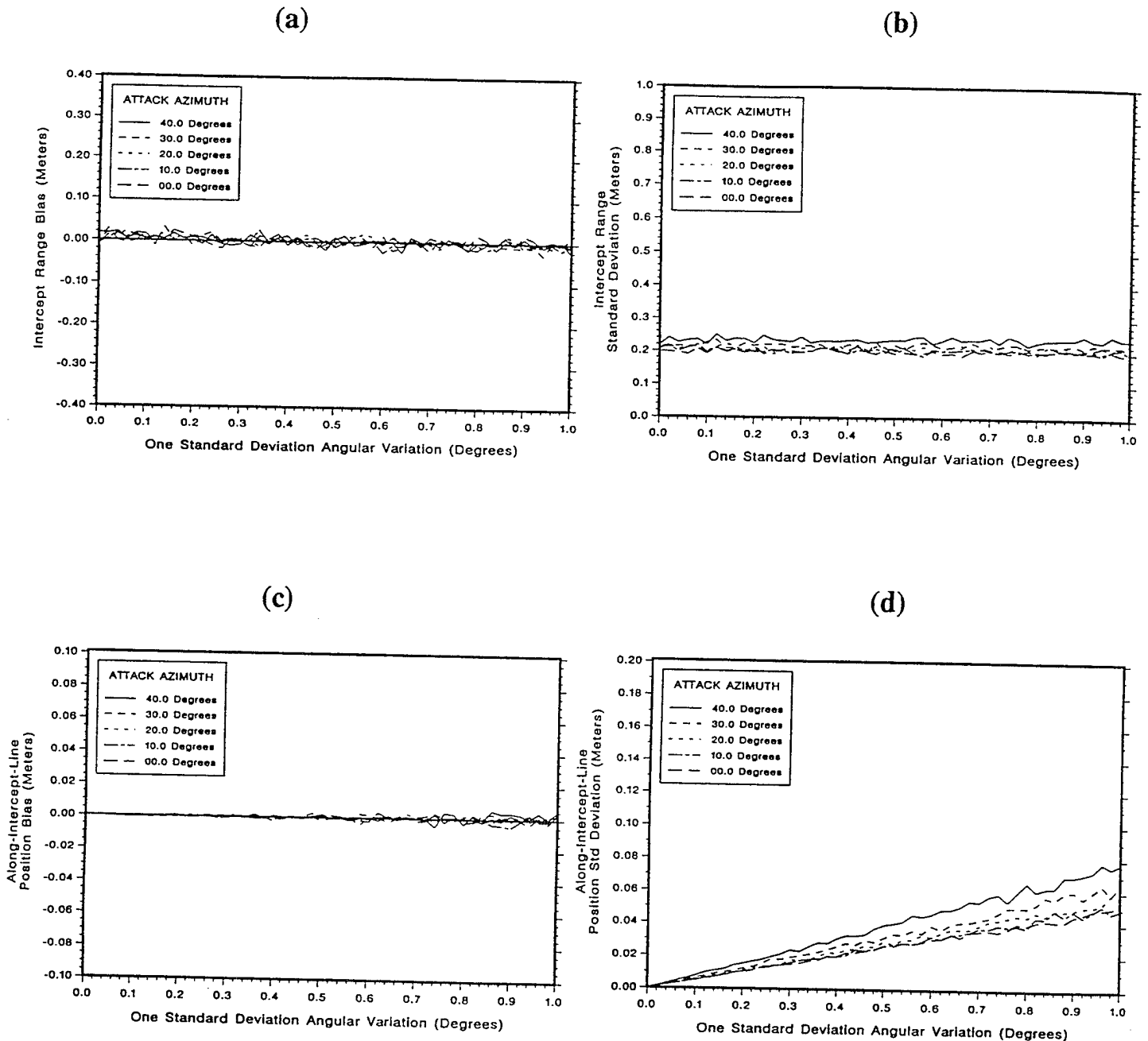
Figure A-8. LOB Tracker with 0.0 to 1.0 Degree Angular Variations, Includes Range
Sensor, Recursive Least-Squares Estimation, 10 Meter Intercept:
(a) Intercept Range Bias, (b) Intercept Range Standard Deviation,
(c) Along-Intercept-Line Position Bias, and (d) Along-Intercept-Line
Position Standard Deviation

73

LOB and Range Sensors with Weighted
Least Squares Estimation

(a)
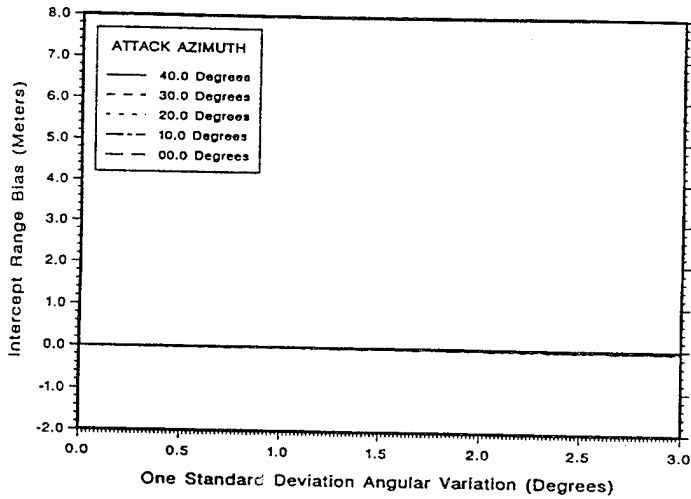
(b)
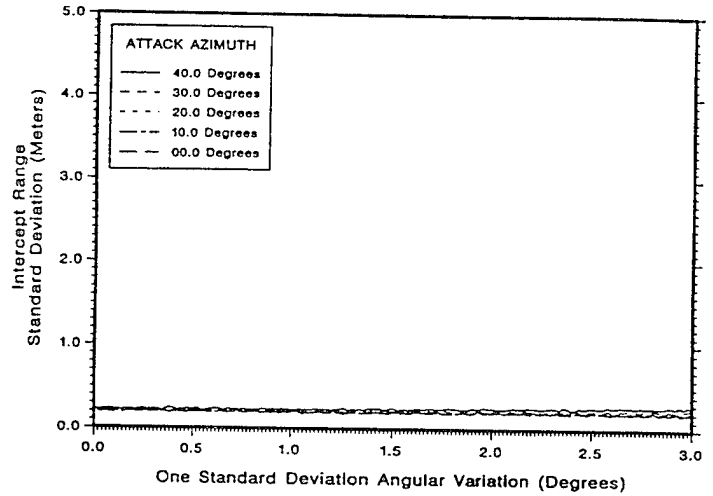
(c)

(d)

Figure A-9. LOB Tracker with 0.0 to 3.0 Degree Angular Variations, Includes Range Sensor, Weighted Estimation, 10 Meter Intercept: (a) Intercept Range Bias, (b) Intercept Range Standard Deviation, (c) Along-Intercept-Line Position Bias, and (d) Along-Intercept-Line Position Standard Deviation

74

LOB and Range Sensors with Weighted
Least Squares Estimation

(a)

(b)

(c)

(d)

Figure A-10. LOB Tracker with 0.0 to 1.0 Degree Angular Variations, Includes Range Sensor, Weighted Estimation, 10 Meter Intercept: (a) Intercept Range Bias, (b) Intercept Range Standard Deviation, (c) Along-Intercept-Line Position Bias, and (d) Along-Intercept-Line Position Standard Deviation

LOB, Velocity, and Range Sensors
with Kalman Estimation

(a)

(b)

(c)

(d)

Figure A-11.   LOB Tracker with 0.0 to 3.0 Degree Angular Variations, Includes Velocity
and Range Sensors, Kalman Estimation, 10 Meter Intercept: (a) Intercept
Range Bias, (b) Intercept Range Standard Deviation, (c) Along-Intercept-Line
Position Bias, and (d) Along-Intercept-Line Position Standard Deviation

LOB, Velocity, and Range Sensors
with Kalman Estimation

(a)

(b)

(c)

(d)

Figure A-12. LOB Tracker with 0.0 to 1.0 Degree Angular Variations, Includes Velocity and Range Sensors, Kalman Estimation, 10 Meter Intercept: (a) Intercept Range Bias, (b) Intercept Range Standard Deviation, (c) Along-Intercept-Line Position Bias, and (d) Along-Intercept-Line Position Standard Deviation

77

INTENTIONALLY LEFT BLANK

APPENDIX B:

SIMULATION RESULTS FOR 5-METER INTERCEPT RANGE

INTENTIONALLY LEFT BLANK

This appendix provides plotted results from the LOB2D simulation model (discussed in section 5) for the discussions provided in section 7 of the report. Each figure in this appendix contains four plots:

a) Intercept range bias as a function of angular variation.

b) Intercept range standard variation as a function of angular variation.

c) Along-intercept-line position bias as a function of angular variation.

d) Along-intercept-line position standard deviation as a function of angular variation.

There are two figures (eight plots) for each of the six cases discussed in section 7:

a) Figures B-1 and B-2: LOB (angle-only sensors) system, recursive least squares estimation.

b) Figures B-3 and B-4: LOB (angle-only sensors) system, weighted least squares estimation.

c) Figures B-5 and B-6: LOB system with velocity sensor, Kalman estimation.

d) Figures B-7 and B-8: LOB system with range sensor, recursive least squares estimation.

e) Figures B-9 and B-10: LOB system with range sensor, weighted least squares estimation.

f) Figures B-11 and B-12: LOB system with velocity and range sensors, Kalman estimation.

LOB Sensors with Recursive
Least Squares Estimation

(a)
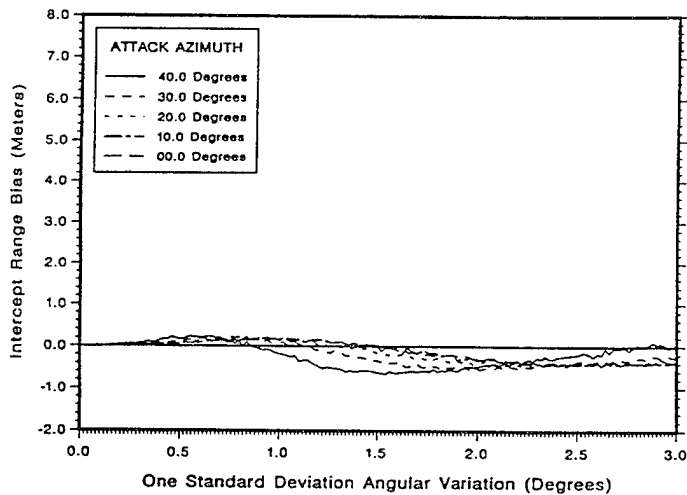
(b)
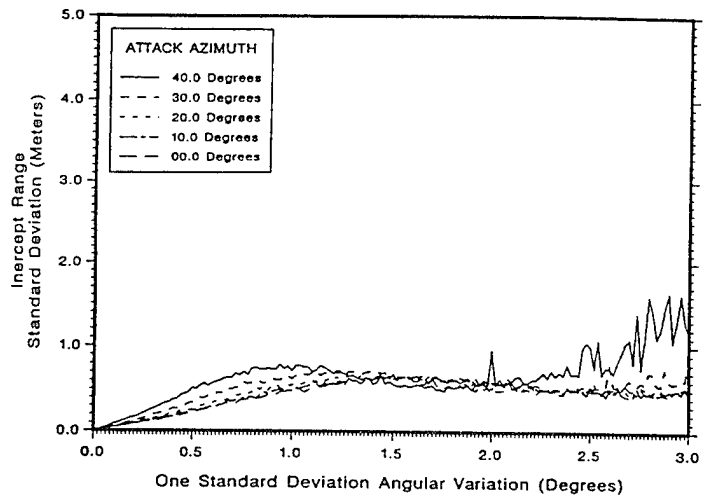
(c)
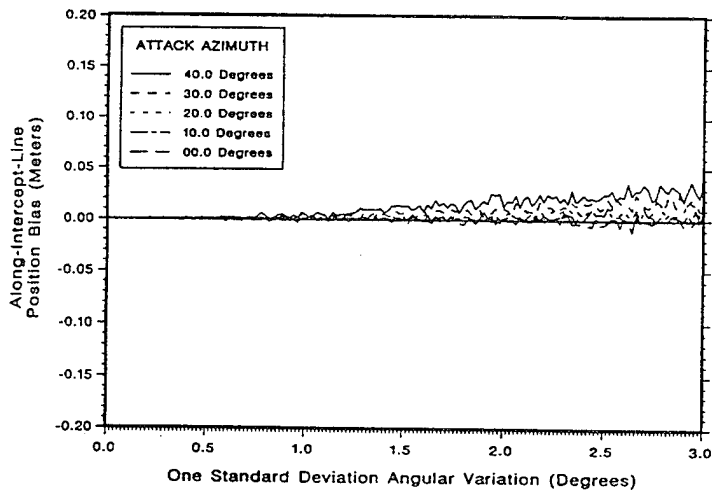
(d)
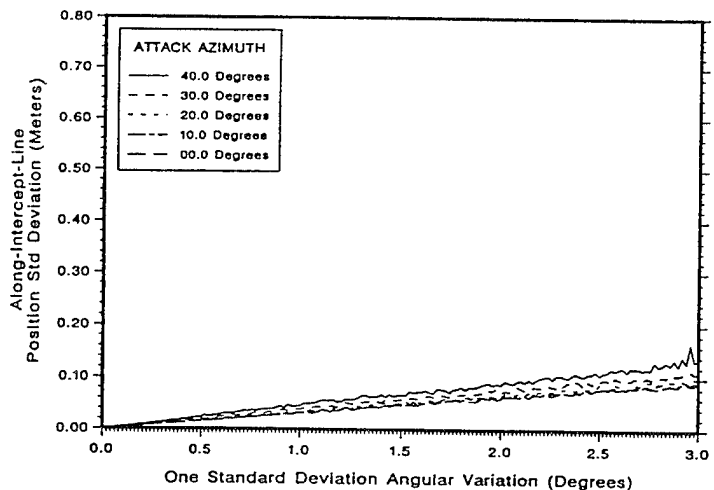
Figure B-1. LOB Tracker with 0.0 to 3.0 Degree Angular Variations, Recursive Least-Squares Estimation, 5 Meter Intercept: (a) Intercept Range Bias, (b) Intercept Range Standard Deviation, (c) Along-Intercept-Line Position Bias, and (d) Along-Intercept-Line Position Standard Deviation

82

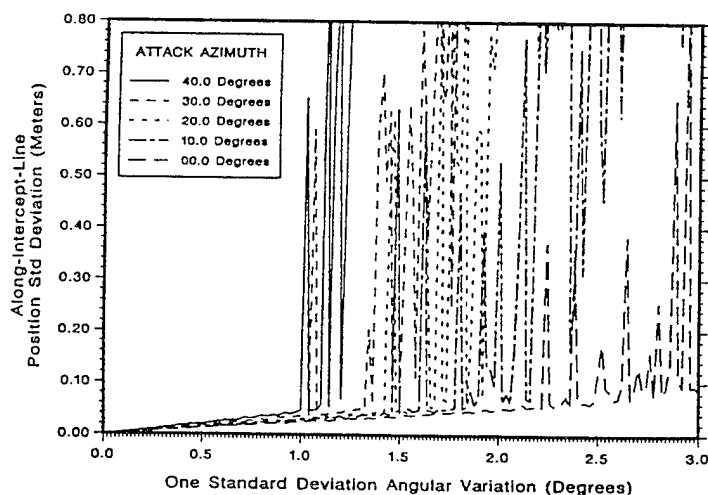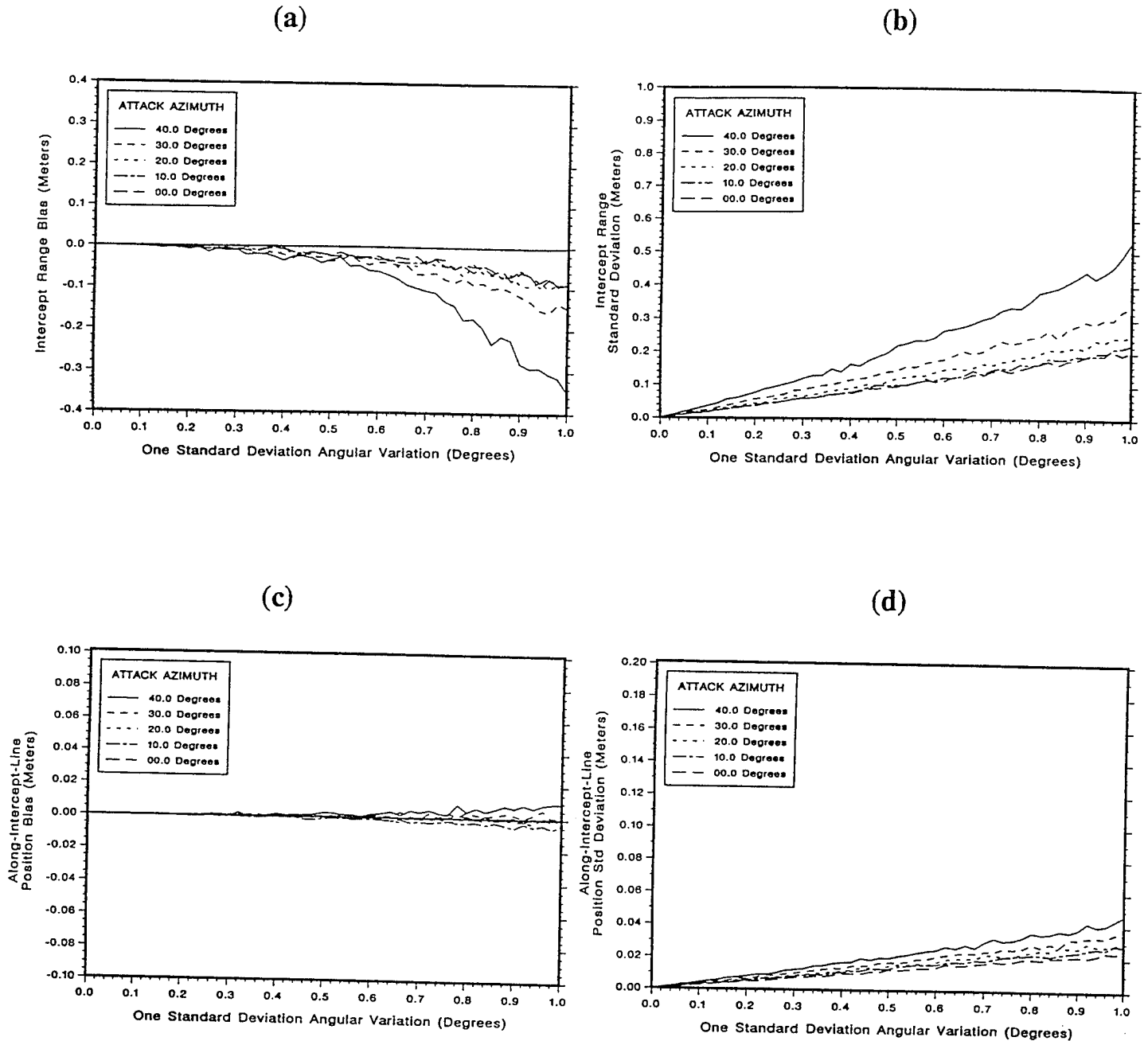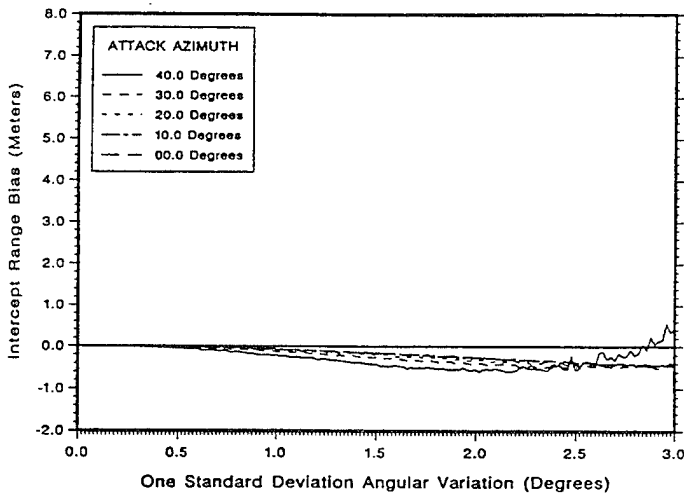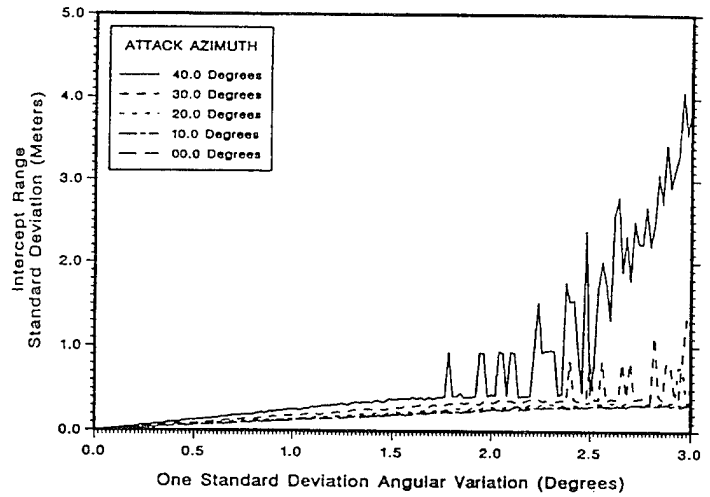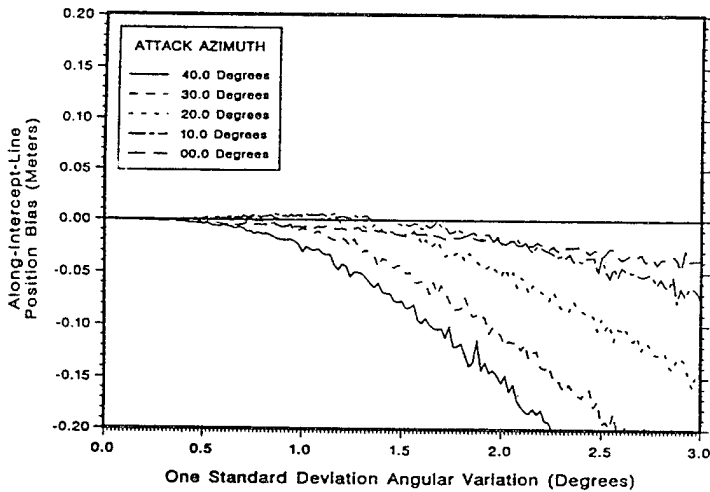## LOB Sensors with Recursive
Least Squares Estimation

(a)

(b)

(c)

(d)
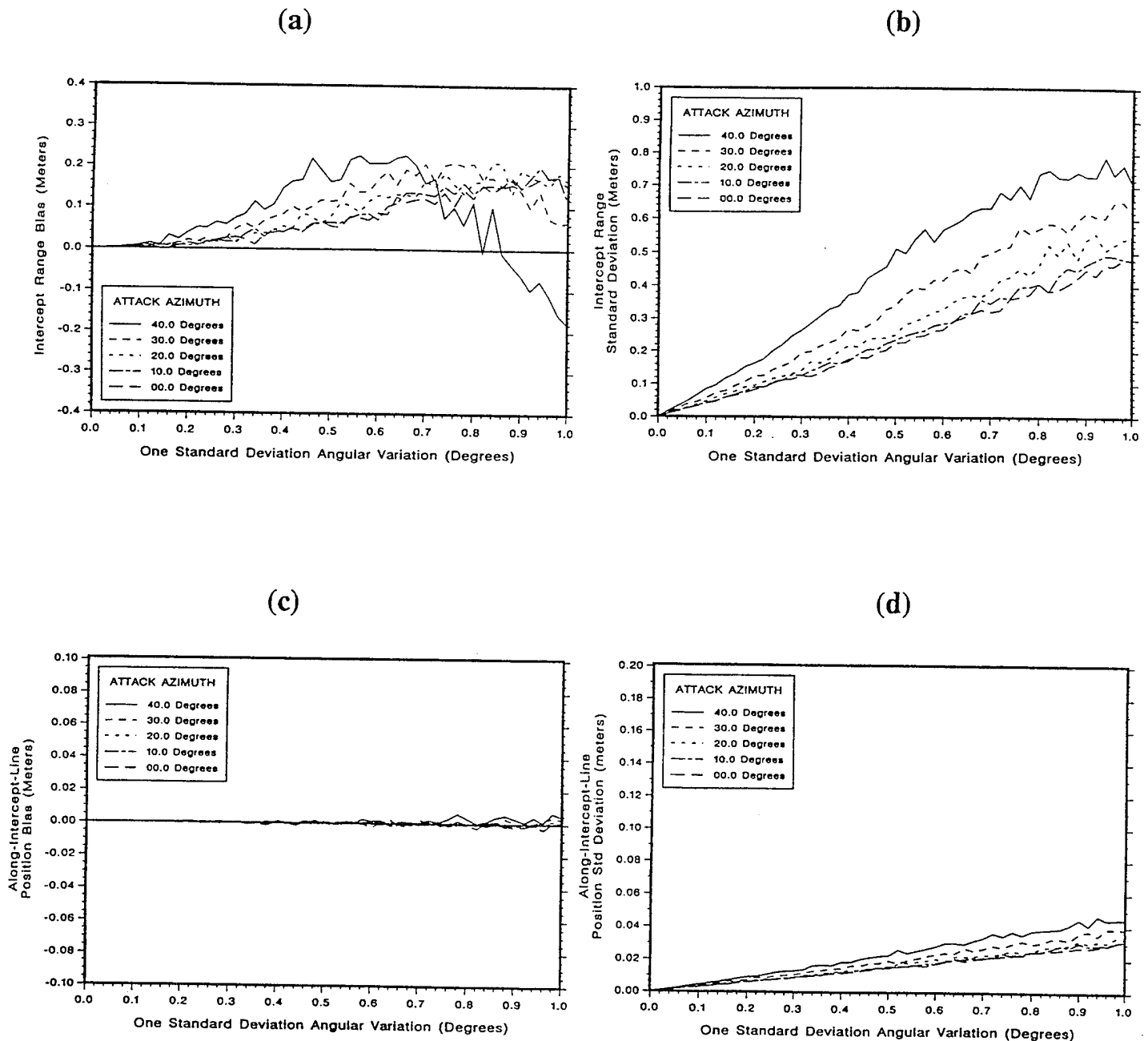
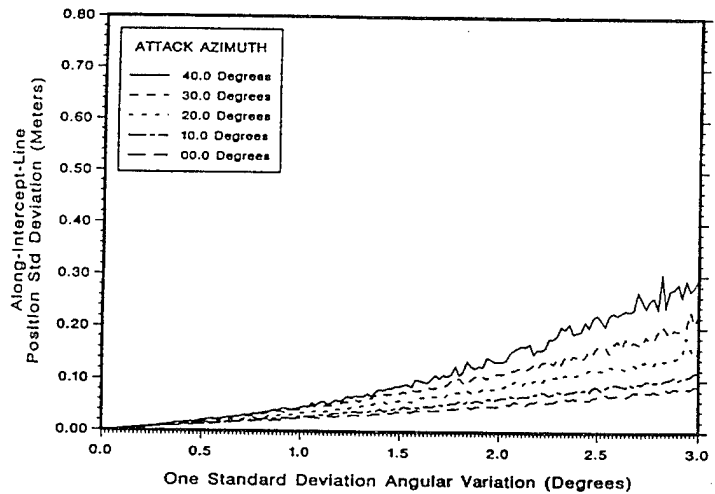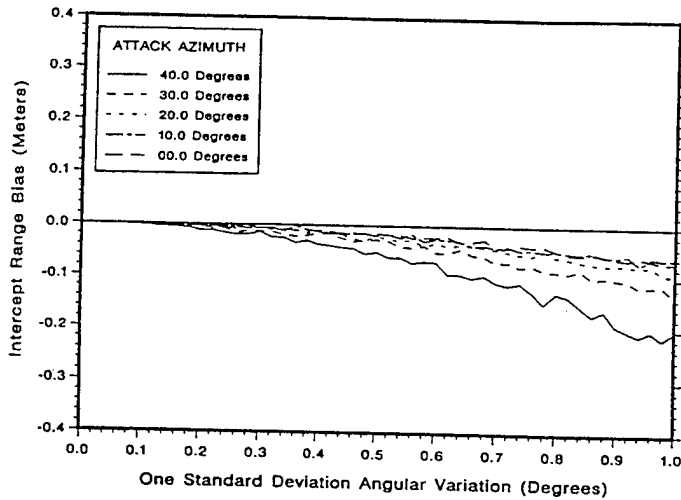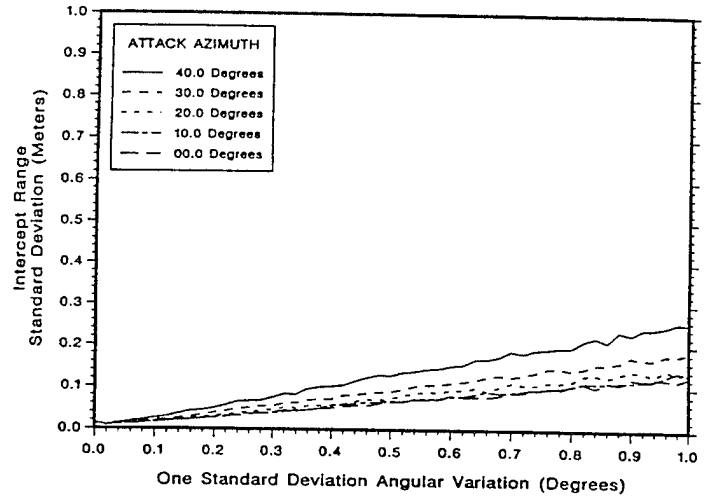**Figure B-2.** LOB Tracker with 0.0 to 1.0 Degree Angular Variations, Recursive Least-Squares Estimation, 5 Meter Intercept: (a) Intercept Range Bias, (b) Intercept Range Standard Deviation, (c) Along-Intercept-Line Position Bias, and (d) Along-Intercept-Line Position Standard Deviation

LOB Sensors with Weighted
Least Squares Estimation

(a)
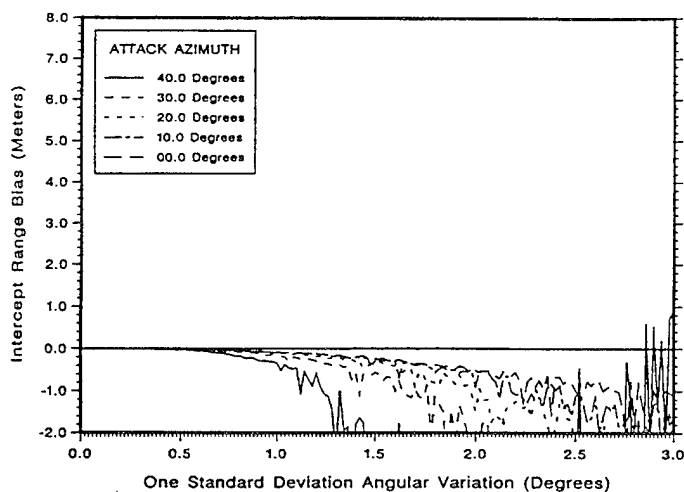
(b)
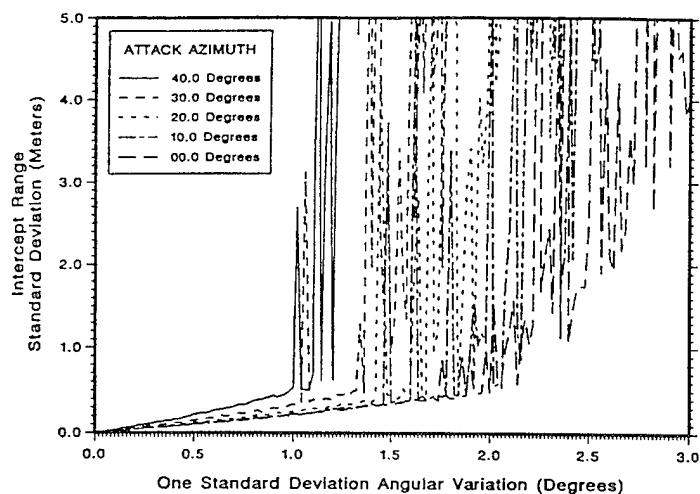
(c)
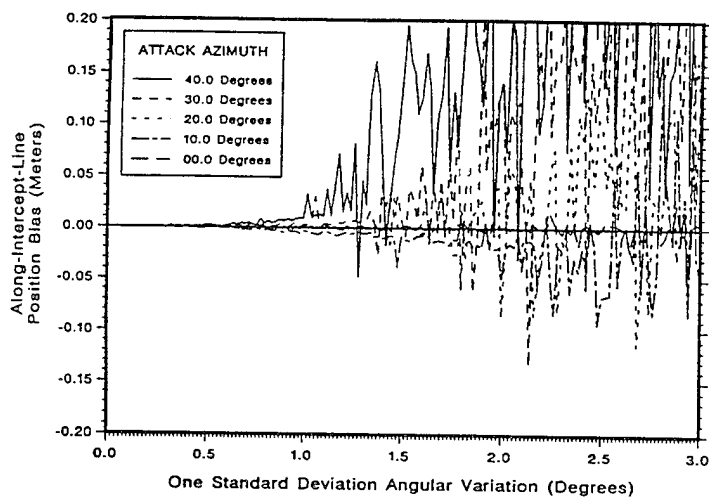
(d)

Figure B-3.   LOB Tracker with 0.0 to 3.0 Degree Angular Variations, Weighted Estimation, 5 Meter Intercept: (a) Intercept Range Bias, (b) Intercept Range Standard Deviation, (c) Along-Intercept-Line Position Bias, and (d) Along-Intercept-Line Position Standard Deviation

84

LOB Sensors with Weighted
Least Squares Estimation

(a)

(b)

(c)

(d)

Figure B-4. LOB Tracker with 0.0 to 1.0 Degree Angular Variations, Weighted Estimation, 5 Meter Intercept: (a) Intercept Range Bias, (b) Intercept Range Standard Deviation, (c) Along-Intercept-Line Position Bias, and (d) Along-Intercept-Line Position Standard Deviation

85

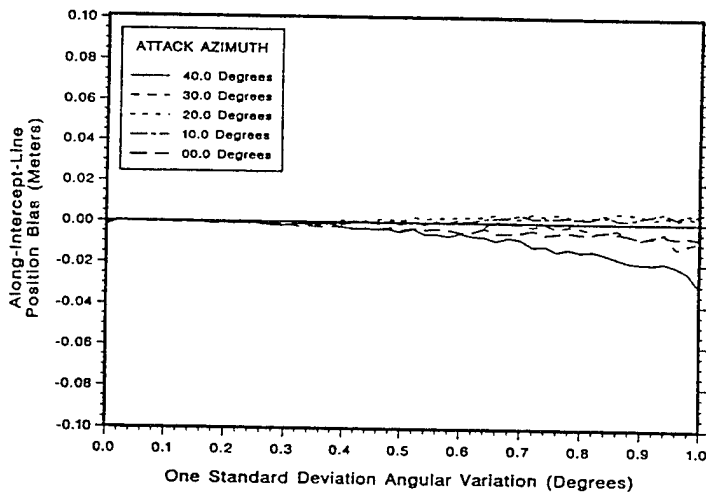# LOB and Velocity Sensors
with Kalman Estimation

(a)
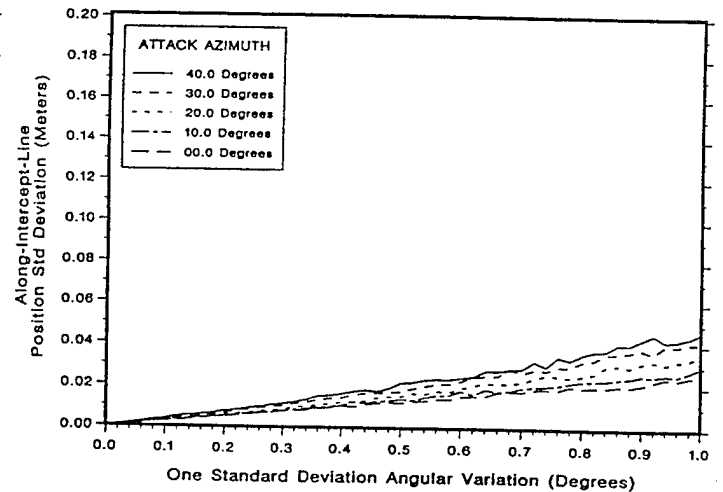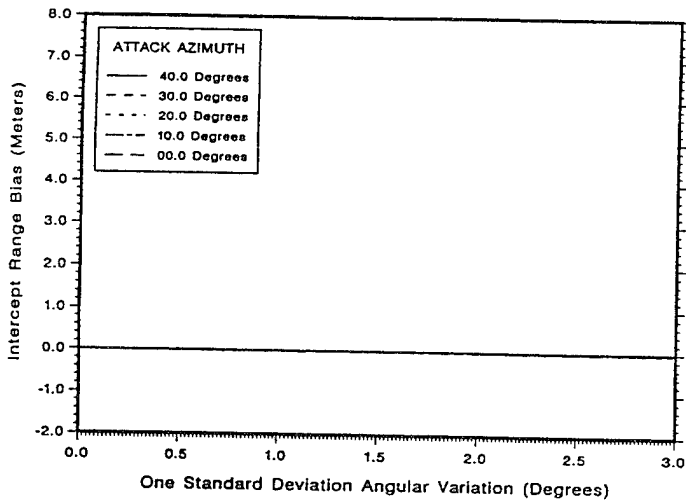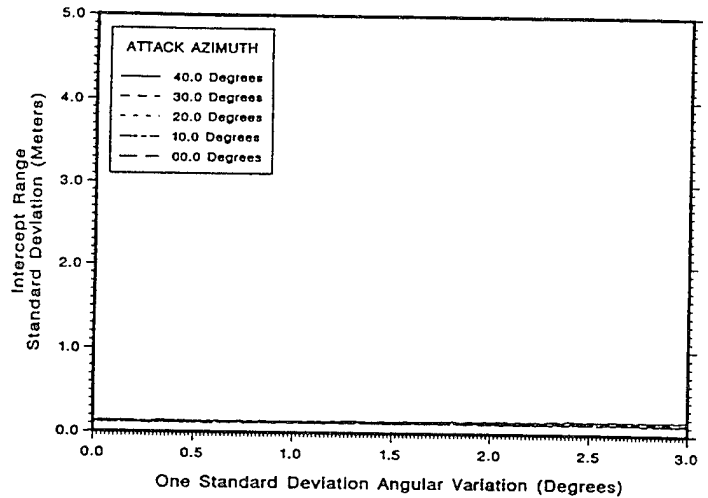
(b)

(c)

(d)

Figure B-5. LOB Tracker with 0.0 to 3.0 Degree Angular Variations, Includes Velocity Sensor, Kalman Estimation, 5 Meter Intercept: (a) Intercept Range Bias, (b) Intercept Range Standard Deviation, (c) Along-Intercept-Line Position Bias, and (d) ong-Intercept-Line Position Standard Deviation

LOB and Velocity Sensors
with Kalman Estimation

(a)

(b)

(c)

(d)

Figure B-6. LOB Tracker with 0.0 to 1.0 Degree Angular Variations, Includes Velocity Sensor, Kalman Estimation, 5 Meter Intercept: (a) Intercept Range Bias, (b) Intercept Range Standard Deviation, (c) Along-Intercept-Line Position Bias, and (d) Along-Intercept-Line Position Standard Deviation

LOB and Range Sensors with Recursive
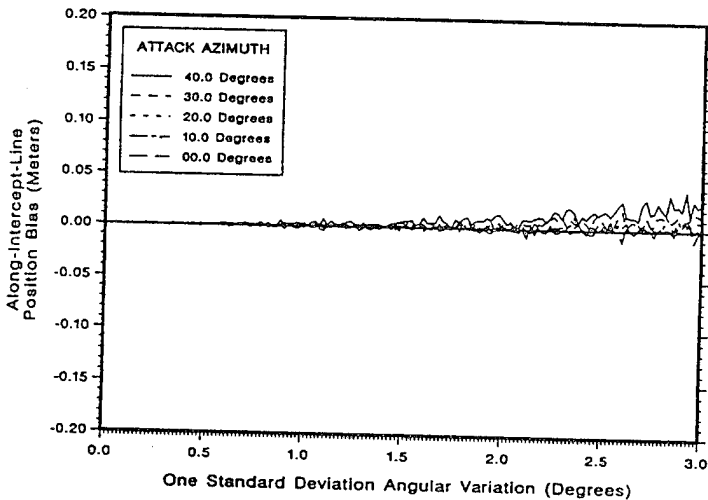# Least Squares Estimation
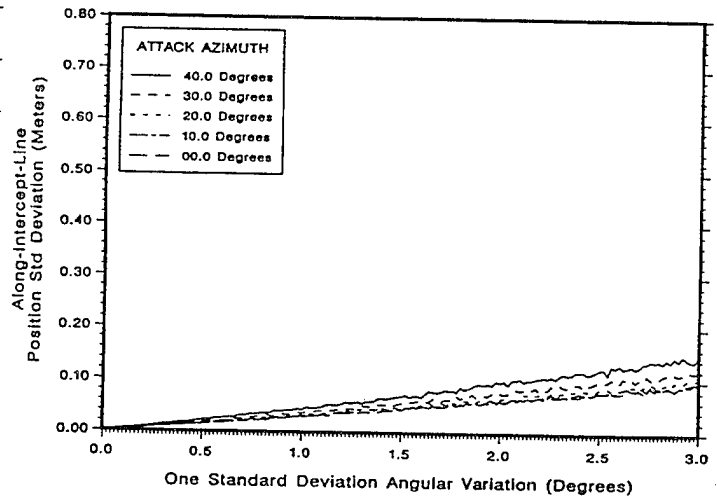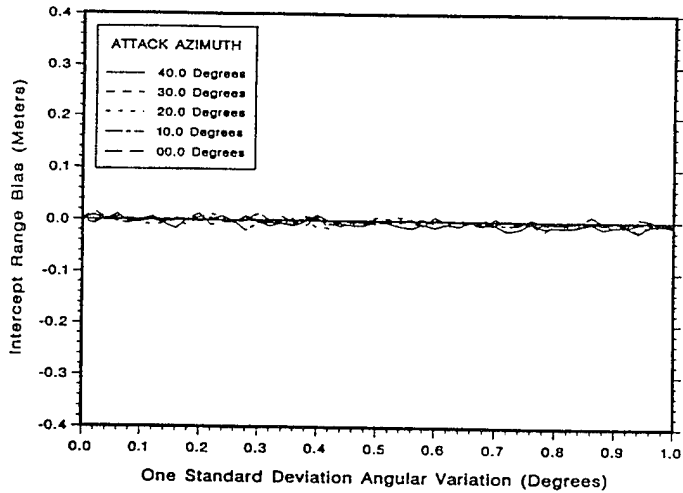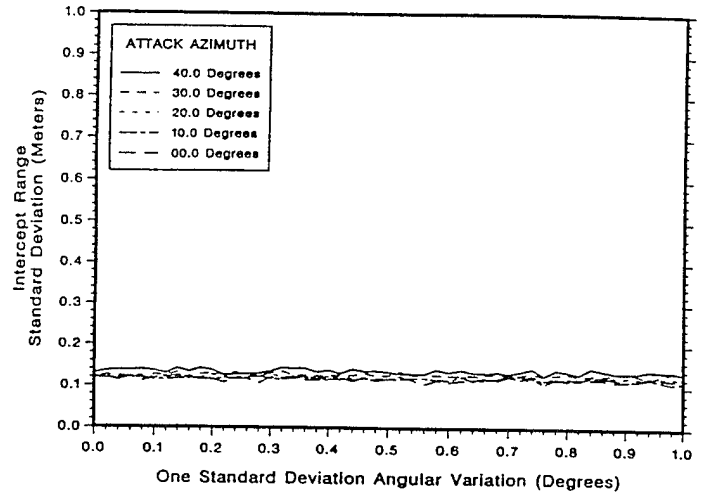
(a)

(b)

(c)

(d)

Figure B-7.   LOB Tracker with 0.0 to 3.0 Degree Angular Variations, Includes Range
Sensor, Recursive Least-Squares Estimation, 5 Meter Intercept:
(a) Intercept Range Bias, (b) Intercept Range Standard Deviation,
(c) Along-Intercept-Line Position Bias, and (d) Along-Intercept-Line
Position Standard Deviation

LOB and Range Sensors with Recursive
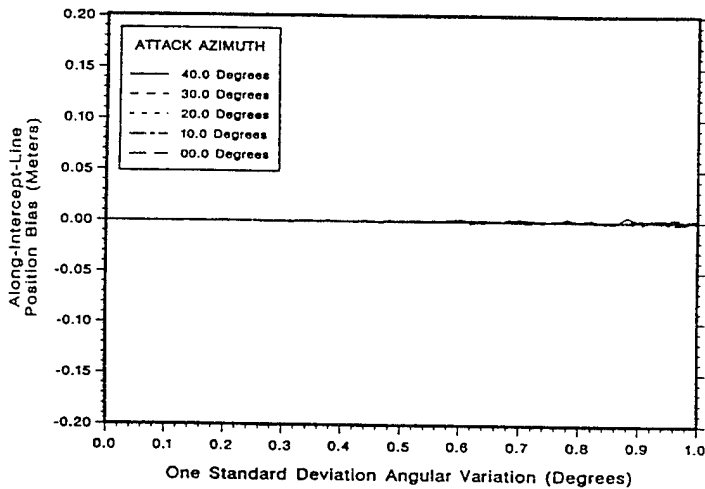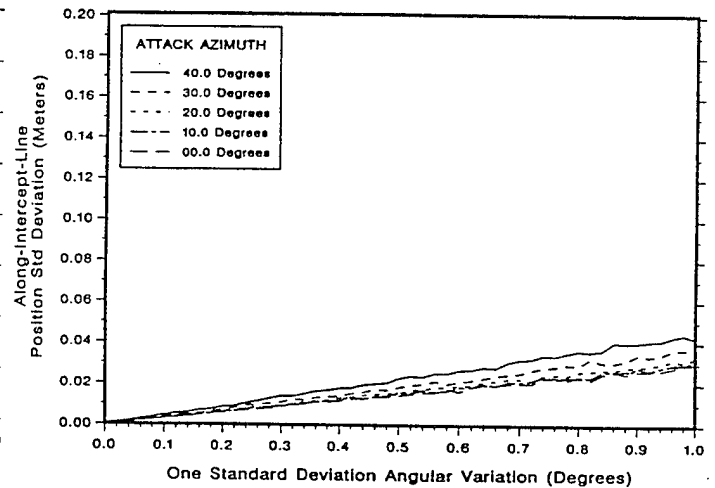# Least Squares Estimation
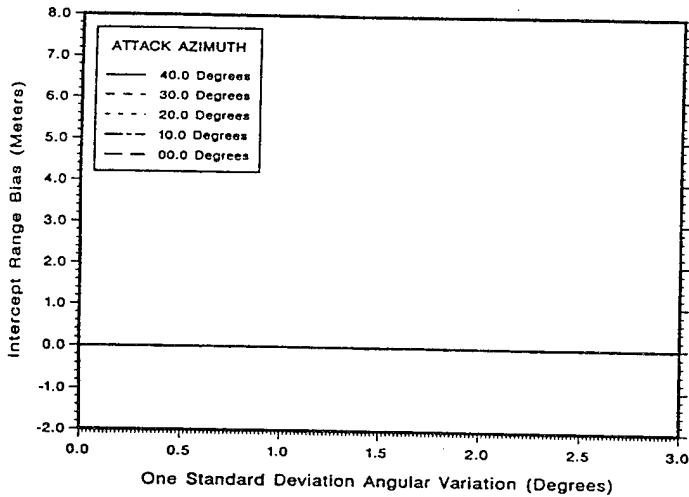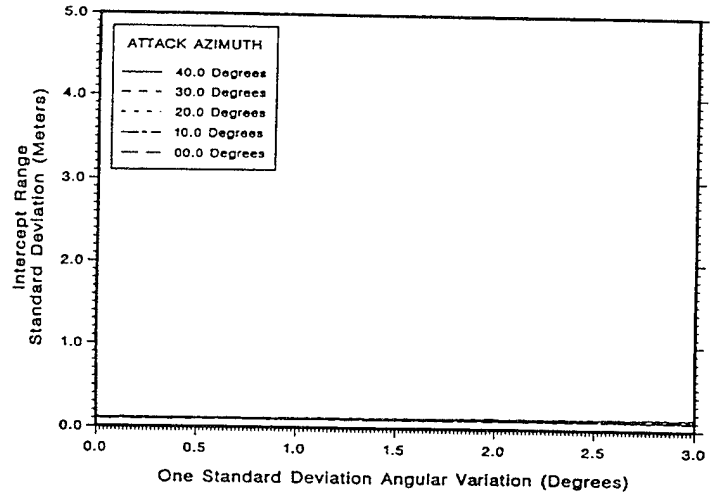
(a)

(b)

(c)

(d)

Figure B-8.   LOB Tracker with 0.0 to 1.0 Degree Angular Variations, Includes Range
Sensor, Recursive Least-Squares Estimation, 5 Meter Intercept:
(a) Intercept Range Bias, (b) Intercept Range Standard Deviation,
(c) Along-Intercept-Line Position Bias, and (d) Along-Intercept-Line
Position Standard Deviation

89

LOB and Range Sensors with Weighted
Least Squares Estimation

(a)

(b)

(c)

(d)

Figure B-9. LOB Tracker with 0.0 to 3.0 Degree Angular Variations, Includes Range Sensor, Weighted Estimation, 5 Meter Intercept: (a) Intercept Range Bias, (b) Intercept Range Standard Deviation, (c) Along-Intercept-Line Position Bias, and (d) Along-Intercept-Line Position Standard Deviation

LOB and Range Sensors with Weighted
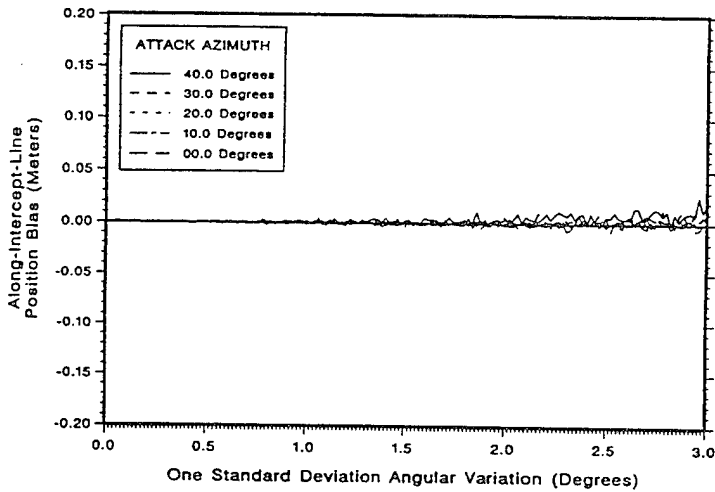# Least Squares Estimation
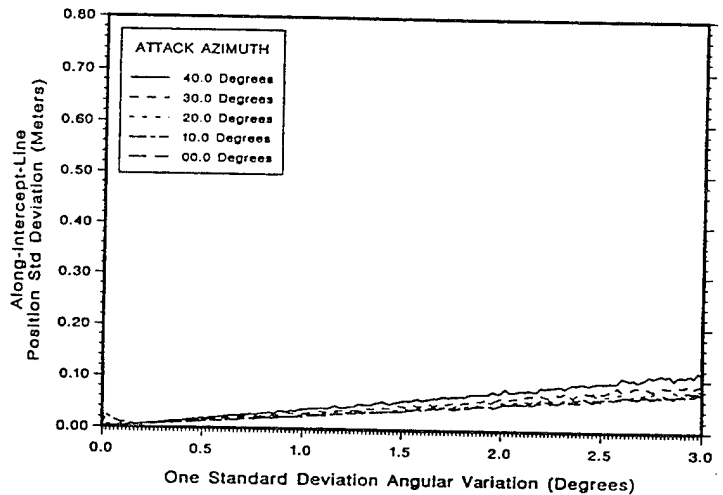
(a)

(b)

(c)

(d)

Figure B-10. LOB Tracker with 0.0 to 1.0 Degree Angular Variations, Includes Range
Sensor, Weighted Estimation, 5 Meter Intercept: (a) Intercept Range
Bias, (b) Intercept Range Standard Deviation, (c) Along-Intercept-Line
Position Bias, and (d) Along-Intercept-Line Position Standard Deviation

LOB, Velocity, and Range Sensors
with Kalman Estimation

(a)

(b)

(c)

(d)
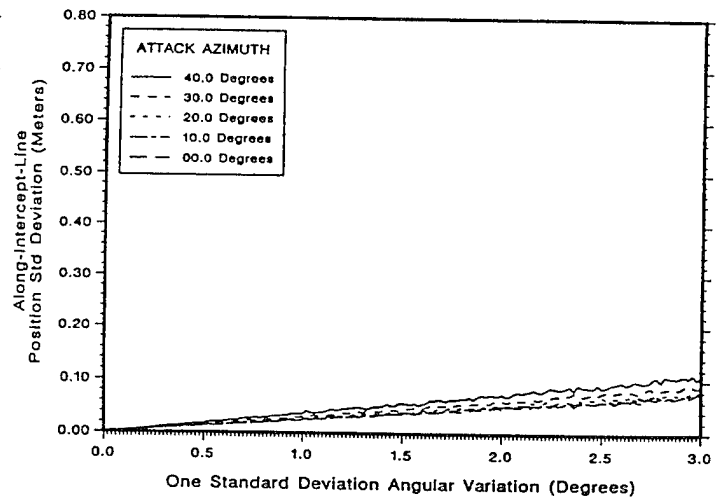
Figure B-11. LOB Tracker with 0.0 to 3.0 Degree Angular Variations, Includes Velocity and Range Sensors, Kalman Estimation, 5 Meter Intercept: (a) Intercept Range Bias, (b) Intercept Range Standard Deviation, (c) Along-Intercept-Line Position Bias, and (d) Along-Intercept-Line Position Standard Deviation

92

LOB, Velocity, and Range Sensors
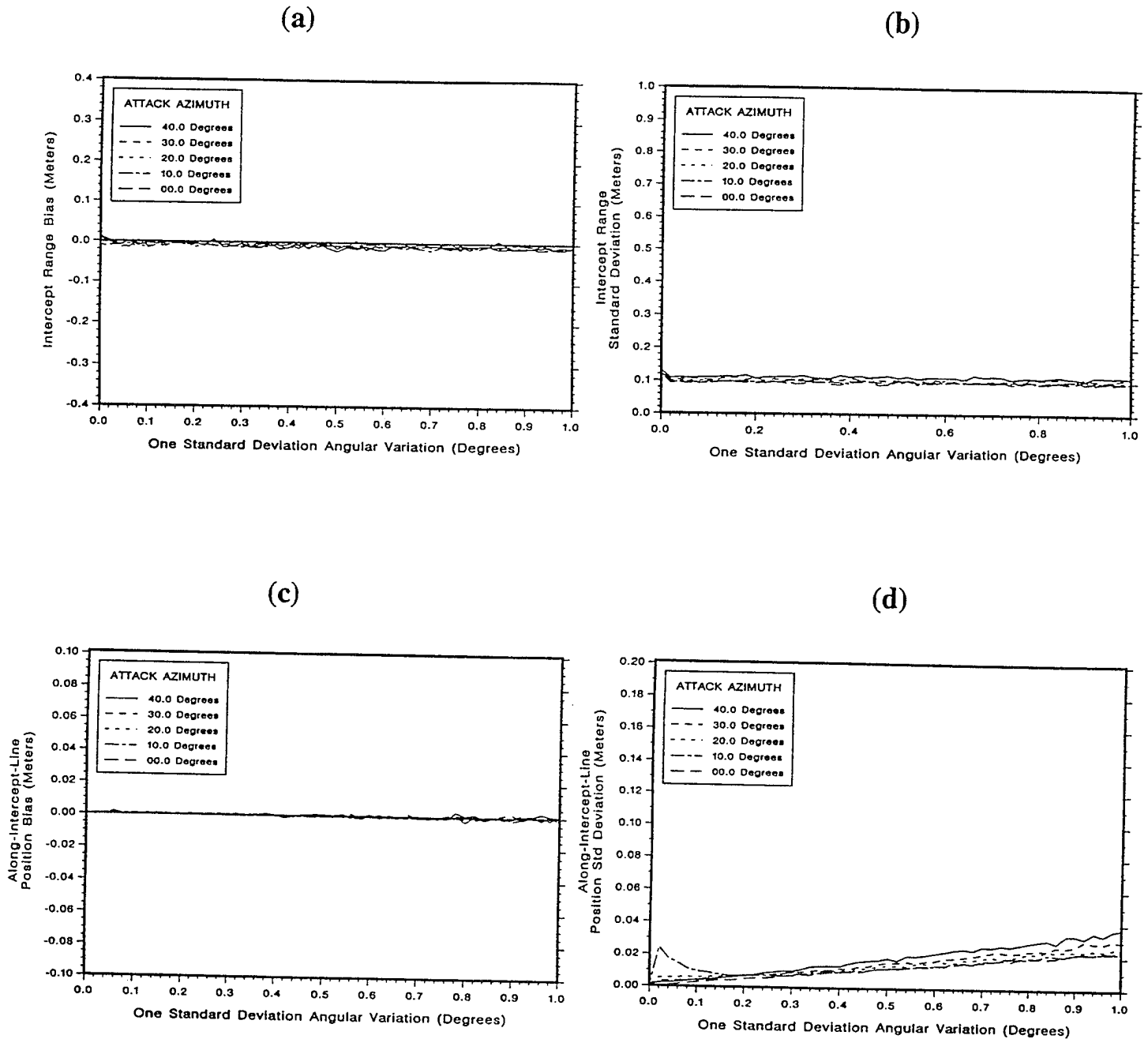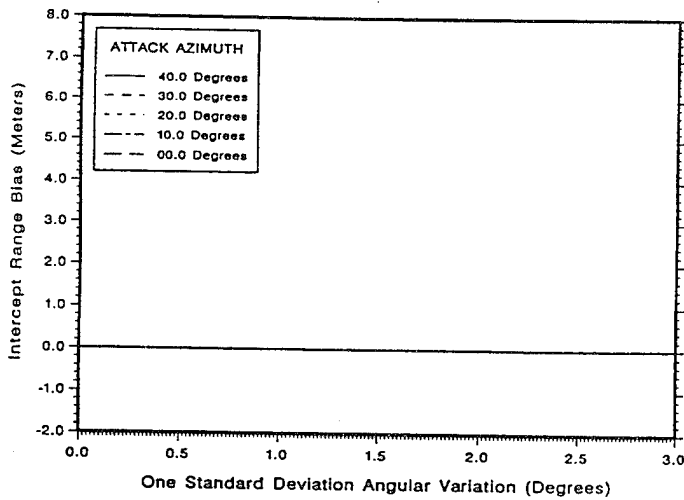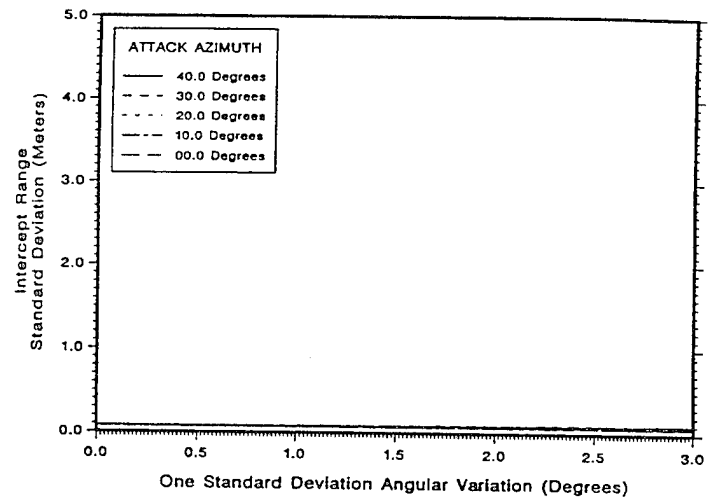# with Kalman Estimation
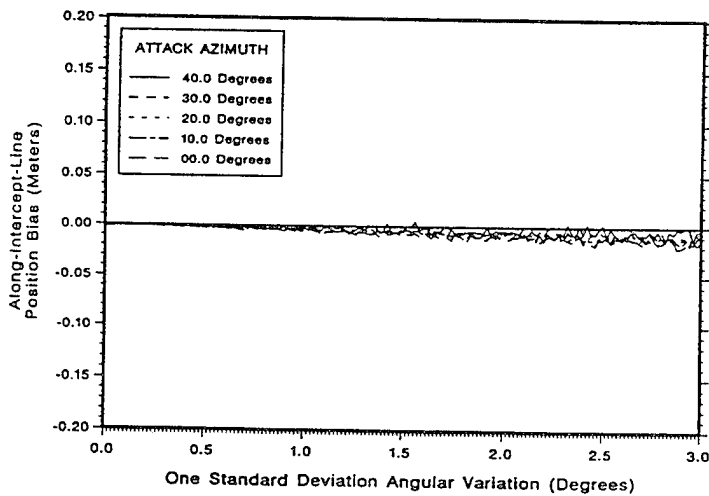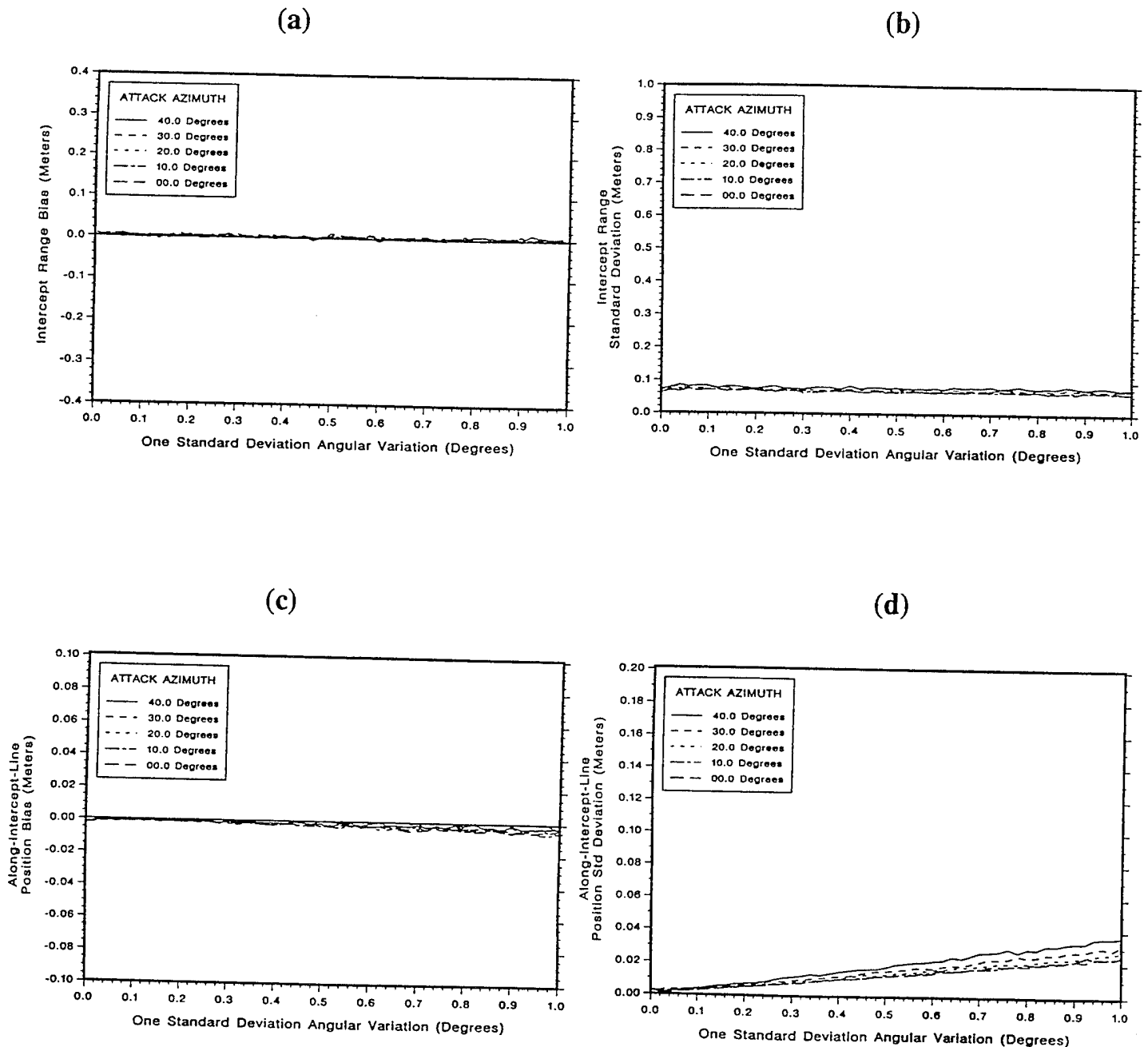

Figure B-12.   LOB Tracker with 0.0 to 1.0 Degree Angular Variations, Includes Velocity
and Range Sensors, Kalman Estimation, 5 Meter Intercept: (a) Intercept
Range Bias, (b) Intercept Range Standard Deviation, (c) Along-Intercept-Line
Position Bias, and (d) Along-Intercept-Line Position Standard Deviation

93

INTENTIONALLY LEFT BLANK

NO. OF
COPIES   ORGANIZATION

2   DEFENSE TECHNICAL INFO CTR
     ATTN DTIC DDA
     8725 JOHN J KINGMAN RD
     STE 0944
     FT BELVOIR VA 22060-6218

1   DIRECTOR
     US ARMY RESEARCH LAB
     ATTN AMSRL OP SD TA
     2800 POWDER MILL RD
     ADELPHI MD 20783-1145

3   DIRECTOR
     US ARMY RESEARCH LAB
     ATTN AMSRL OP SD TL
     2800 POWDER MILL RD
     ADELPHI MD 20783-1145

1   DIRECTOR
     US ARMY RESEARCH LAB
     ATTN AMSRL OP SD TP
     2800 POWDER MILL RD
     ADELPHI MD 20783-1145

     ABERDEEN PROVING GROUND

5   DIR USARL
     ATTN AMSRL OP AP L (305)

NO. OF
COPIES ORGANIZATION

ABERDEEN PROVING GROUND

35   DIR USARL
        ATTN   AMSRL SL BV
                        WILLIAM E. BAKER
                        JOSEPH C. COLLINS
                        LINDA L. C. MOSS
                AMSRL SL I
                        RICHARD SANDMEYER
                AMSRL CI S
                        BARRY A. BODT
                        MALCOLM S. TAYLOR
                AMSRL WT WB
                        ANDREW A. THOMPSON (5 CPS)
                        EUGENE FERGUSON
                        GARY DURFEE (5 CPS)
                        THOMAS HARKINS
                        BILL D'AMICO
                        RICHARD MCGEE
                AMSRL WT PB
                        DAVID W. WEBB
                AMSRL WT WD
                        THOMAS KOTTKE
                        GEORGE THOMSON
                        ANDRUS NIILER
                AMSRL SS SD
                        H. BRUCE WALLACE (2 CPS)
                AMSRL WT WE
                        JOSEPH K. WALD
                        FRED BUNN
                        PATRICK CORCORAN
                        PETER FAZIO
                        JAMES RAPP
                AMSRL CI CA
                        AIVARS CELMINS
                AMSRL CI CC
                        RICHARD KASTE
                AMSRL WT
                        DONALD ECCLESHALL
                AMSRL WT WC
                        GARY HAAS

3   DIR ARDEC
        ATTN   AMSTA AR FSF T (BLDG 120)
                        MIGUEL ANDRIOLA
                        RINA CARTER
                        ELIZABETH LAURIE
                APG, MD 21001-5068

96

USER EVALUATION SHEET/CHANGE OF ADDRESS

This Laboratory undertakes a continuing effort to improve the quality of the reports it publishes. Your comments/answers to the items/questions below will aid us in our efforts.

1. ARL Report Number __ARL-TR-961_____ Date of Report __February 1996_____

2. Date Report Received _____

3. Does this report satisfy a need? (Comment on purpose, related project, or other area of interest for which the report will be used.) _____

_____

_____

4. Specifically, how is the report being used? (Information source, design data, procedure, source of ideas, etc.) ____

_____

_____

5. Has the information in this report led to any quantitative savings as far as man-hours or dollars saved, operating costs avoided, or efficiencies achieved, etc? If so, please elaborate. _____

_____

_____

6. General Comments. What do you think should be changed to improve future reports? (Indicate changes to organization, technical content, format, etc.) _____

_____

_____

_____

CURRENT
ADDRESS

Organization _____

Name _____

Street or P.O. Box No. _____

City, State, Zip Code _____

7. If indicating a Change of Address or Address Correction, please provide the Current or Correct address above and the Old or Incorrect address below.

OLD
ADDRESS

Organization _____

Name _____

Street or P.O. Box No. _____

City, State, Zip Code _____

(Remove this sheet, fold as indicated, tape closed, and mail.)
(DO NOT STAPLE)

DEPARTMENT OF THE ARMY

OFFICIAL BUSINESS

BUSINESS REPLY MAIL
FIRST CLASS PERMIT NO 0001,APG,MD

POSTAGE WILL BE PAID BY ADDRESSEE

**DIRECTOR
U.S. ARMY RESEARCH LABORATORY
ATTN: AMSRL-WT-WB
ABERDEEN PROVING GROUND, MD 21005-5066**

NO POSTAGE
NECESSARY
IF MAILED
IN THE
UNITED STATES